

Identification of critical residues in the carboxy-terminal extension of the mitochondrial
DNA polymerase in *Saccharomyces cerevisiae*

by

Robin John Lester Imperial

A Thesis submitted to the Faculty of Graduate Studies of
The University of Manitoba
in partial fulfillment of the Requirements for the Degree of

MASTER OF SCIENCE

Department of Microbiology

University of Manitoba

Winnipeg

Copyright © 2011 by Robin John Lester Imperial

Thesis Abstract

Mip1p is the highly processive monomeric mitochondrial DNA polymerase in *Saccharomyces cerevisiae*. Despite differences in enzyme structure, substrate topology, and possible nucleoid interactions, Mip1p continues to be used as a model for human mitochondrial DNA polymerase (POLG) variants associated with various human mitochondrial diseases. Structurally, Mip1p functions as a monomer, whereas, the POLG holoenzyme contains a catalytic subunit (POLGA) complexed with a dimeric form of an accessory subunit (POLGB) which functions by loading the enzyme onto mitochondrial DNA and enhancing processivity. However, Mip1p does contain a 279-residue carboxyl-terminal extension (CTE) absent in the structure of POLG. The function of the CTE has not yet been determined although studies of truncation variants identify 74 N-terminal residues are essential for Mip1p wild-type activity. Furthermore, regions encompassing Mip1p residues N1033 – E1038 and Y1039 – A1049 are suggested to function in mitochondrial DNA maintenance and fidelity, respectively. This study has developed a mutagenic strategy to systematically replace the residues in the mitochondrial DNA maintenance region with glycine in order to identify residues critical for Mip1p function. Using *in vivo* respiratory competence and erythromycin resistance assays accompanied by an *in vitro* non-radioactive DNA polymerase assay, this study has identified two key residues, E1036 and D1037 that may function in the exonuclease-polymerase coupling mechanism of Mip1p.

Acknowledgements

I have been very fortunate in my life to have known and been surrounded by such amazing people. I am indebted to my supervisor, mentor and friend, Dr. Deborah Court. Her wisdom, guidance and advice have helped me to become not only a better scientist, but also a better person.

I would like to thank Dr. William Navarre at the University of Toronto who first sparked my interest in research. Without him and the members of the Navarre Lab, I wouldn't be where I am today. My thesis work would not be completed without the help of my committee members Dr. Brian Mark and Dr. Dan Gietz. Thank you both for your input and candor.

I will treasure my time at the University of Manitoba. The staff, faculty and students have been supportive, knowledgeable and encouraging. In particular, I would like to thank Dr. Georg Hausner for his persistence in offering me a position in his lab. I must respectfully decline. To the members of the Court Lab: Wailing Thao, Summer Pham, Aaron Dubyna, Emma Hauch, Suman Lakhi, Maggie Ong, Ameet Bharaj and Lan Li, thank you for all the laughs.

My family has always been a source of support and inspiration. Mom, Dad, Rochelle, Shirley, Adonis, Helene, Philippe, Grace, Noel, Evangeline, Mike, Henry, Tess and all my nieces and nephews, I love you. To my Winnipeg family, especially Larissa, thank you for your love and support. Showtime: Like Eli, I did it.

This work was made possible by the Natural Sciences and Engineering Research Council (NSERC) through a Discovery Grant awarded to Dr. Deborah Court.

Table of Contents

Thesis Abstract.....	i
Acknowledgements	ii
Table of Contents	iii
List of Tables	v
List of Figures.....	vi
List of copyrighted material for which permission was obtained	viii
List of Abbreviations	ix
CHAPTER ONE: LITERATURE REVIEW AND INTRODUCTION	1
1.1 <i>Saccharomyces cerevisiae</i> , the model eukaryotic organism	1
1.2 Model for mitochondrial study.....	2
1.3 Mip1p	4
1.4 Consequences of mtDNA instability: using Mip1p to model POLG mutations	25
1.5 Yeast mitochondrial nucleoid.....	29
1.5.1 Mitochondrial DNA packaging	30
1.5.2 The dynamic mitochondrial nucleoid: evolutionary tinkering and nucleoid remodelling.....	32
1.5.3 Mitochondrial nucleoid tethering	35
1.6 Mechanisms of mitochondrial DNA replication	36
1.7 Goals of this study.....	37
CHAPTER TWO: STRAINS, MATERIALS AND METHODS	39
2.1 Strains, vectors and primers	39
2.2 Media.....	46
2.3 Methods.....	47
2.3.1 Isolation of yeast genomic DNA	47

2.3.2 Transformation of yeast strains	48
2.3.3 Transformation of <i>Escherichia coli</i> DH5 α	50
2.3.4 Creation of <i>mip1</i> mutants for <i>in vivo</i> studies.....	51
2.3.4.1 Mip1p(E1036G) Δ 205.....	51
2.3.4.2 Mip1pR1034G.....	52
2.3.5 Replenishment of mitochondrial DNA	63
2.3.6 Respiratory competence	64
2.3.7 Erythromycin resistance.....	65
2.3.8 Construction of mutant vectors for overexpression	65
2.3.9 Induction.....	66
2.3.10 Isolation of mitochondrial membrane fractions	67
2.3.11 Western blotting.....	69
2.3.12 Non-radioactive <i>in vitro</i> DNA polymerase assay	70
2.3.13 Data analysis	72
CHAPTER THREE: RESULTS	73
3.1 Computational results.....	73
3.3 <i>In vivo</i> analysis	81
3.4 Creation of plasmids for overexpression of <i>mip1</i> variants.....	88
3.5 Overexpression and isolation of Mip1p variants.....	88
3.6 Western blot	91
3.7 Non-radioactive <i>in vitro</i> DNA polymerase assay	91
CHAPTER FOUR: DISCUSSION AND FUTURE STUDIES.....	106
4.1 Discussion	106
4.2 Future studies	109
REFERENCES.....	117

List of Tables

Table 2.1 <i>Saccharomyces cerevisiae</i> and bacterial strains used in this study.....	39
Table 2.2 Vectors used in this study	40
Table 2.3 Primers used in this study	41
Table 3.1 NetSurfP numerical analysis of the predicted 15-residue helix in the Mip1p CTE.....	76
Table 3.2 Activity of Mip1p variants at 30°C	103
Table 3.3 Activity of Mip1p variants at 37°C	104
Table 3.4 Relative activity rates of Mip1p variants at 30°C and 37°C between sampled time points.....	105

List of Figures

Figure 1.1 Map of human POLG variants isolated from patients diagnosed with their respective disease.....	5
Figure 1.2 Alignment of sequenced eukaryotic representatives of gamma subfamily mtDNA polymerases and diseases associated with respective human POLG residues.....	7
Figure 1.3 3D model of the catalytic subunit of human POLG, POLGA.....	19
Figure 1.4 Secondary structure analysis and identification of two regions within the CTE critical for Mip1p function.....	23
Figure 2.1 Schematic of the one-step gene replacement cloning strategy employed to create <i>MIP1E1036G::CaURA3</i>	55
Figure 2.2 Adapted <i>delitto perfetto</i> cloning strategy for the creation of Mip1p genomic variant	57
Figure 3.1 NetSurfP alpha helix prediction plot of the Mip1p residues Q1026 – R1075 located in the CTE..	74
Figure 3.2 Verification of <i>delitto perfetto</i> cloning strategy in creating <i>mip1R1034G</i>	79
Figure 3.3 Respiratory competence of S150 and R1006 at 30°C. A. Chart representing the respiratory competence of a population of cells from strains S150 and RI006 grown for 4 days at 30°C on a fermentable carbon source.	82
Figure 3.4 Erythromycin resistance of S150 and RI006 over the course of 2 weeks growth on a fermentable carbon source at 30°C.....	84
Figure 3.5 Respiratory competence of S150 and R1004 at 30°C.....	86
Figure 3.6 Sequencing chromatogram of <i>mip1</i> variant plasmids.....	89
Figure 3.7 Western blot of a <i>mip1</i> variant	92

Figure 3.8 – 3.13 *In vitro* relative activity of Mip1p variants at 30°C and 37°C over 15 minutes..... 94

Figure 4.1 Amino acid alignment of representative mitochondrial DNA polymerases from *Homo sapiens* (HS), *Xenopus laevis* (Xl) mouse (mm), *Drosophila melanogaster* (Dm), *Saccharomyces cerevisiae* (Sc) and *Schizosaccharomyces pombe* (Sp)..... 114

List of copyrighted material for which permission was obtained

Lee, Y. S., Kennedy, W. D. and Yin, Y. W., (2009) Structural Insight into Processive Human Mitochondrial DNA Synthesis and Disease-Related Polymerase Mutations. *Cell* **139**: 312-24. Reproduced/amended with permission.

List of Abbreviations

AMP	Ampicillin
AP	alkaline phosphatase
ATP	Adenosine triphosphate
bp	base pair
BSA	Bovine Serum Albumin
CaURA3	<i>Candida albicans</i> gene encoding Orotidine-5'-phosphate (OMP) decarboxylase required for uracil biosynthesis
dATP	deoxyadenosine triphosphate
dCTP	deoxycytosine triphosphate
ddNTP	dideoxy nucleoside triphosphate
dGTP	deoxyguanosine triphosphate
DIG-11-dUTP	Digoxigenin-11-2'-deoxy-uridine-5'-triphosphate
DMSO	Dimethylsulfoxide
DNA	deoxyribonucleic acid
dNTP	deoxynucleoside triphosphate
dsDNA	double-stranded DNA
dTTP	deoxythymidine triphosphate
<i>E. coli</i>	<i>Escherichia coli</i>
EDTA	Ethylenediaminetetraacetic acid
Er	Erythromycin
EtBr	Ethidium Bromide
EtOH	Ethanol
FOA	5-fluoroorotic acid
HA	human influenza hemagglutinin epitope tag
His	Histidine
HIV	Humain Influenze Virus
IgG	Immunoglobulin G
Ilv5p	Bifunctional acetohydroxyacid reductoisomerase and mtDNA binding protein
kb	Kilobase
kda	Kilodalton
LB	Luria Broth
LEU	Leucine
LiAc	Lithium Acetate

LOH	Loss of Heterozygosity
Mip1p	Mitochondrial DNA Polymerase gamma in <i>Saccharomyces cerevisiae</i>
Mip1p[Σ]	Mitochondrial DNA Polymerase gamma derived from <i>Saccharomyces cerevisiae</i> Σ1278b
Mip1pN1033G	Mitochondrial DNA Polymerase gamma of the Σ1278b lineage with a single amino acid substitution of glycine for asparagine at residue 1036 of Mip1p
Mip1pR1034G	Mitochondrial DNA Polymerase gamma of the Σ1278b lineage with a single amino acid substitution of glycine for arginine at residue 1036 of Mip1p
Mip1pL1035G	Mitochondrial DNA Polymerase gamma of the Σ1278b lineage with a single amino acid substitution of glycine for leucine at residue 1036 of Mip1p
Mip1pE1036G	Mitochondrial DNA Polymerase gamma of the Σ1278b lineage with a single amino acid substitution of glycine for glutamate at residue 1036 of Mip1p
Mip1p(E1036G)Δ205	Mitochondrial DNA Polymerase gamma of the Σ1278b lineage with a single amino acid substitution of glycine for glutamate at residue 1036 and replacement of the 205 residues from the carboxyl end of Mip1p with <i>CaURA3</i>
Mip1pD1037G	Mitochondrial DNA Polymerase gamma of the Σ1278b lineage with a single amino acid substitution of glycine for aspartate at residue 1036 of Mip1p
mL	millilitre
mtDNA	mitochondrial DNA
NaCl	Sodium Chloride
nm	Nanometer
nt	Nucleotide
nucDNA	nuclear DNA
PCR	polymerase chain reaction
PEG	poly ethylene glycol

PEO	Progressive external ophthalmoplegia
PMSF	phenylmethylsulfonyl fluoride
POLG	Human mitochondrial DNA polymerase gamma
POLGA	Human mitochondrial DNA polymerase gamma catalytic subunit
POLGB	Human mitochondrial DNA polymerase gamma accessory subunit
ρ	status of mitochondrial DNA, ρ^+ indicates intact mitochondrial DNA, ρ^o indicates mitochondrial DNA depletion, ρ^- indicates highly mutated mitochondrial DNA
RNA	Ribonucleic Acid
RNR1	yeast gene encoding ribonucleotide reductase
ROS	Reactive Oxygen Species
rpm	rotations per minute
SC	Simple complete
sdH₂O	sterile, distilled water
SDS	sodium dodecyl sulfate
SEM	Buffer containing sucrose, EDTA and MOPS
<i>SML1</i>	yeast gene encoding a ribonucleotide reductase inhibitor involved in regulating dNTP production
TAE	Buffer containing Tris base, acetic acid and EDTA
TBS	Tris-buffered Saline buffer
TE	Tris-EDTA buffer
tRNA	transfer RNA
TRP	tryptophan
TTC	2,3,5-triphenyl tetrazolium chloride
μg	microgram
URA	Uracil
UV	ultraviolet
w/v	weight:volume ratio
YBB	Yeast Breaking Buffer
YP10D	media: yeast extract, peptone, 10% dextrose
YPD	media: yeast extract, peptone, 2% dextrose
YPG	media: yeast extract, peptone, 3% glycerol

CHAPTER ONE: LITERATURE REVIEW AND INTRODUCTION

1.1 *Saccharomyces cerevisiae*, the model eukaryotic organism

Baker's yeast, *Saccharomyces cerevisiae*, is a valuable resource for investigating eukaryotic processes. It is among the most studied organisms to date with the entire genome completely sequenced in 1996 and available electronically (<http://www.yeastgenome.org>). Genetic manipulations can be done with relative ease using a wide range of auxotrophic markers (Brachmann *et al.* 1998). Rather than using restriction sites in cloned genes to create null mutations that could be moved into chromosomal DNA, which may leave behind a functional portion of the gene, a PCR-mediated method was developed to completely and efficiently replace the gene of interest with a selectable auxotrophic marker (Baudin *et al.*, 1993, Lorenz *et al.*, 1995). This method exploits the endogenous yeast recombination machinery. Linear PCR products of an auxotrophic marker amplified with at least 40 base pairs (bp) of homology on both 5' and 3' ends to the upstream and downstream areas of the gene of interest are transformed into the yeast strain. The PCR product efficiently undergoes homologous recombination at the desired locus resulting in the seamless replacement of the gene of interest and the creation of a null mutation immediately available for study. Following this method, constructions of vectors for study have become restriction enzyme free. Linear DNA fragments containing homologous ends cotransformed with linearized vector DNA into yeast cells utilize the same endogenous machinery to create circular plasmids with high specificity and efficiency (reviewed in Wang, 2004).

The single-celled nature of *S. cerevisiae* and its relative ease to be cultured both in haploid and diploid states provide an advantage over studies done in mammalian cell lines. Mutations created in a haploid cell that, cause depletion of a cytoplasmic constituent, can be replenished by mating with an isogenic strain. For example, the majority of the yeast mitochondrial proteome is nuclear encoded. Mutation involving members of the mitochondrial proteome with roles in mitochondrial DNA (mtDNA) maintenance may cause unwanted depletion or disruption of functional mtDNA. Mating with an isogenic strain re-introduces intact and functional mtDNA. The, now diploid, strain can then be sporulated for haploid studies (Foury, 1989). Furthermore, potentially lethal mutations can be introduced into a diploid cell, thereby masking its effect. Upon sporulation, the effect of these mutations can be determined.

1.2 Model for mitochondrial study

S. cerevisiae has garnered particular interest from the mitochondrial disease research community. Mitochondria are double-membrane enclosed organelles and the home to several essential eukaryotic cell processes that are conserved across all eukaryotes: metabolism of fatty-acids, iron, amino acids, steroids, and apoptosis (Stumpf, 1969, Kohlhaw *et al.*, 2003, Midzak *et al.*, 2011, Stella *et al.*, 2011). Most notably, mitochondria are considered the “powerhouse” of the cell (reviewed in McBride *et al.*, 2006). ATP is generated through catabolism of fermentable sugar molecules via glycolysis and/or more efficiently by the mitochondrial oxidative phosphorylation machinery. *S. cerevisiae* is a facultative-anaerobe. As such, it is capable of surviving in

the absence of oxidative phosphorylation driven ATP generation. Studies affecting the integrity of aerobic respiration can be conducted in the yeast background with easily recognizable cell growth phenotypes for analysis.

The major constituents of the oxidative phosphorylation machinery are encoded in the mitochondrial genome. Factors that affect the maintenance or expression of these genes result in a ρ^- or ρ^o phenotype (Ephrussi *et al.*, 1949, Dujon *et al.*, 1981). ρ^-/ρ^o mutants are unable to grow on a non-fermentable carbon source and when grown on a fermentable carbon source produce colonies much smaller (“petite”) than the robust ρ^+ (“grande”) cells. The phenotypes described are in reference to the state of the mitochondrial genome. ρ^o mutants are depleted in mtDNA and thus are not able to express the mtDNA-encoded components of the oxidative phosphorylation machinery, while, ρ^- mutants contain highly mutated mtDNA resulting from genetic rearrangements or point mutations.

mtDNA replication in humans is governed by POLG (Polymerase Gamma, Lee *et al.* 2009). The homologous counterpart in yeast is Mip1p (MItochondrial Polymerase 1, Foury 1989, 1992). They share high homology and have highly conserved exonuclease and polymerase motifs in each respective domain (Figure 1.1 and section 1.3). Therefore, it was accepted that Mip1p could be a suitable substitute for POLG for assessing mutations that could cause human disease stemming from mtDNA replication (Barrientos, 2003). Currently, an online database exists that maps polymorphisms in POLG associated with disease (<http://tools.niehs.nih.gov/polg>, Figure 1.1) and equivalent

mutations introduced into Mip1p for study are shown (Figure 1.2). These mutations can be characterized *in vitro* through polymerase assays or *in vivo* through the ability to respire and resistance to erythromycin. Respiratory competence is determined by the ability to grow on a non-fermentable carbon source and can be assessed by the appearance of *petites* over continued growth on a fermentable carbon source. Erythromycin resistance is a function of the stability of mtDNA. Specific point mutations within the mtDNA-encoded 21S rRNA genes confer resistance of the cell to erythromycin (Dujon, 1981, Netter *et al.*, 1974, Sor and Fukuhara 1983). Thus, the acquisition of erythromycin resistance provides insights into the fidelity of mtDNA replication.

1.3 Mip1p

Mitochondrial DNA polymerases belong to the gamma subfamily of family A DNA polymerases. Characteristically, these enzymes are found to be resistant to aphidicolin and sensitive to di-deoxynucleotidetriphosphates (ddNTPs) (Foury, 1989). They contain 3' - 5' exonuclease activity supplied via a domain harbouring 3 conserved "exonuclease" motifs in the N-terminus of the protein and 5' - 3' polymerase activity courtesy of 3 conserved "polymerase" motifs in the C-terminus of the protein (Figure 1.3, Ito and Braithwaite, 1990, Lecrenier *et al.*, 1997). This subfamily also contains 6 gamma specific sequences located in the polymerase domain and between the polymerase and exonuclease domain in the spacer region (Kaguni, 2004). The prototypical DNA polymerase of this group is *Escherichia coli* DNA polymerase I.

Figure 1.1 Map of human POLG variants isolated from patients diagnosed with their respective disease (Figure was taken from <http://tools.niehs.nih.gov/polg>).

Figure 1.2 Alignment of sequenced eukaryotic representatives of gamma subfamily mtDNA polymerases and diseases associated with respective human POLG residues. Highlighted in blue are residues conserved across mammalian polymerase gamma representatives. Highlighted in yellow are residues conserved across all eukaryotic representatives sampled in this alignment. Disease causing variants of POLG that are highly conserved among mammalian sampled or all eukaryotic sampled representatives are indicated with * (Figure was taken from <http://tools.niehs.nih.gov/polg>).

Consensus	(276)	VGHNVSFDRAHIREQYLIQGSRRFLDTMSMHMAISGLSSFQORSLWM AKQGKHK	
		331 * * * *	385
hum pol gamma aa seq	(322)	VC-- PTKQGQKSQRKARRG --- PAISSWDWLDISSVNSLAEVHRLYVGGPPLEKE	324P→S SNP
Pan troglodytes (chimpanzee)	(319)	VC-- PSTKQGQKSQRKARRG --- PAISSWDWLDISSVNSLAEVHRLYVGGPPLEKE	S332V
Macaca mulatta (rhesus monkey) pol gamma	(311)	VC-- GSTKQGQKSQRKARRG --- PAISSWDWLDISSVNSLAEVHRLYVGGPPLEKE	T326fs61X-Alpers
mus pol gamma	(305)	TC-- QSTKRGQKSQRK-ANG --- PAISSWDWMDISSANNLADVHNLYVGGPPLEKE	W347_L356del-Alpers
rat pol gamma	(305)	TC-- HPTKRGQKSQRK-ANG --- PAISSWDWMDISSANNLADVHNLYVGGPPLAKE	
Xenopus pol gamma	(296)	GL-- QEVKQHIKKTFSNFSG --- SPISSWDWVNLSSINNLADVHALYVGGPPLEKE	
Drosophila pol gamma	(305)	----- KE ----- PAEEDLGLWLEQSLNLSVEVHRLYCGGDTLSKE	
scyeast pol gamma mip1	(274)	----- KKEAEVESEVHPEISIEDYDDPWLNVSLNLSKDVAKFHCK-IDIDKT	
S. pombe pol gamma	(277)	S OSTETS E DDDD S SFDD D YQ-- NYLKQEPWLAHSVNSLKDVAKFHCN-ITLDKS	
Neurospora pol gamma	(297)	REKAEHESASVEL Q EVL Q GS L T A E A D L W V K S I N S I R D V A Q F H L N-VKID K	
Consensus	(331)	Q TK GQKSQR G PAISSWDWLDISS NSLADVH LYVGGPPLEKE	
		386 * * * * EXOIII * * * *	440
hum pol gamma aa seq	(373)	P REL F V K G T N K DIRE N F Q D L M Q Y C A Q D V W A T H E V F Q Q L P L F L E R C P H P V T L A G M	R374X -Alpers
Pan troglodytes (chimpanzee)	(370)	P REL F V K G T N K DIRE N F Q D L M Q Y C A Q D V W A T H E V F Q Q L P L F L E R C P H P V T L A G M	G380D-PEO
Macaca mulatta (rhesus monkey) pol gamma	(362)	P REL F V K G T N K DIRE N F Q D L M Q Y C A Q D V W A T H E V F Q Q L P L F L E R C P H P V T L A G M	392L→V SNP
mus pol gamma	(355)	P REL F V K G S M R DIRE N F Q D L M Q Y C A R D V W A T F E V F Q Q L P L F L E R C P H P V T L A G M	L392V-muscle weakness, optic atrophy
rat pol gamma	(355)	P REL F V K G S M R DIRE N F Q D L M Q Y C A R D V W A T F E V F Q Q L P L F L E R C P H P V T L A G M	R417T - Alpers
Xenopus pol gamma	(347)	A REL F V K G S M S DIR T E F Q E L M R Y C A L D V Q A T H E V F Q E Q F P L F M E R C P H P V T L S G M	C418R - Alpers
Drosophila pol gamma	(340)	P R N I F V E G T L E Q V R Q S F O S I T N Y C A S D V E A T H R I L R V L Y P L Y A E R F P H P A S L A G M	L424Gfs28X-PEO
scyeast pol gamma mip1	(321)	D R D F F A S T D K S T L I E N F Q K L V N Y C A T D V T A T S Q V F D E I F P V F L K K C P H P V S F A G L	Alpers
S. pombe pol gamma	(329)	K R D D F A S L E K E P L Q K L N E I T Y C A H D T Y S T H Q V F K K V F Q F L E V C P H A T F S A M	G426S - Epilepsy...
Neurospora pol gamma	(351)	I R D V E A E T R N V L N Q L D L L T Y C A A D V Q V T H Q V Y Q V V F N F L G V C P H P V S F A L	
Consensus	(386)	PREL F V K G M DIRE N F Q D L M YCA DVWATHEV F Q Q L P L F L E R C P H P V T L A G M	
		441 * * * * * *	495
hum pol gamma aa seq	(428)	L E M G V S Y L P V N Q-N W E R Y L A E A Q G T Y E E L Q R E M K K S L M D L A N D A C Q L L S G E R Y K E	L428P-Alpers,...
Pan troglodytes (chimpanzee)	(425)	L E M G V S Y L P V N Q-N W E R Y L A E A Q G T Y E E L Q R E M K K S L M D L A N D A C Q L L S G E R Y K D	M430L-PEO
Macaca mulatta (rhesus monkey) pol gamma	(417)	L E M G V S Y L P V N Q-N W E R Y L A E A Q G T Y E E L Q R E M K K S L M D L A N D A C Q L L S G E R Y K E	G431V-PEO
mus pol gamma	(410)	L E M G V S Y L P V N Q-N W E R Y L T E A Q N T Y E E L Q R E M K K S L M D L A N D A C Q L L S G E R Y K E	S433C-PEO, ataxia, ...
rat pol gamma	(410)	L E M G V S Y L P V N Q-N W E R Y L T E A Q S T Y E E L Q R E M K K S L M E L A N D A C Q L L S G E R Y K E	T452X-PEO
Xenopus pol gamma	(402)	L E M G V S Y L P V N Q-N W E R Y L D E A Q T S Y E E L Q E M K K S L M K L A N D A C Q L I T K D A Y K E	L463F-PEO
Drosophila pol gamma	(395)	L E M G S A Y L P V N S-N W E R Y I R E A Q L T Y E D L S I E A K Y H L G R R A E E A C S L L D D O Y R Q	A467T-PEO, SANDO, MERRF, & Alpers...
scyeast pol gamma mip1	(376)	K S L S K C I L P T K L N D N D Y L N S S E S L Y Q S K V Q I E S K I V Q I I K I V L L K D K P D F Y L	N468D-PEO
S. pombe pol gamma	(384)	L S L S V F L P V N H - S W T Y I N G V E E Q Y Q Q M I Q L V D Q K L S Q Y E K A K D L I N T K D T V L	Y479X

Neurospora pol gamma	(406)	RHLASVILPVNK--TWDTYIETAEATYLQMLHGQERLFTLMERTLDYKADPEKYL	
Consensus	(441)	LEMGSVYLPVNVQ NWEERYL EAQ TYEELQREMKKSLM LANDACQLLSGERYKE	
		496	550
hum pol gamma aa seq	(482)	DPWLDLEWDLQEFKQKKAKKVKKEPATAS SKLPIEGAG APGDPMDQEDL GPCSEE	
Pan troglodytes (chimpanzee)	(479)	DPWLDLEWDLQEFKQKKAKKVKKEPATAS SKLPIEGAG APGDPMDQEDL GPCSEE	<i>Q497H-Ataxia-Neuropathy</i>
Macaca mulatta (rhesus monkey) pol gamma	(471)	DPWLDLEWDLQEFKQKKAKKVKKEPATAS KLPIEGAG APGDPMDQEDL GP RSEE	<i>S511N-PEO</i>
mus pol gamma	(464)	DPWLDLEWDLQEFKQKKAKKVKK--PAS ASKLPIEGAG PF GDPMDQED PG PPSEE	<i>G517V- Ataxia-Neuropathy</i>
rat pol gamma	(464)	DPWLDLEWDLQEFKQKKAKKVKK--TAS ASKLPIEGAG PF GDPMDQED PG PPSEE	
Xenopus pol gamma	(456)	DPWLDLEWDLQEFKQKKAKKVKK--QKKANEAA ESV GNKLVEDHNE DPG PT EEK	
Drosophila pol gamma	(449)	NLWLDLEWDLQEFKQKKAKKVKK PP -----LPTVEIKDS	
scyeast pol gamma mip1	(431)	KDPWLSQLDWTTRKPLRLTK GV PAK-----	
S. pombe pol gamma	(438)	KDPWLRQLDWTPCNLYRKL KK ATQE-----	
Neurospora pol gamma	(460)	SDPWLSQLDWSGQEI KMAKPKK KG-----	
Consensus	(496)	DPWLDLEWDLQEFKQKKAKKVKK A ASKLPIEGAG GDPMDQED GP SEE	
		551	605
hum pol gamma aa seq	(537)	EEFQQDVMA RAC LQK IKG TT ELLPKRPQHLPGHPG WY RKLC PR L -----	<i>546R→C,S,G SNP</i>
Pan troglodytes (chimpanzee)	(534)	EEFQQDVMA RAC LQK IKG TT ELLPKRPQHLPGHPG WY RKLC PR L -----	<i>K561M- dysmorphia, hypotonia, liver insufficiencies, R562Q-PEO</i>
Macaca mulatta (rhesus monkey) pol gamma	(526)	EEFQQDVMA RAC LQK IKG TT ELLPKRPQHLPGHPG WY RKLC PR L -----	
mus pol gamma	(518)	EELQRSVTA HNR LQ LR ST TDLLPKRPQHLPGHPG WY RKLC PR L -----	<i>H569Q - Alpers</i>
rat pol gamma	(518)	EELQ Q NIMA H TR LQ L K ST TDLLPKRPQHLPGHPG WY RKLC PR L -----	<i>R574W-PEO+myopathy dysphagia & Alpers</i>
Xenopus pol gamma	(509)	EE S RP S MG L Y L ED L KL K L L PL L PK R Q H LP G HP G WY R K L C P R L -----	<i>R579W-PEO</i>
Drosophila pol gamma	(482)	GNTPEERR LQAKF CH L YD Q Q A LL PA RR PL LP G Y PL WY R K L CR K PP A K R E D E I L E D	
scyeast pol gamma mip1	(456)	-----C KL PG F EWY K Q L F SK -----	
S. pombe pol gamma	(463)	-----VP-----V V PK W Y K W A Y C K T -----	
Neurospora pol gamma	(484)	-----D V ER P AL N Q L PG Y P Q W Y K D L F V K V P K E L S G L D E P D	
Consensus	(551)	EE Q A LQ L TT LL PKRPQHLPGHPG WY RKLC PR L	

		606	* * * * *		660	
hum pol gamma aa seq	(581)	---DDPAWTPG PSLLS LQMRVTPK LMALT WDGFPLHYSER HGWGYL VP GRRD NLA				<i>P587L-PEO, Alpers, & inf. hepatocerebral</i>
Pan troglodytes (chimpanzee)	(578)	---DDPAWTPG PSLLS LQMRVTPK LMALT WDGFPLHYSER HGWGYL VP GRRD NLA				<i>P589L - Alpers</i>
Macaca mulatta (rhesus monkey) pol gamma	(570)	---DDPAWTPG PSLLS LQMRVTPK LMALT WDGFPLHYSER HGWGYL VP GRRD NLA				<i>R597W - PEO</i>
mus pol gamma	(562)	---DDPAWTPG PSLLS LQMRVTPK LMALT WDGFPLHYSER HGWGYL VP GRRD NLT				<i>M603L-PEO w/ ptosis</i>
rat pol gamma	(562)	---DDPAWTPG PSLLS LQMRVTPK LMALT WDGFPLHYSER HGWGYL VP GRRD NLT				<i>L605R - Alpers</i>
Xenopus pol gamma	(553)	---ED PDWLP GG ELIS LQ MRLT PK LMRL TD QY PLHYSER HGWGYL VP GRK NNKL				<i>Y614X</i>
Drosophila pol gamma	(537)	---DEEP WSPG AEIS TGM QIA PKLLS LC WE SYPLHYER EQGW GF LV PF RS DS--				<i>R617C-muscle weakness, exercise intolerance, hearing loss, arrhythmia</i>
scyeast pol gamma mip1	(474)	-----DTVEPKITIKS RIIP IL FKLS WENS SVIWS KES GWCF NV PHE QVET--				<i>L623W-Liver Dysf., hypoketotic, & hypogly.</i>
S. pombe pol gamma	(478)	-----EKRAVITAKS RLA IL LR LK WK KH PLA WSD TY GW VFS VERTSKD--				<i>R627W-PEO, Alpers, & SANDO</i>
Neurospora pol gamma	(520)	KEQENRKARHEFIN TVRS IA LL LK LS WE YEL FW SD Q FW TF QV ER--EK--				<i>R627Q-ataxia-myopathy, Alpers, PEO, ataxia-neropathy, & MELAS</i>
Consensus	(606)	DDPAW PG PSLLS LQMRVTPK LMALT WDGFPLHYS HGWGYLVP GRRD NL				<i>R628Q-in one breast tumor</i>
		661	* * * *		715	
hum pol gamma aa seq	(633)	KL PTGT LESAG VVCP YRAIESLYR KHCL EQG KQQL MP Q EAG LAE FFLLT D NSAI				<i>P648R-PEO+MYOPATHY & SANDO</i>
Pan troglodytes (chimpanzee)	(630)	KL PTGT LESAG VVCP YRAIESLYR KHCL EQG KQQL MP Q EAG LAE FFLLT D NSAI				<i>H659Q</i>
Macaca mulatta (rhesus monkey) pol gamma	(622)	KL PTGT LESAG VVCP YRAIESLYR KHCL EQG KQQL MP Q EAG LAE FFLLT D NSAI				<i>662E→K SNP</i>
mus pol gamma	(614)	EL PVSP TESAA VTCP YRAIESLYR KHCL EQG KQQL ET Q ET D LAEFFLLT D SSAM				<i>Q666L</i>
rat pol gamma	(614)	EL PVSP TESAA VTCP YRAIESLYR KHCL EQG KQQL ET Q ET D LAEFFLLT D SSAM				
Xenopus pol gamma	(605)	NNEEEE-- E --I IP CPYRAIED IAE YSK NKT WG CLS Q H ST IP EE FM L T DDNSM				
Drosophila pol gamma	(587)	-----EGVDR IP ME QL L AR CP V PE FAR LS ASKA NS DMA F D M L P				
scyeast pol gamma mip1	(520)	-----YKAKN-----YVLADSV				
S. pombe pol gamma	(522)	-----E IT M L L D -QGLV				
Neurospora pol gamma	(571)	-----A ET F I Q R Q M T P				
Consensus	(661)	P T ESA V CPYRAIESLYR HCL QGKQQL QE LAEEFFLLTD A				

		716		*	*	*	*	*	*	770	
hum pol gamma aa seq	(688)	WQTVEELDYLEVEAEAKMENLR--AAVPGQPLALTARGGPKDTQPSYHHGNGPYN									R709X-PEO
Pan troglodytes (chimpanzee)	(685)	WQTVEELDYLEVEAEAKMENLR--AAVPGQPLALTARGGPKDTQPSYHHGNGPYN									Q715X-Alpers
Macaca mulatta (rhesus monkey) pol gamma	(677)	WQTVEELDYLEVEAEAKMENLR--AAVPGQPLALTAPGGPKDSQPNYHHGNGPYN									c.2157+5_+6gc>ag-Alpers
mus pol gamma	(669)	WQTVEELGCLDVEAEAKMEN----SGLSQPLVLPAAACAPKSSQPTYHHGNGPYN									722R→H SNP
rat pol gamma	(668)	WQTVEELGCLDVEAEATVES----SGLSQPLVPPACAPKTSQPTYHHGNGPYN									H734R
Xenopus pol gamma	(656)	WQKVEELSRTEMDLSSEVPATAKAKRNNSSSEHPVKLEMEFDSLFDNHHGNSPCG									G737R- Alpers, CMT, & Parkinsonism
Drosophila pol gamma	(625)	GOVEQHLGKREHYKLSQKQ-----QR-----LETQYQGSVWCV									
scyeast pol gamma mip1	(532)	SEEEE-----IRTHN									
S. pombe pol gamma	(533)	PCSREE-----DT									
Neurospora pol gamma	(582)	VQFEDP-----DVDDR									
Consensus	(716)	WQTVEEL LEVEAEA E QPL PK QP YHHGNGPYN									
		771	*	*	*	*	*	*	*	825	
hum pol gamma aa seq	(741)	DVDIPGCWFFKLPKDKGNSCNVGSFFAKDFLPKMGDGLQA-GPGGASGPRALEI									G746S-PEO
Pan troglodytes (chimpanzee)	(738)	DVDIPGCWFFKLPKDKGNSCNVGSFFAKDFLPKMGDGLQA-GPGGASGPRALEI									W748S- Alpers & ataxia neuropathy
Macaca mulatta (rhesus monkey) pol gamma	(730)	DVDIPGCWFFKLPKDKGNSCNVGSFFAKDFLPKMGDGLQA-GPGGASGPRALEI									F749S-Alpers
mus pol gamma	(719)	DVNI PGCWFFKLPKDKGNVNVGSFFAKDFLPKMGDGLQA-GPGGASGPRALEI									L752P-Epilepsy
rat pol gamma	(718)	DVDIPGCWFFKLPKDKGNVNVGSFFAKDFLPKMGDGLQA-GPGGASGPRALEI									K755E-Liver Dysf., hypoketotic, & hypogly
Xenopus pol gamma	(711)	DVNVSGCWFFKLPKDKGNVNVGSFFAKDFLPKMGDGLQA-STGDSGATRALEI									G763R-PEO & SANDO
Drosophila pol gamma	(660)	KVLDDCCFFLKLPHKNGPSFRVGNLSDKDFLNKFAENVLSSGDESCQAAAVIDI									A767D-Alpers
scyeast pol gamma mip1	(543)	LGLQCTGVLPKVPHPNGPTFNCTNLLTKSNHFFKGVLESE---LHCAIQI									G785fs21X-PEO
S. pombe pol gamma	(541)	KLQYNNYIFKVPKDKGPEARCVRHSPNHITHTSKRVFYNQ---IMKWLKKALEM									
Neurospora pol gamma	(593)	LRMDVDHKYKLPKDKGPNARCVMARKYLYYFKGILSS---EYPYAKEALEM									
Consensus	(771)	DVDIPGCWFFKLPKDKGN NVGSFFAKDFLPKMGDGLQA GPGGASGPRALEI									
		826		*	*			*	*	880	
hum pol gamma aa seq	(795)	NKMISFWRNAHKRISSQMVVWLPKRSALPRAVIRHFDYDE---EGLYGAILPQVVT									A804T - Fatigue...
Pan troglodytes (chimpanzee)	(792)	NKMISFWRNAHKRISSQMVVWLPKRSALPRAVIRHFDYDE---EGLYGAILPQVVT									R807P-PEO
Macaca mulatta (rhesus monkey) pol gamma	(784)	NKMISFWRNAHKRISSQMVVWLPKRSALPRAVIRHFDYDE---EGLYGAILPQVVT									R807C- SANDO
mus pol gamma	(773)	NKMISFWRNAHKRISSQMVVWLPKRSALPRAVIRHFDYDE---EGLYGAILPQVVT									c.2480+1g>a-Alpers
rat pol gamma	(772)	NKMISFWRNAHKRISSQMVVWLPKRSALPRAVIRHFDYDE---EGLYGAILPQVVT									IVS15-9-c.2485del 12bp-Alpers
Xenopus pol gamma	(765)	NKMISFWRNAHKRISSQMVVWLMKKNELHHTITNDYEFDE---ENKYGAILAQVVS									IVS16-10c>t-ataxia, neuropathy...
Drosophila pol gamma	(715)	ARMMSYRNRRDRIMGQLVWVLDLSDQQLPNEFTG--EKCCQ---PIAYGATCPQVVA									Y831C-PEO & Parkinsonism
scyeast pol gamma mip1	(595)	NSSGSYNMSARERIQSQFVVPSCKFPNEFQSLSAKSSLNNEKTNDLAIIPKIVP									Y831F
S. pombe pol gamma	(593)	SAGCSYNSSARDRIRSQMVVWVWVVDKDAELGVPSVSD--G-----FGIILPCIIIP									Y831S
Neurospora pol gamma	(645)	NASCSYNISARERIKQKVVVYEDQLPPSRQFVNKDADSN---TPIGGFVLPQVIVP									
Consensus	(826)	NKMISFWRNAHKRISSQMVVWLPKRSALPR V RHP DE E YGAILPQVVT									

		881		PolA	935	
			** ** *	* * * *	** ** *	
hum pol gamma aa seq	(847)	AGTITRRAVEPTWLTASNARPD	RVGSELKAMVQAPP	GYTLVGADVDSQELWIAAV		
Pan troglodytes (chimpanzee)	(844)	AGTITRRAVEPTWLTASNARPD	RVGSELKAMVQAPP	GYTLVGADVDSQELWIAAV		G848S-PEO & Alpers, & MELAS
Macaca mulatta (rhesus monkey) pol gamma	(836)	AGTITRRAVEPTWLTASNARPD	RVGSELKAMVQAPP	GYTLVGADVDSQELWIAAV		T849H-Alpers
mus pol gamma	(825)	AGTITRRAVEPTWLTASNARPD	RVGSELKAMVQAPP	GYVVLVGADVDSQELWIAAV		T851A- Alpers
rat pol gamma	(824)	AGTITRRAVEPTWLTASNARPD	RVGSELKAMVQAPP	GYVVLVGADVDSQELWIAAV		R852C-Alpers
Xenopus pol gamma	(817)	AGTITRRAVEPTWLTASNARAD	RVGSELKAMVQVPP	GYHLIGADVDSQELWIAAI		R853Q-Myocerebrohepat.
Drosophila pol gamma	(765)	CGTLTRRAMEPTWMTASNSR	PPDLGSELRSVMVQAPP	GYRLVGADVDSQELWIASV		R853W-PEO w/ptosis & Parkinsonism
scyeast pol gamma mipl	(650)	MGTITRRAVENANLTASNAKAN	RISSSELKIQVKAPP	GYCFVGVADVDSQELWIASL		V855A-muscle weakness
S. pombe pol gamma	(638)	MGTITRRAVENTWLTASNASKN	RLGSELKAMIRAPD	GYTFVGVADVDSQELWIVAL		A862T-Ataxia & PEO
Neurospora pol gamma	(697)	MGTITRRAVERTWLTASNAKKN	RVGSELKAMVRAPP	GYVFLVGADVDSQELWIASV		N864S-PEO
Consensus	(881)	AGTITRRAVEPTWLTASNARPD	RVGSELKAMVQAPP	GYLVGADVDSQELWIAAV		R869Q - Myopathy, ataxia, Ptosis, & neuropathy
						E873X- Alpers
						Q879H-Alpers
						T885S-Alpers
						L886P-Alpers
						G888S-Alpers
						A889T-PEO
						E895G-Myopathic MDS
		936		PolB	990	
			* * *	* * *	* * *	
hum pol gamma aa seq	(902)	LGD AHFAGMHGCTAFGWM	TLQGRKSRGTDLH	SKTATTVGISREHAKIFNYGRIY		
Pan troglodytes (chimpanzee)	(899)	LGD AHFAGMHGCTAFGWM	TLQGRKSRGTDLH	SKTATTVGISREHAKIFNYGR		T914P-PEO, Alpers...
Macaca mulatta (rhesus monkey) pol gamma	(891)	LGD AHFAGMHGCTAFGWM	TLQGRKSRGTDLH	SKTATTVGISREHAKVFN		W918R - PEO
mus pol gamma	(880)	LGD AHFAGMHGCTAFGWM	TLQGRKSRGTDLH	SKTAAATVGISREHAKIFNYGR		G923D-PEO
rat pol gamma	(879)	LGD AHFAGMHGCTAFGWM	TLQGRKSRGTDLH	SKTAAATVGISREHAKVFN		G923R
Xenopus pol gamma	(872)	LGE AHFAGIHGCTAFGWM	TLQGRKSSGTDLH	SKTASTVGISREHAKVFN		K925Rfs42X-Epilepsy, ...
Drosophila pol gamma	(820)	LGD AYACCEHGAFLE	GWMTLSGSKNGS	DMHSLITAKAVGISRDHAKVIN		D930N-Alpers
scyeast pol gamma mipl	(705)	VGS IIFN-VHGGTAIC	WMCLEETKNEG	TDLHTKTAQILGCSRNEAKIFNYGR		H932Y-PEO, & SANDO
S. pombe pol gamma	(693)	MGS SQFR-LHGATA	LGMMLGKKS	EGTDLHSKTAAAILGVS		R943C-Myocerebrohep
Neurospora pol gamma	(752)	VGDATFK-LHGGNA	IGFMTLEGT	KSQGTDLHRTASILG		R943H-PEO
Consensus	(936)	LGD AHFAGMHGCTAFGWM	TLQGRKSRGTDLH	SKTATTVGISREHAKVFN		R953C-PEO
						Y955C-PEO, & Parkinsonism...

		991		1045	
		* * * *		*	
hum pol gamma aa seq	(957)	AGQPF	FAERLLMQFNHRLTQEQAAEKAAQOMYAATKGLRWYRLSDEGEWLVR	EINLP	<i>A957S-PEO</i>
Pan troglodytes (chimpanzee)	(954)	AGQPF	FAERLLMQFNHRLTQEQAAEKAAQOMYAATKGLRWYRLSDEGEWLVR	EINLP	<i>A957P-Alpers</i>
Macaca mulatta (rhesus monkey) pol gamma	(946)	AGQPF	FAERLLMQFNHRLTQEQAAEKAAQOMYAATKGLRWYRLSDEGEWLVR	EHLPL	<i>F961S - adPEO</i>
mus pol gamma	(935)	AGQSF	FAERLLMQFNHRLTRQEAEEKAAQOMYAVTKGLRRYRLSADGEWLVKQINLP		<i>R964C-Mitoch. tox.to</i>
rat pol gamma	(934)	AGQSF	FAERLLMQFNHRLSRQEAADKAAQOMYAVTKGLRRYRLSDDGEWLVKQINVE		<i>NRTI'S</i>
Xenopus pol gamma	(927)	AGQPF	FAERLLMQFNHRLTQEQAAEKAAQOMYAVTKGIRRYILSKEGEWLVEELGIS		<i>L965X-PEO</i>
Drosophila pol gamma	(875)	AGQLF	ASTLLRQFNPTFSASEAKAKAMKFSITKGGKRVYRLREFPHDELEDRAYS		<i>L966R-Alpers</i>
scyeast pol gamma mipl	(759)	AGAKF	ASQLLKRFPNPSLTDEETKKIANKLYENTPKGKTK-RSK-----		<i>S998W</i>
S. pombe pol gamma	(747)	AGLKHT	FLLMQMNPTLKTAAKELAKKLYASTKGVKSKMSKRLQEMGLPKLIT--		
Neurospora pol gamma	(806)	AGLKF	ASQLLRQFNPSLTAETTAIATKLYDATKGAKTNRKS-----		
Consensus	(991)	AGQ	FAERLLMQFNHRLT QEAEEKAAQOMYA TKGLR YRLS EGEWLV L P		
		1046		1100	
		*		*	
hum pol gamma aa seq	(1012)	VDRTEGG	WISLQDLRQVRETARKSQWKK-WEVVAERAWKGGTESEMFKLESIA		<i>W1020X-Alpers</i>
Pan troglodytes (chimpanzee)	(1009)	VDRTEGG	WISLQDLRQVRETARKSQWKK-WEVVAERAWKGGTESEMFKLESIA		<i>R1047Q-PEO</i>
Macaca mulatta (rhesus monkey) pol gamma	(1001)	VDRTEGG	WISLQDLRQVREEAARKSHRKK-WEVIAERAWKGGTESEMFKLESIA		<i>R1047W-Alpers & PEO</i>
mus pol gamma	(990)	VDRTE	DGWVSLQDLRMIRREASRKSRWKK-WEVASERAWTGGTESEMFKLESIA		<i>G1051R-PEO, & SANDO</i>
rat pol gamma	(989)	VDRTE	DGWVSLQDLRIRREASRKSRWKK-WEVVTERRAWTGGTESEMFKLESIA		
Xenopus pol gamma	(982)	VERGE	ENSVNLQDLRKIQKDATKRERK--WNLVSRRIWTTGGTESQMPFKLETIA		
Drosophila pol gamma	(930)	SYEAS	RLAIQ-----RNRTLAEVFHRPNWQGGTESAMFNRLLEETIA		
scyeast pol gamma mipl	(800)	-----	-----LFKKFWYGGSESILFNKLESIA		
S. pombe pol gamma	(800)	-----	-----FWSQGTESFVFNKLEAMA		
Neurospora pol gamma	(848)	-----	-----LYKRPFRGCTESFVFNMLEEFA		
Consensus	(1046)	VDRTE	GW SLQDLRK RE RKS KK WEV ERAW GGTESEMFKLESIA		
		1101		1155	
		* * *		* ** *** *	
hum pol gamma aa seq	(1066)	TSDI	IPRTPVVGCCISRALEPSA---VQGEFFMTSRVNWWVQSSAVDYLHLMVLVAMK		<i>P1073L-Alpers-like</i>
Pan troglodytes (chimpanzee)	(1063)	TSDI	IPRTPVVGCCISRALEPSA---VQGEFFMTSRVNWWVQSSAVDYLHLMVLVAMK		<i>G1076V-PEO</i>
Macaca mulatta (rhesus monkey) pol gamma	(1055)	TSDI	IPRTPVVGCRISRALEPSA---VQGEFFMTSRVNWWVQSSAVDYLHLMVLVAMK		<i>I1079L-adPEO</i>
mus pol gamma	(1044)	MSD	TPRTPVVGCCISRALEPSV---VQGEFFITSRVNWVQSSAVDYLHLMVLVAMK		<i>F1092L</i>
rat pol gamma	(1043)	MSD	TPRTPVVGCCISRALEPSV---VQGEFFMTSRVNWWVQSSAVDYLHLMVLVAMK		<i>S1095R-adPEO</i>
Xenopus pol gamma	(1035)	MS	PSKTPVVGCRISRALEETA---VKGEFFITSRVNWVQSSAVDYLHLMVLVAMK		<i>R1096C-PEO & Alpers</i>
Drosophila pol gamma	(970)	TGS	QPTFFLGGRLSRALADTGPQEORELPTRINWVQSSAVDFLHLMVSMR		<i>R1096H-Alpers</i>
scyeast pol gamma mipl	(822)	EQET	PKTPVVGCGITYSLMKKN--LRANSFLPSTRINWAIQSSGVDYLHLLCCSME		<i>S1104C-PEO</i>
S. pombe pol gamma	(818)	QLP	SPRTPVVDAGIQQALSSKN--LSKNSFMTSRVNWIQSSAVDYLHLLVSMN		<i>A1105T-PEO</i>
					<i>V1106I-PEO</i>

Neurospora pol gamma (871) EQERPRTPVLGAGITEALMSRWVS-RGGELTSRINWAIQSSGVDYLHLIIAMD H1110Y-mtDNA depletion
 Consensus (1101) SD PRTPVLCG ISRALPEPS VQGEFMTSRVNVVQSSAVDYHLHMLVAMK

Pol C

1156 * * * * * * * * * * 1210

hum pol gamma aa seq (1118) WLFEEFAIDGRFCISIHDEVRYLVREEDRYRAALALQITNLLTRCMFAYKLGND R1128H-Microrcephaly
 Pan troglodytes (chimpanzee) (1115) WLFEEFAIDGRFCISIHDEVRYLVREEDRYRAALALQITNLLTRCMFAYKLGND H1134R-mtDNA depletion
 Macaca mulatta (rhesus monkey) pol gamma (1107) WLFEEFAIDGRFCISIHDEVRYLVREEDRYRAALALQITNLLTRCMFAYKLGND E1136K- mtDNA depletion
 mus pol gamma (1096) WLFEEFAIDGRFCISIHDEVRYLVREEDRYRAALALQITNLLTRCMFAYKLGND R1138C-PEO
 rat pol gamma (1095) WLFEEFAIDGRFCISIHDEVRYLVREEDRYRAALALQITNLLTRCMFAYKLGND 1142R→W SNP
 Xenopus pol gamma (1087) WLFAYDIDGRFCISIHDEVRYLVHSHKDRYRAALALQITNLLTRCMFASRLGIQD 1143E→G SNP, PEO, ...
 Drosophila pol gamma (1025) WLMG---SHVRFCLSFHDELRYLVKKEELSPKAALAMHITNLMTRSFVSRIGIQD 1146R→C SNP
 scyeast pol gamma mip1 (875) YIIKKYNLEARLCISIHDEIRFLVSEKDKYRAAMALQISNIWTRAMFCQQMGINE c.3482+2t>c(splice)-
 S. pombe pol gamma (871) HLIKYYLEARLSLTVHDEVRYLVSSDKKYRVAFALQVANLWTRAFFCQRLGINE Alpers
 Neurospora pol gamma (924) YLTRRNLACRLATVHDEIRYLAEPDKYRVAMALQIANLWTRVMFAQQVGIQD M1163R-Alpers
 Consensus (1156) WLFEEFAIDGRFCISIHDEVRYLVREEDRYRAALALQITNLLTRCMFAYKLGND F1164I-PEO
 F1164L

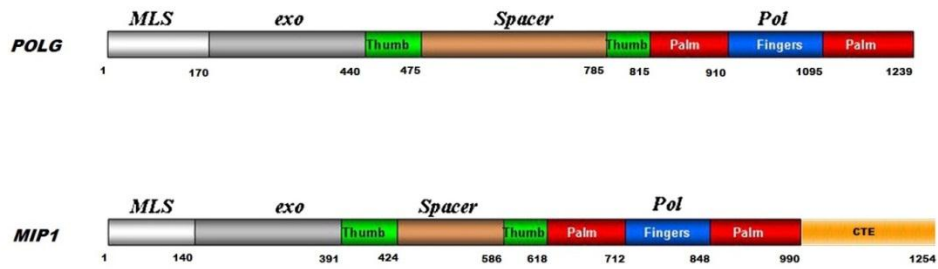
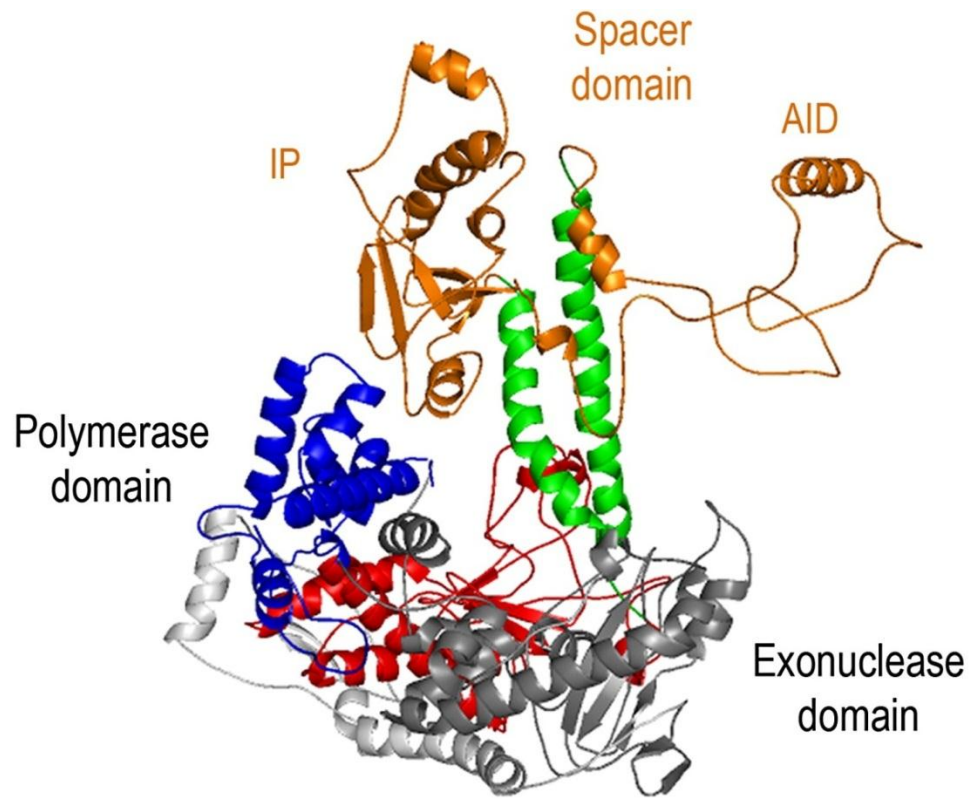
1211 * * * * * * * * * * 1265

hum pol gamma aa seq (1173) LPQSVAFFSAVDIDRCLRKEVTMDCKTPSNPTGMERRYGIPQGEALDIYQIIELT L1173fs stop- Alpers
 Pan troglodytes (chimpanzee) (1170) LPQSVAFFSAVDIDRCLRKEVTMDCKTPSNPTGMERRYGIPQGEALDIYQIIELT S1176L-PEO
 Macaca mulatta (rhesus monkey) pol gamma (1162) LPQSVAFFSAVDIDRCLRKEVTMDCKTPSNPTGMERRYGIPQGEALDIYQIIELT D1184N-PEO
 mus pol gamma (1151) LPQSVAFFSAVDIDQCLRKEVTMDCKTPSNPTGMERRYGIPQGEALDIYQIIELT R1187W-?
 rat pol gamma (1150) LPQSVAFFSAVDIDQCLRKEVTMDCKTPSNPTGMERYKYGIPQGEALDIYQIIELT K1191N-Alpers
 Xenopus pol gamma (1142) VPQSVAFFSAVDIDKCLRKEVTMDCKTPSNPNMSEKRYGIPQGEALDIYQILKVT K1191R-Myocerebrohep.
 Drosophila pol gamma (1077) LPMVAFFSSVEVDTVLRKECTMDCKTPSNPHGLRIGYGIQPGQSLSVAEATEKA D1196N-Myopathy
 scyeast pol gamma mip1 (930) LPQNCAFFSQVDIDSVIRKEVNMDCITPSNKTAI PHGEALDINQLLDRSNSKLGK T1199 ins.a-ataxia, PEO...
 S. pombe pol gamma (926) LPQSVAFFSAVDIDHVLRRDVKMDCVTPSNKPVI PPGEELTIESVLEKLEQSGQS G1205A-hearing loss,
 Neurospora pol gamma (979) LPQSCAFFSAVDIDHVLRRKEVDMDCITPSNPIAHGESIDIFQIEKGGDAKLD failure to thrive, &
 Consensus (1211) LPQSVAFFSAVDID CLRKEVTMDCKTPSNPTGMERRYGIPQGEALDIYQIIELT ETC complex defic.
 Y1210fs-1216stop-
 Alpers
 c.3643+2t>c(splice)-
 Alpers

		1266		1320	
			*	*	
hum pol gamma aa seq	(1228)	KGSLEKRSQPGP	-----		
Pan troglodytes (chimpanzee)	(1225)	KGSLEKRSQPGP	-----		1230S→F SNP
Macaca mulatta (rhesus monkey) pol gamma	(1217)	KGSLEKRSQPGP	-----		1236Q→H SNP, PEO
mus pol gamma	(1206)	KGSLEKRSQPGP	-----		Alpers
rat pol gamma	(1205)	KGSLEKRSQPGP	-----		
Xenopus pol gamma	(1197)	KGVV	-----		
Drosophila pol gamma	(1132)	GSNDVSQWDWIKKS	-----		
scyeast pol gamma mip1	(985)	PNLDIDSKVSYAYNYREPVFEEYNKSYTPEFLKYFLAMQVQSDKRDVNRLEDEY	-----		
S. pombe pol gamma	(981)	LEPTEIQCFVDVKATTSABEITEEDKKNIAYLKAQAFY	-----		
Neurospora pol gamma	(1034)	DSIVPQSQYAPRLENIPYTPRVFVMQRLRERAEAGDHQAFLEFRFIRAQITNSDEEL	-----		
Consensus	(1266)	KGSLEKRSQPGP	-----		
		1321		1375	
hum pol gamma aa seq	(1240)	-----			
Pan troglodytes (chimpanzee)	(1237)	-----			
Macaca mulatta (rhesus monkey) pol gamma	(1229)	-----			
mus pol gamma	(1218)	-----			
rat pol gamma	(1217)	-----			
Xenopus pol gamma	(1201)	-----			
Drosophila pol gamma	(1146)	-----			
scyeast pol gamma mip1	(1040)	LRECTSKEYARDGNTAEYSLLDYIKDVEKGKRTKVRIMGSNFLDGTKNADQRI	-----		
S. pombe pol gamma	(1019)	-----			
Neurospora pol gamma	(1089)	KRIIAETRYSDPYGAFSLASNGRVSGNPHQRHAAVHASTKTAAAPSKPSIASRFD	-----		
Consensus	(1321)	-----			
		1376		1430	
hum pol gamma aa seq	(1240)	-----			
Pan troglodytes (chimpanzee)	(1237)	-----			
Macaca mulatta (rhesus monkey) pol gamma	(1229)	-----			
mus pol gamma	(1218)	-----			
rat pol gamma	(1217)	-----			
Xenopus pol gamma	(1201)	-----			
Drosophila pol gamma	(1146)	-----			
scyeast pol gamma mip1	(1095)	RLPVNMPDYPTLHKIANDSAIPEKQLLENRRKKENRIDDENKKLTRKKNTTPME	-----		
S. pombe pol gamma	(1019)	-----			
Neurospora pol gamma	(1144)	SVSQASRIKSVAAGSDEPTIRATKAQGKAMAKASGTKLAASKDITVLNVTIKKKV	-----		
Consensus	(1376)	-----			

		1431		1485
	hum pol gamma aa seq	(1240)	-----	
	Pan troglodytes (chimpanzee)	(1237)	-----	
Macaca mulatta (rhesus monkey)	pol gamma	(1229)	-----	
	mus pol gamma	(1218)	-----	
	rat pol gamma	(1217)	-----	
	Xenopus pol gamma	(1201)	-----	
	Drosophila pol gamma	(1146)	-----	
scyeast pol gamma	mipl	(1150)	RKYKRVYGGRKAFEAFYECANKPLDY	LETEKQFFNIPIDGVIDDVLDKSNYKK
	S. pombe pol gamma	(1019)	-----	
Neurospora pol gamma		(1199)	AAPEMAAVPSTSESSEKSKASATTT	TTTTENATASPSSSSNVDAKKTSKTKPTHK
	Consensus	(1431)		
		1486		1537
	hum pol gamma aa seq	(1240)	-----	
	Pan troglodytes (chimpanzee)	(1237)	-----	
Macaca mulatta (rhesus monkey)	pol gamma	(1229)	-----	
	mus pol gamma	(1218)	-----	
	rat pol gamma	(1217)	-----	
	Xenopus pol gamma	(1201)	-----	
	Drosophila pol gamma	(1146)	-----	
scyeast pol gamma	mipl	(1205)	KPSQARTASSSPIRKTAKAVHSKKL	PARKSSTNRLVELELDITISREY--
	S. pombe pol gamma	(1019)	-----	
Neurospora pol gamma		(1254)	KETEGEFFPSLDDPVIAARLEAVSK	TSPGTRASVAAKLDALASFCHASCCGC
	Consensus	(1486)		

Figure 1.3 3D model of the catalytic subunit of human POLG, POLGA. This structure follows the canonical “right hand” DNA polymerase structure. The exonuclease, linker and polymerase domains are labelled. The “thumb”, “fingers” and “palm” subdomains are highlighted in green, blue and red, respectively. Sequence alignment of Mip1p with other gamma subfamily polymerases has identified these salient features and its approximate location in Mip1p (This figure was adapted with permission from Lee *et al.* 2009).



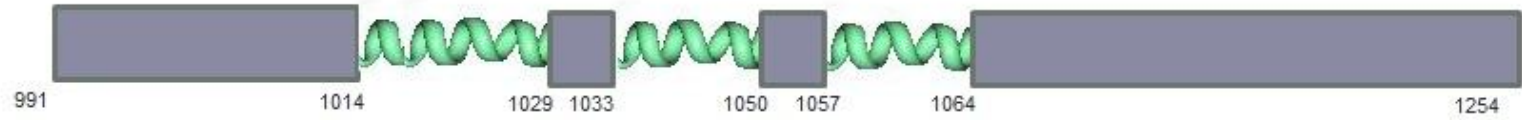
Currently, 3D crystal structures are available for several family A DNA polymerases (Beese *et al.*, 1993, Eom *et al.*, 1996, Kiefer *et al.*, 1998, Doublet *et al.*, 1998), including the human mtDNA polymerase γ (Lee *et al.*, 2009). All follow the canonical “right-hand” model (Figure 1.3, Joyce & Steitz, 1995, Kaguni, 2004, Graciewicz, 2006). The palm subdomain is composed of a DNA binding channel surrounded by polymerase and exonuclease domains (Kaguni, 2004). Thumb and finger subdomains are highly variable among family A DNA polymerases but have been implicated in template strand and dNTP binding (Beese *et al.*, 1993, Polesky *et al.*, 1990, Hu *et al.* 1995).

Gamma polymerases of higher eukaryotes typically exist in a heterooligomeric structure. In *Drosophila melanogaster*, the main catalytic subunit requires an accessory subunit to form a heterodimeric holoenzyme (Oliveira and Kaguni 2009). Alternatively, the human version forms a heterotrimeric holoenzyme made up of a single catalytic subunit (POLGA) complexed with a homodimer accessory subunit (POLGB). The accessory subunit function is essential for mtDNA maintenance and is thought to act by increasing the processivity of the holoenzyme and facilitating recognition of primer RNA during the initiation of mtDNA replication (Iyengar *et al.*, 2002, Carrodeguas *et al.*, 1999, Fan *et al.*, 1999, Carrodeguas and Bogenhagen, 2000). Processivity is defined as the extent of polymerization following a single binding event (Foury, 1992). Curiously, the accessory subunit is notably absent in yeast mitochondria (Lucas, 2004). With consideration of recombination-dependent mtDNA priming (see section 1.6), the accessory subunit may have become dispensable in the evolution of *Ascomycetes*.

Recently, it has been shown that the catalytic subunit of *S. cerevisiae* gamma polymerase, Mip1p, functions as a highly processive monomer *in vitro* (Foury, 1992, Viikov, 2010).

Another glaring difference of note, is the presence of a long 279-residue carboxy terminal extension (CTE) following the polymerase domain in Mip1p not found in higher metazoans (Foury 1989, Figure 1.3). Sequence alignment analysis among fungal mtDNA polymerases show moderate to high conservation of the first 63 residues of the CTE proximal to the polymerase domain (Young, *et al.* 2006) while the remaining 216 residues exhibit very poor conservation. However, alignment of the CTEs of *Saccharomycetales* polymerases displayed moderate to high conservation of the first polymerase proximal 97 residues. Interestingly, secondary structure analysis of the CTE has identified three putative helices, all located within the conserved 97 residues. The first helix is 11 residues in length, starts at Mip1pP1014 and is very hydrophobic and highly conserved. The second helix is 15 residues in length, 13 of which are polar residues, starts at Mip1pN1033 and is moderately conserved (Figure 1.4). The third helix starts at Mip1pY1057, is 7 residues in length, amphipathic and poorly conserved. Although the function of this domain is not yet known, recent analysis of truncation variants has identified regions essential to the fidelity and functionality of the gene. Deletion of the entire 279-residue long CTE (Mip1p Δ 279) resulted in a non-functional Mip1p as seen in the production of ρ^o mutants. However, it was shown that only the first two helices are required for wild-type function of the enzyme. Furthermore, truncation mutant Mip1p Δ 216, in which the 15-residue helix is disrupted, was found to have an error-prone mtDNA polymerase phenotype. Additionally, complete removal of the 15-residue helix in truncation mutant Mip1p Δ 222 complete abrogates Mip1p activity.

Figure 1.4 Secondary structure analysis and identification of two regions within the CTE critical for Mip1p function. Three putative helices are located within the CTE (Young, 2006). Truncation studies have identified two regions: N1033 – E1038 required for mtDNA maintenance and Y1039 – A1049 required for mtDNA fidelity.



mtDNA maintenance



mtDNA fidelity

Therefore, the region spanning Mip1pN1033 – Mip1pE1038 is essential for Mip1p functionality and the region spanning Mip1pY1039 – Mip1pA1049 is required for Mip1p fidelity (Young, 2008, Figure 1.4).

While the divergence of the metazoan mitochondrial DNA polymerase to possess an accessory subunit and yeast mitochondrial DNA polymerase to possess a carboxyl-terminal extension is unclear, the idea of these proteins being derived from the chromosome of the eubacterial progenitor of mitochondria has recently been refuted. Phylogenetic analysis of the A family DNA polymerases suggests that mitochondrial DNA polymerases are phage T-odd phage derived (Filee *et al.*, 2002). The T7 DNA polymerase does require an accessory subunit (thioredoxin) for processivity (Tabor *et al.*, 1987) and fidelity (Kunkel *et al.*, 1994). However, while the catalytic subunits appear related, human POLGB does not structurally resemble thioredoxin, indicating divergent evolution of the two systems (Fan *et al.*, 2006).

1.4 Consequences of mtDNA instability: using Mip1p to model POLG mutations

Recently, genetic analyses of several debilitating and deadly human diseases have focused in on the role that mitochondria play in these diseases. Individuals with these diseases show varying degrees of heteroplasmy – mixtures of wild-type and mutant mitochondria. The severity of the disease generally correlates with ratio of mutated mtDNA to intact mtDNA. Onset of the disease will occur when the mutant load exceeds a certain threshold (Ylikallio *et al.* 2011). The threshold level may differ for different mutations and tissues. Cell culture studies of systems harbouring the A3243G mutation in the mitochondrial gene encoding tRNA^{leu(UUR)}, commonly associated with mitochondrial

encephalomyopathy lactic acidosis and strokes (MELAS) syndrome, show that as little as 10% of wild-type DNA is sufficient to mask the mutant phenotype (Chromyn *et al.*, 1992, King *et al.*, 1992). The uniparental inheritance of mtDNA suggests that mutations may accumulate slowly over successive generations until the threshold is reached. However, recent studies have shown strong purifying selection against mtDNA mutations in transmission of mtDNA through a murine germ line (Fan *et al.*, 2008, Stewart *et al.*, 2008).

Differences in degrees of heteroplasmy, however, may not be the sole determinants for disease expression. The wide range of diseases and severity of disease that arise from a single mutation in mitochondrial DNA suggests that other factors, including genetic background and environmental factors may facilitate the manifestation of the disease (Hughes, 1995). To address the role POLG plays in mtDNA disease, researchers have looked to *S. cerevisiae* to study the effects of disease-related mutations in humans by introducing the equivalent changes into the homologous mitochondrial proteins in yeast (reviewed in Barrientos, 2003 and Rinaldi *et al.*, 2010).

Mutations introduced into Mip1p that affect mtDNA replication have been assessed for their role in disease. Unfaithful replication of mtDNA is thought to be involved in ageing and cancer (Ishikawa, 2008, Veatch *et al.*, 2009, Desler, 2011). The accumulation of reactive oxygen species (ROS) during oxidative phosphorylation causes mutations in the mitochondrial genome and thus has a direct impact on energy production of the cell, which is thought to be a focal point in ageing (Desler, 2011). Additionally, these mutations could be the result of a defective mitochondrial DNA polymerase as seen in the premature ageing of mice expressing such a polymerase (Trifunovic *et al.*, 2004).

Veatch *et al.* (2009) consider an alternate model in which mtDNA plays a more indirect role in ageing through a phenomenon they called “Loss of Heterozygosity” (LOH). LOH occurs when a functional dominant allele suppressing the recessive defective allele is lost. In this model, nuclear genomic instability resulting in ageing and cancer (Brown, 1997) are caused by a decrease in iron-sulfur clusters (ISC) required by nuclear DNA maintenance proteins. These ISCs are produced in the mitochondria by nuclear-encoded proteins, for which, import is fuelled by the electric membrane potential of the mitochondrial membrane created by the oxidative phosphorylation machinery. With the machinery partially encoded on mtDNA, faithful replication of mtDNA is required to maintain ISC-levels in the cell. Thus, destabilization of mtDNA over time results in LOH.

Perhaps, the most studied Mip1p-modelled human disorder is progressive external ophthalmoplegia (PEO) (Van Goethem *et al.*, 2001, Stuart *et al.*, 2006). PEO is characterized by multiple point mutations and deletions in mtDNA. Physiologically, PEO causes a progressive weakening of eye muscles to the point of paralysis (reviewed in Cohen and Naviaux, 2010). The resulting inability to look left or right can be accompanied by dysphagia, weakness of limb and neck muscles as well as depression. Interestingly, POLG point mutations associated with the disease can be found throughout the protein (Figure 1.2). Equivalent point mutations in Mip1p have been shown to result in ρ^-/ρ^0 phenotypes characteristic of a mtDNA disorder. Other POLG mutations have been implicated in diseases such as Parkinson’s Disease (Luoma, 2007, Hudson 2007, Tiangyou 2006, Davidzon, 2006) Alpers’ syndrome (Stumpf, 2010).

The yeast model has also been used to assess ways to rescue particular forms of POLG. The effect of increasing deoxynucleotide triphosphate (dNTP) pool concentrations was assessed in yeast harbouring equivalent mutations to two different POLG variants associated with PEO *in vivo* (Baruffini *et al.*, 2006). It was shown previously that increasing dNTP pool concentrations can rescue mtDNA replication in some Mip1p yeast mutants (Lecrenier and Foury, 1995). Baruffini *et al.* hypothesized that one of the PEO-associated mutations, Y955C, caused the polymerase to stall due to decreased affinity for incoming nucleotides and that stalling would be compounded by a local depletion of a particular nucleotide after synthesizing a run of that nucleotide in succession. Increasing dNTP pool concentrations through overexpression of ribonucleotide reductase (*RNR1*) (Di Fonzo *et al.*, 2003, Elledge *et al.*, 1987) or the deletion of the gene for its inhibitor *SML1* (Wang *et al.*, 1997, Zhao *et al.*, 1998) did in fact decrease the occurrence of *petites*, but did not have an effect on the acquisition of erythromycin resistance. It was also noted, that increasing dNTP pool concentrations could also cause a reduction in the formation of *petites* in a yeast strain harbouring a Mip1p variant equivalent to POLG(G268A). The authors hypothesized that this reduction was due to the dNTP pool concentration increasing the DNA repair efficiency of the cell through an unknown mechanism.

Another use for POLG mutant modelling in yeast is in investigating the toxicity of stavudine, a nucleoside reverse transcriptase inhibitor used in highly active antiretroviral therapy for HIV-infected patients. It has been previously reported that, although this treatment has significantly extended the life-expectancy of HIV-infected patients, it could have toxic effects as seen with patients possessing POLG allelic variants

R964C (Yamanaka *et al.*, 2007) and E1143G (Chiappini *et al.*, 2009). When modelled in *S. cerevisiae*, cells with the equivalent mutations showed an increase *petite* frequency compared to wild-type. These findings suggest that patients harbouring these variants are more susceptible to mitochondrial damage from stavudine (Baruffini, 2010).

The use of Mip1p to model POLG mutations has provided researchers with quantifiable data that helps to better understand the clinical manifestations of the disease. However, discrepancies do exist. Szczepanowska *et al.* (2010) found that the equivalent POLG W312R mutation in Mip1p generated severe mutagenic phenotypes that did not agree with the late disease onset of PEO by this POLG variant seen in a previous study (Horvath, 2006). This could be reflective of the differences in the nature of human and yeast mtDNA as well as the constituents that comprise the mtDNA replisome.

1.5 Yeast mitochondrial nucleoid

Generally speaking, mitochondrial genomes are surrounded by a matrix of proteins termed the nucleoid. There are multiple copies of mtDNA within each nucleoid. These protein components serve to maintain, replicate and transcribe mtDNA, as well as act as heritable units in aiding transmission of mtDNA into newly formed buds during mitosis (reviewed in Chen and Butow, 2005). Not surprisingly, mtDNA polymerase gamma is a vital component in the nucleoid complex. The human mitochondrial nucleoid is approximately 70 nm in diameter, compared to 400 nm in diameter for *S. cerevisiae* (Chen & Butow, 2005). While they share the same core functions, mitochondrial nucleoids in some species, may provide extra functions (Table 1). For example, human mitochondrial nucleoids contain the DNA helicase, TWINKLE, and the DNA POLG

accessory subunit, POLGB. Neither of these proteins is present in the mitochondrial nucleoid of *S. cerevisiae* (Lucas, 2004). Conversely, *S. cerevisiae* mitochondrial nucleoid proteins include aconitase and Ilv5p, which in addition to playing a role in maintaining mtDNA, also participate in the Krebs's cycle and branched chain amino acid synthesis respectively (For a comprehensive list yeast mitochondrial nucleoid components see Nosek, 2006). This dynamic nature of the nucleoid implies that interactions among its constituents, in particular, mitochondrial DNA polymerase, may not apply universally, and functions within this complex are dependent on species and metabolic requirements (see section 1.4.2).

The human mitochondrial genome exists as a circular double-stranded DNA (dsDNA) molecule, 16.5 kb in length (Spelbrink 2010, Holt *et al.* 2007; Chen & Butow, 2005). It encodes 2 ribosomal RNAs, 22 tRNAs and 13 polypeptides that form parts of the oxidative phosphorylation machinery. The mitochondrial genome of *Saccharomyces cerevisiae*, however, is 85 kb in length and exists mainly as linear tandem repeats with a small portion existing in a circular monomeric dsDNA form (Williamson, 2002, Maleszka, 1991). It encodes the same RNA products and an overlapping collection of proteins that include Var1p of the mitochondrial ribosome. While both molecules encode a similar set of products, the yeast genome contains considerably more mobile genetic elements than its metazoan counterpart.

1.5.1 Mitochondrial DNA packaging

Eukaryotic nuclear DNA (nucDNA) is packaged by histone proteins (H2A, H2B, H3 and H4) that form an octamer (nucleosome) and bind DNA by wrapping it around the

octamer (Kishimoto, et al., 2006). This action compacts the nucDNA and protects it from nucleolytic degradation and, in addition, acts as a transcriptional regulatory mechanism. The periodic wrapping of nucDNA around the histones has been demonstrated by DNA footprinting studies using micrococcal nuclease, which digests nucDNA into a series of fragments that correlate to the nucleosome repeat of 160 bp (Lohr *et al.*, 1977, Miyakawa *et al.*, 2008). To elucidate whether mtDNA contains a similar structure the same DNA footprinting assay was carried out, but no such pattern was discernable (Miyakawa *et al.*, 2008). The authors of that study suggested two possible reasons why no such structure was seen in mtDNA nucleoids. First, mitochondrial nucleoid proteins may bind along the contours of mtDNA uniformly rather than at intervals as was seen with nucDNA. Alternatively, the positioning of the mitochondrial nucleoid proteins protecting mtDNA may be irregular. With no discernable structure it is difficult to predict the exact interactions occurring between the nucleoid proteins and mtDNA.

In *S. cerevisiae*, the mitochondrial nucleoid protein identified as the major mtDNA packaging protein is Abf2p (Sia *et al.*, 2009). Abf2p belongs to a group of proteins classified as high mobility group (HMG) proteins (Diffley and Stillman, 1991) which contain a DNA-binding conserved structural motif (Stros *et al.* 2007). Recently, HMG-box proteins in the nucleus have been implicated in remodelling the nucleosome (reviewed in Travers, 2003). The tight binding of the histone octamer prevents access to the DNA template from transcription and replication machinery. Loosening of the chromatin structure through DNA bending and unwinding by HMG-box proteins can affect the strength of the nucleosome interaction. Thus, modulation of the nucleosome by HMG-box proteins may play an important role in regulation of transcription and

replication. Abf2p is composed of two HMG-boxes (Sia *et al.*, 2009). It has been shown to bind, bend and compact mtDNA (Stigter, 2004, Friddle *et al.*, 2004). There is an estimated one Abf2p molecule per 15 – 30 bp of mtDNA (Diffley and Stillman, 1992). In addition to DNA packaging, Abf2p is linked to the regulation of mtDNA copy number. Moderate over-expression of Abf2p (2 – 3-fold) increased the amount of mtDNA by 50 – 150% (Zeleneya-Troitskaya *et al.*, 1998). Surprisingly, Abf2p was also correlated with an increase in nucDNA replication. Increased amounts of Abf2 resulted in increased cell size and proliferation compared to wild-type cells (Blank *et al.* 2008).

Other HMG-box proteins found to be associated with the yeast mitochondrial nucleoid are mitochondrial aconitase, Aco1p and mitochondrial branched-chain amino acid synthesis protein, Ilv5p. Interestingly, both proteins are bi-functional (Chen and Butow, 2005). In addition to being involved in mtDNA maintenance, Aco1p converts citrate into isocitrate in the Krebs cycle. During active respiration, the expression of Aco1p is robust and has been suggested to provide mtDNA with extra protection against ROS (Chen and Butow, 2005). Ilv5p binds to mtDNA with levels proportional to the mitochondrial concentration of Ilv5p (Macierzanka *et al.*, 2008) and is suggested to play a role in parsing the mitochondrial nucleoid (Chen and Butow, 2005).

1.5.2 The dynamic mitochondrial nucleoid: evolutionary tinkering and nucleoid remodelling

Based on the discoveries of bi-functional proteins such as Aco1p and Ilv5p, Kucej and Butow (2008) have alluded to the idea of *evolutionary tinkering* with respect to mitochondrial nucleoids. They suggested that the original endosymbiont's nucleoid-

associated proteins have been lost and compensated for by seizing host cell proteins during the course of evolution and thus reinventing the mitochondrial nucleoid. In yeast, Ilv5p plays roles in the branched-chain amino acid synthesis pathway and mtDNA maintenance. However, this particular pathway is absent in higher metazoans. Furthermore, the *Escherichia coli* ortholog of Ilv5p has been shown to complement the branched-chain amino acid synthesis function of Ilv5p but not the mtDNA stabilization or parsing defects in *S. cerevisiae ilv5Δ* mutants (Bateman, 2002), suggesting that the nucleoid must undergo remodelling in response to metabolic cues (Kucej *et al.*, 2008). Analysis of Ilv5p levels via sucrose-gradient-centrifugation of mitochondrial extracts from cells grown with or without amino acids reveals that Ilv5p co-fractionates predominantly in the nucleoid fraction in the latter condition (Kucej *et al.*, 2008). Therefore, Ilv5p is actively recruited to the nucleoid under amino-acid starvation conditions.

Conversely, when using the sucrose-gradient-centrifugation method to compare Aco1p levels in the presence of glucose or a non-fermentable carbon source, no significant difference in nucleoid:matrix ratios were observed (Kucej *et al.*, 2008). Although Aco1p is not actively recruited to the nucleoid under those conditions, previous results from DiRisi *et al.* using DNA-microarrays found an increase in *ACO1* expression during growth in the presence of glycerol (1997). Thus, under conditions that require increased protection of mtDNA from reactive oxygen species from oxidative phosphorylation, *ACO1* expression increases, thereby increasing the amount of Aco1p localizing with the nucleoid without actively recruiting it.

Hsp60p is an essential mitochondrial protein. It is a chaperonin that facilitates the proper folding of mitochondrial proteins (Cheng, *et al.*, 1989) and has been shown to interact with mtDNA (Kaufman *et al.*, 2000). The proposed function of Hsp60 in the nucleoid is to assist in division (Kaufman *et al.*, 2003). Under the same conditions used to analyze Aco1p, Hsp60p exhibited higher levels in the nucleoid than the matrix when grown in the presence of glucose. Therefore, Hsp60p is recruited to the nucleoid when grown in the presence of glucose.

While some nucleoid proteins are able to associate and disassociate from the nucleoid, the mtDNA molecule itself does not have that dynamic ability. Gilkerson *et al.* in 2008 used cybrid cell lines to generate mtDNA heteroplasmy with wild-type and mtDNA isolated from human patients with Kearns-Sayre syndrome. These experiments gave visual evidence for the “genetic autonomy” of nucleoids. Using deletion-specific FISH probes for visualizing mtDNA from the 2 different cell lines, the authors found very little colocalization of signals (Gilkerson *et al.*, 2008). This indicates that there are low levels of mtDNA mixing between adjacent nucleoids and thus, mitochondrial nucleoids maintain genetic autonomy. These findings are consistent with the “faithful nucleoid” model proposed by Jacobs *et al.* (2000).

The recruitment and difference in localization of nucleoid proteins show that the nucleoid is a dynamic entity that modulates its composition in response to metabolic and environmental cues. Nucleoid proteins surround, interact and protect mtDNA, which in itself is a static entity that lacks the ability to diffuse into neighbouring nucleoids.

1.5.3 Mitochondrial nucleoid tethering

Studies have noted the appearance of mitochondrial nucleoids as discrete punctate structures that colocalize with mtDNA seemingly along the inner mitochondrial membrane (Berger and Yaffe, 2000, Dimmer *et al.* 2005, Hobbs *et al.*, 2001, Meeusen and Nunnari 2003, Chen and Butow, 2005, Kucej, 2008). It was proposed that the nucleoid not only functions to maintain, transcribe and replicate mtDNA, but also acts as a segregative unit involved in the transmission of the mitochondrial genome during mitotic division (reviewed in Lipinski, 2010, and Solieri, 2010). The position of the nucleoid along the inner mitochondrial membrane is likely attributed to a protein complex tethering it to the inner membrane. This tether may include a complex of Mdm10p, Mdm12p, Mdm34p, Mgm101p and Mmm1p (Meeusen and Nunnari, 2003, Kornmann, 2010, Spelbrink, 2010). This complex, curiously, is implicated in several different processes. First, it was noted that Mgm101p is a DNA-binding protein required for the repair of oxidatively-damaged mtDNA (Meeusen, 1999) which colocalizes with mitochondrial outer membrane proteins: Mdm10p, Mdm12p, and Mdm34p (Boldogh *et al.*, 2003) and immunoprecipitates with Mmm1p (Meeusen and Nunnari 2003, Youngman *et al.*, 2004, Kornmann, 2010). Mdm10p, Mdm12p and Mdm34p act as anchors in the outer membrane, while Mmm1p, originally thought to be a mitochondrial outer membrane protein, has now been re-categorized as an endoplasmic reticulum membrane protein that colocalizes with this complex (Meeusen and Nunnari, 2003, Kornmann, 2010). Together these components comprise a three-membrane spanning complex (TMS, Kornmann, 2010) that resides in close proximity to mitochondrial attachment points of the cell's actin skeleton (Meeusen and Nunnari, 2003). Interestingly,

this complex is not associated with every nucleoid in the mitochondria and not every nucleoid is actively replicating mtDNA. BrdU-labelling of mtDNA shows that the complex is associated only with nucleoids involved in actively replicating mtDNA (Meeusen and Nunnari, 2003). Altogether, these findings support the idea that the TMS is involved in tethering the mitochondrial nucleoid to cell division machinery. Furthermore, other studies have shown that the association of the endoplasmic reticulum with mitochondria at these loci also provide routes for phospholipid biosynthesis, cellular calcium-ion regulation, and mitochondrial protein import (Kornmann 2010).

1.6 Mechanisms of mitochondrial DNA replication

The exact mechanism for mitochondrial DNA (mtDNA) replication has not yet been completely elucidated. However, upon discovery of *ori* replication sequences in the human mitochondrial genome, it became tentatively accepted that mtDNA replication was initiated through RNA-priming by human mitochondrial RNA polymerase, mtRPOL (Chang and Clayton, 1985, Tiranti *et al.*, 1997) and continued through asymmetric strand displacement mechanism (reviewed in Graciewicz, 2006 and Holt, 2009).

Several *ori* sequences are found scattered throughout the *S. cerevisiae* mitochondrial genome. However, only a handful of these sequences are thought to be functional (reviewed in Solieri, 2010). The detection of RNA priming ability by the yeast mitochondrial RNA polymerase, Rpo41p, led researchers to believe that mtDNA replication was primed by Rpo41p at these sites and may undergo a mechanism similar to that of humans (reviewed in Solieri, 2010 and Lecrenier and Foury, 2000). However, a study conducted by Fangman *et al.* (1990) showing the ability of yeast cells to stably

maintain an *ori* devoid 35 bp mitochondrial genome suggests that Rpo41p-primed mtDNA synthesis is not the sole process in charge of replicating mtDNA. This idea was further supported by the ability of yeast cells to stably maintain mtDNA in an Rpo41p null background (Fangmann *et al.*, 1990, Lorimer *et al.*, 1995).

Recent studies have implicated, Mhr1p, a mitochondrial ATP-driven protein involved in homologous pairing of single-stranded and double-stranded DNA, its functionally redundant brother Cce1p, and Ntg1p, a mitochondrial protein involved in DNA repair and recombination, in priming mitochondrial DNA synthesis through recombination (Ling and Shibata, 2004, Phadnis *et al.*, 2006, Lipinski 2010). The proposed recombinant priming model involves the creation of a double-stranded break in the circular monomeric *S. cerevisiae* form of mtDNA by Ntg1p followed by the pairing of a resulting single strand to an adjacent intact circular monomer (reviewed in Solieri, 2010). The discovery of linear concatameric and circular forms of mtDNA led researchers to propose that recombinant-dependent initiation of mtDNA replication is followed by rolling circle replication (Maleszka *et al.*, 1991). Of note, it was discovered that the linear concatameric form of mtDNA was preferentially localized in the mother cells while the circular monomer form was the major species in buds (Ling and Shibata, 2002).

1.7 Goals of this study.

Despite differences in mtDNA structure, mitochondrial nucleoid dynamics and mitochondrial DNA polymerase structure, *S. cerevisiae* is still considered to be a very good model for investigating human mitochondrial diseases stemming from mtDNA

dysfunction. Although, the exact mechanism of mtDNA replication is still not completely understood, 3D structures of related polymerase gamma proteins have given insight into the functional components of each respective protein and their mechanisms. However, the 3D structure of Mip1p has yet to be elucidated and the role of the CTE remains enigmatic. The purpose of this study was to examine the CTE. The goals were:

1. Create a strategy to introduce point mutations into an essential region of the CTE for *in vivo* studies.
2. Quantitate *in vivo* and *in vitro* the effects of the resulting changes.
3. Determine essential residues of the CTE.

CHAPTER TWO: STRAINS, MATERIALS AND METHODS

2.1 Strains, vectors and primers

Table 2.1 *Saccharomyces cerevisiae* and bacterial strains used in this study.

Strain	Genotype	Reference
S150	<i>MATa leu2-3,112 his3-Δ1 trp1-289 ura3-52 MIP1[Σ]^a HAP1</i>	Steger <i>et al.</i> , 1990
RI001	[S150] <i>URA3</i>	Young, 2008
RI002	[S150] <i>SpHIS5^b</i>	This study
RI003	[S150] <i>SpHIS5, mip1::CORE</i>	This study
RI004	[S150] <i>mip1RI034G</i>	This study
RI005	[S150] <i>Δmip1::trp1-dsRED</i>	Young, 2006
RI006	[S150] <i>mip1E1036G::CaURA3</i>	This study
<i>Escherichia coli</i> DH5α	<i>supE44 lacU169 (80 lacM15) hsdR17 recA1 endA1 gyrA96 thi-1 relA1</i>	Hanahan, 1983

^a *MIP1[Σ]* allele derived from *Saccharomyces cerevisiae* strain Σ1278b

^b *HIS5* protrophic marker cloned into a region of the genome immediately downstream of the *MIP1* locus

Table 2.2 Vectors used in this study

Vector	Selection	Gene for overexpression	Reference
pMIP Σ	<i>amp^R</i> , <i>LEU</i>	<i>MIP1[Σ]</i> ^a	Young, 2006
pGSKU ^b	<i>amp^R</i> ,		Storici, 2003
pKT128 ^c	<i>amp^R</i>		Sheff and Thorn, 2004
pKT209	<i>amp^R</i>		Sheff and Thorn, 2004
pN1033G	<i>amp^R</i> , <i>LEU</i>	<i>mip[Σ]N1033G</i>	This study
pR1034G	<i>amp^R</i> , <i>LEU</i>	<i>mip[Σ]R1034G</i>	This study
pL1035G	<i>amp^R</i> , <i>LEU</i>	<i>mip[Σ]L1035G</i>	This study
pE1036G	<i>amp^R</i> , <i>LEU</i>	<i>mip[Σ]E1036G</i>	This study
pD1037G	<i>amp^R</i> , <i>LEU</i>	<i>mip[Σ]D1037G</i>	This study
pE1038G	<i>amp^R</i> , <i>LEU</i>	<i>mip[Σ]E1038G</i>	This study
pMIP1F3 ^d	<i>amp^R</i>		Young, 2006

^a Plasmids harbouring *MIP1[Σ]* and *mip1[Σ]* variants have their respective genes under the control of a *GALI* promoter and are C-terminally tagged with 6xHIS and HA epitopes.

^b Template DNA for amplification of CORE cassette. CORE cassette contains: I-*SceI* HO endonuclease under control of *GALI* promoter, *KIURA3*, and *KanMX4*

^c Template DNA for amplification of *SpHIS5*.

^d Linearized vector used as template DNA for *in vitro* analysis of Mip1p mutants.

Table 2.3 Primers used in this study

Primer	Sequence (5' → 3')	Template DNA	Description
EGMutFwd	TACTCCAGAGTTCTTAAAATATTTTCTTGCGA TGCAAGTCCAGTCAGATAAGCGCGATGTGAA TCGGCTAGGTGATGAGT ^a	-	Forward primer used to amplify fragment 1 of the <i>mip1E1036G</i> mutation
EGMutRev	CCGGCGGGGACGAGGCAAGCTAAACCTAAG CGTATTCTTTGGATGTACACTCCCGCAGATAC TCATCACCTAGCCGATTC ^b	-	Reverse primer used to amplify fragment 1 of the <i>mip1E1036G</i> mutation
UniCaURA3Fwd	GTTTAGCTTGCCTCGTCC	pKT209	Forward primers used to amplify fragment 2 of the <i>mip1E1036G</i> mutation
CTEFcnRev	CGCTGGCCGGGTGACCCGGCGGGGACGAGG CAAGCTAAACCTAAGCGTATTCTTTGGATGT ACACTC	pKT209	Reverse primers used to amplify fragment 2 of the <i>mip1E1036G</i> mutation
Mip1DSBFwd	TCTTAAAATATTTTCTTGCGATGCAAGTCCAG TCAGATAAGCGCGATGTGTAGGGATAACAGG <u>GTAATTTGGATGGACGCAAAGAAGT</u> ^c	pGSKU	Forward primer used to amplify the CORE ^d cassette with homology to the <i>MIP1</i> ^e locus for recombination
Mip1DSBRev	TCGACATCCTTTATATAGTCTAGGAGGCTGT ACTCTGCAGTGTTCATCTTCGTACGCTGCA GGTCGAC	pGSKU	Reverse primer used to amplify the CORE cassette with homology to the <i>MIP1</i> locus for recombination
Mip1SpHIS5Fwd	GAAATTTGGTTGAGCTGGAAAGGGACATTAC TATTTCTAGAGAGTACTAGTCGCCCGTACATT	pKT128	Forward primer used to amplify <i>SpHIS5</i> with

	TAGCCCATACA		homology to the area of the genome immediately downstream of the <i>MIP1</i> locus for recombination
Mip1SpHIS5Rev	TAATGTGCTGTATATATAAATAACAAATGCGA AAGCTAATGCAGATTTTGCTGGATGGCGGCG TTAGTATCGAAT	pKT128	Forward primer used to amplify <i>SpHIS5</i> with homology to the area of the genome immediately downstream of the <i>MIP1</i> locus for recombination
Mip1DSBVerFwd	CCTTGAGGCAAGGCTTTGCATTTC	<i>MIP1</i> locus	Forward primer used to verify the insertion of the CORE cassette into the <i>MIP1</i> locus and used for sequencing possible mutants
Mip1DSBVerRev	TCCTTCTTTCTCCTGTTCTCCAGC	<i>MIP1</i> locus	Reverse primer used to verify the insertion of the CORE cassette and downstream region of the <i>mip1</i> locus
Mip1SpHIS5VerFwd	TGTATGGTGGCAGGAAGGCATTTG	Immediately following the <i>MIP1</i> locus	Forward primer used to verify the insertion of <i>SpHIS5</i> immediately downstream of the <i>MIP1</i> locus
Mip1SpHIS5VerRev	ACACATCGCCTCCAGAAAGTG TTC	Immediately following the	Reverse primer used to verify the insertion of <i>SpHIS5</i> immediately downstream of the <i>MIP1</i>

		<i>MIPI</i> locus	locus
DSBMutFwd	GTATCACAATATGCCTATAACTACAGAGAAC CTG	<i>MIPI</i> locus and overlap extension of mutant DNA fragments	Forward primer used to amplify the 5' mutant DNA fragment and for overlap extension PCR of the 5' and 3' mutant DNA fragments
DSBMutRev	CCATAATACGTACTTTAGTCCTTTTGCCCTTC	<i>MIPI</i> locus and overlap extension of mutant DNA fragments	Reverse primer used to amplify the 3' mutant DNA fragment and for overlap extension PCR of the 5' and 3' mutant DNA fragments
N1033GFM	GCGCGATGT <u>GGT</u> TCGGCTAGAAG	<i>MIPI</i> locus	Forward primer to amplify the 3' N1033G Mutant DNA fragment. To be used with DSBMutRev
N1033GRM	CTTCTAGCCGA <u>ACC</u> ACATCGCGC	<i>MIPI</i> locus	Reverse primer to amplify the 5' N1033G Mutant DNA fragment. To be used with DSBMutFwd

R1034GFM	GCGCGATGTGGGTAAGCTAGAAGATG	<i>MIPI</i> locus	Forward primer to amplify the 3' N1033G Mutant DNA fragment. To be used with DSBMutRev
R1034GRM	CATCTTCTAGCTT <u>ACCC</u> CACATCGCGC	<i>MIPI</i> locus	Reverse primer to amplify the 5' N1033G Mutant DNA fragment. To be used with DSBMutFwd
L1035GFM	CGATGTGAATCGGGGTGAAGATGAGTATC	<i>MIPI</i> locus	Forward primer to amplify the 3' N1033G Mutant DNA fragment. To be used with DSBMutRev
L1035GRM	GATACTCATCTT <u>CACCC</u> GATTACATCG	<i>MIPI</i> locus	Reverse primer to amplify the 5' N1033G Mutant DNA fragment. To be used with DSBMutFwd
E1036GFM	GTGAATCGGCTAGGTGATGAGTATCTG	<i>MIPI</i> locus	Forward primer to amplify the 3' N1033G Mutant DNA fragment. To be used with DSBMutRev
E1036GRM	CAGATACTCAT <u>CACCT</u> AGCCGATTAC	<i>MIPI</i> locus	Reverse primer to amplify the 5' N1033G Mutant DNA fragment. To be used with DSBMutFwd

D1037GFM	GATGTGAATCGGCTAGAG <u>GGTT</u> GAGTATCTG	<i>MIPI</i> locus	Forward primer to amplify the 3' N1033G Mutant DNA fragment. To be used with DSBMutRev
D1037GRM	CAGATACTCA <u>ACCT</u> CTAGCCGATTCACATC	<i>MIPI</i> locus	Reverse primer to amplify the 5' N1033G Mutant DNA fragment. To be used with DSBMutFwd
E1038GFM	GGCTAGAAGAG <u>GGT</u> GTATCTGCGGG	<i>MIPI</i> locus	Forward primer to amplify the 3' N1033G Mutant DNA fragment. To be used with DSBMutRev
E1038GRM	CCCGCAGATAC <u>ACCT</u> CTTCTAGCC	<i>MIPI</i> locus	Reverse primer to amplify the 5' N1033G Mutant DNA fragment. To be used with DSBMutFwd

^a. Double underlined sequence indicates mutation.

^b **Bold sequences** indicate a stop codon.

^c Underlined sequence highlights the target for the I-SceI HO endonuclease.

^d CORE Cassette (See Table 2.2)

2.2 Media

For growth of *Escherichia coli* cells, Luria-Bertani medium (LB, 1% Bacto-tryptone, 0.5% Bacto-yeast extract, 1% NaCl and 1.5% Bacto-agar for solid media) was used. To select for successful transformations of plasmid DNA into *E. coli* cells, LB media was supplemented with Ampicillin at concentrations of 50 µg/mL for liquid LB and 100 µg/mL for LB plates.

General growth of yeast cells was done in Yeast Peptone Dextrose media (YPD, 1% yeast extract, 2% peptone, 2% dextrose and 2% Bacto-agar for solid media). To select for respiratory competent mutants, Yeast Peptone Glycerol media was used (YPG, 1% yeast extract, 2% peptone, 2% glycerol and 2% Bacto-agar for solid media). Growth of RI005 used for constructing plasmids was carried out in YP10D broth (1% yeast extract, 2% peptone, 10% dextrose). Synthetic complete (SC, 0.67% Difco® yeast nitrogen base, 4% dextrose, all amino acids and 2% Bacto-agar for plates) media, pH 5.6, was used to grow and select for yeast strains based on the auxotrophic markers used. SC-TRP, SC-LEU, SC-HIS, and SC-URA media denotes SC media containing all amino acids except tryptophan, leucine, histidine, or uracil, respectively. To select against cells containing a uracil marker, SC+FOA (SC media supplemented with 1 mg/mL 5-Fluororotic acid, Zymo Research, Irvine, CA) was used. YPD+G418 (200 mg/L, Sigma-Aldrich, St. Louis, MO) was used to select for successful integration of the CORE cassette. Sporulation media (1% potassium acetate, 0.1% bacto-yeast extract, 0.05% dextrose, 2% bacto-agar) was used following sexual mating between ρ^+ and ρ^0 cells.

For induction of Mip1p, yeast cells harbouring the overexpression vector were first grown in liquid Synthetic media lacking leucine and containing raffinose as the sole carbon source (SRaff-LEU, 0.67% Difco® yeast nitrogen base, 4% (w/v) raffinose, all amino acids except leucine). Cells were induced by the addition of 3x Yeast Peptone Galactose medium (3xYPGal, 3% yeast extract, 6% peptone, 6% galactose) to the SRaff-LEU cultures. For induction of the I-SceI HO endonuclease in the *in vivo* mutant cloning strategy, synthetic complete media with galactose was used (SC2Gal, 0.67% Difco® yeast nitrogen base, 2% galactose, all amino acids). Assessment of erythromycin resistance by yeast strains was carried out on yeast glycerol media supplemented with erythromycin (YG-Er, 2% yeast extract, 3% glycerol, 50 mM potassium phosphate, pH 6.5, 4 g/L erythromycin, Sigma-Aldrich, St. Louis, MO).

2.3 Methods

2.3.1 Isolation of yeast genomic DNA

Yeast cells were grown overnight in 5 mL of YPD at 30°C with shaking. The following day, 3 mL of culture was centrifuged at 5,000 rpm for 2 minutes at room temperature. The supernatant was discarded via aspiration and the cell pellet was washed with 1 mL of 1.2 M sorbitol with 50 mM EDTA, pH 8.5. The resulting pellets were combined and resuspended in 1 mL 1.2 M sorbitol with 50 mM EDTA, pH 8.5 and 0.113 mg/mL lyticase (Sigma-Aldrich, St. Louis, MO). This mixture was incubated at 30°C for 1 hour with shaking. Next, the mixture was centrifuged at 5,000 rpm for 2 minutes at room temperature. The supernatant was aspirated and the cell pellet was resuspended in 1 mL solution of 50 mM EDTA, pH 8.5, and 0.2% SDS and incubated at 65°C for 15

minutes. 100 μ L of 5 M potassium acetate was added to the now lysed cells and the mixture was chilled on ice for 10 minutes. Following this, the mixture was centrifuged at 13,000 rpm for 10 minutes at 4°C. 500 μ L of the supernatant was then aliquoted into 2 microfuge tubes. To each 500 μ L aliquot, 1 mL of 95% ethanol (EtOH) and 75 μ L of 3 M sodium acetate were added and mixed. These tubes were then incubated at -20°C for at least 1 hour. The ethanol-DNA mixture was centrifuged at 13,000 rpm for 15 minutes at 4°C. The supernatant was discarded and the DNA pellet was washed with 1 mL ice-cold 70% EtOH. The supernatant was discarded, and the DNA pellet was then air-dried. Finally, each pellet was resuspended in 30 μ L of TE buffer (10 mM Tris-Cl, pH 8.0, 1 mM EDTA) with RNaseA (50 μ g/mL, Sigma-Aldrich, St. Louis, MO).

2.3.2 Transformation of yeast strains

Electroporation of yeast strains was adapted from Thompson *et al.* (1998). The desired yeast strain was inoculated into YPD for 1-2 days growth at 30°C with shaking. The day of the transformation, the strain was subcultured in the same medium to an OD_{600 nm} of 0.35 and allowed to grow at 30°C with shaking to a final OD_{600 nm} between 1 and 1.5 was reached. Cells were centrifuged at 5,000 rpm for 5 min at room temperature. The supernatant was discarded and the cells were resuspended in 16 mL of 0.1 M lithium acetate (LiAc), 10 mM dithiothreitol (DTT), 10 mM Tris-Cl, pH 7.5, 1 mM EDTA (TE) and incubated at room temperature for 1 hour. The LiAc/DTT/TE treated cells were centrifuged at 5,000 rpm for 5 min at 4°C and washed twice with 16 mL of ice-cold sterile double-distilled water (sdH₂O) followed by one wash with 6.4 mL of 1 M sorbitol. Following the sorbitol wash, cells were resuspended with 54 μ L of 1 M sorbitol and 44 μ L of the cell suspension was aliquoted to fresh microfuge tubes. Purified DNA was

added to the aliquots, mixed and then added to 0.2 cm electroporation cuvettes. Cells were electroporated using the “SC2” setting on the BioRad Micropulser and immediately, but gently, resuspended in 1 mL of 1 M sorbitol. The electroporated cells were centrifuged at 5,000 rpm for 2 minutes and 800 μ L of the supernatant was discarded. The cells were resuspended in the remaining supernatant and plated onto the desired selection media.

Yeast cells were also transformed using the Gietz “High Efficiency Transformation Protocol” (2002). The yeast strain was inoculated in 10 mL of YPD and grown overnight at 30°C with shaking. The cells were subcultured into 50 mL YPD to an $OD_{600\text{ nm}}$ 0.5. These cells were grown at 30°C to an $OD_{600\text{ nm}}$ 2.0 and centrifuged at 5,000 rpm for 2 minutes at room temperature. Next, the cells were washed with 25 mL of sdH_2O and resuspended in 1 mL of sdH_2O . The cell/water suspension was transferred to a microfuge tube and centrifuged at 13,000 rpm for 30 seconds. The supernatant was aspirated and the pellet was resuspended in sdH_2O to a final volume of 1 mL. 100 μ L aliquots of these cells were taken and transferred into fresh microfuge tubes. The aliquots were then centrifuged at 13,000 rpm to remove the supernatant. These pellets were resuspended in 360 μ L of “transformation mix” (240 μ L PEG 3350 50% w/v, 36 μ L 1.0 M LiAc, 50 μ L boiled salmon sperm DNA, 34 μ L of DNA) and incubated at 42°C for 40 minutes. The cells were centrifuged at 13,000 rpm for 30 seconds and the supernatant is aspirated off. The cell pellet was then resuspended in 200 μ L of sdH_2O and plated onto selection media.

2.3.3 Transformation of *Escherichia coli* DH5 α

Electrocompetent *E. coli* DH5 α were prepared by growth to mid-log phase in 1 L of Luria Broth (LB, 10 g Bacto-tryptone, 5 g yeast extract, 10 g NaCl) followed by subsequent washes in ice-cold 10% glycerol. 5 mL of LB starter culture was inoculated from a single *E. coli* DH5 α colony and allowed to grow overnight at 30°C with shaking. The entire starter culture was subcultured into 500 mL of fresh LB and grown to an OD_{578 nm} of 0.5. The culture was then chilled on ice for 30 minutes and centrifuged at 6,000 rpm for 15 minutes at 4°C. Pellets were subsequently washed with 500 mL of ice-cold 10% glycerol. Next, they were washed with 250 mL ice-cold 10% glycerol. Finally, cells were washed with 5 mL of ice-cold 10% glycerol and then resuspended in 500 μ L of 10% ice-cold glycerol and 40 μ L aliquots were transferred to fresh microfuge tubes to be frozen down and stored at -60°C.

Electroporation of electrocompetent *E. coli* DH5 α was carried out using the “Ec1” program of the BioRad Micropulser. The desired amount of DNA was mixed with a 40 μ L aliquot of frozen electrocompetent *E. coli* and transferred to a 0.2 cm electroporation cuvette. The mixture was pulsed and gently resuspended with 1 mL of ice-cold LB. These cells were transferred to a fresh microfuge tube and allowed to recover at 37°C for 1 hour. The cells were centrifuged at 13,000 rpm for 1 minute at room temperature and 900 μ L of supernatant was removed. The cell pellet was resuspended in the remaining supernatant and plated in its entirety onto LB medium with the desired antibiotic for selection.

2.3.4 Creation of *mip1* mutants for *in vivo* studies

2.3.4.1 Mip1p(E1036G) Δ 205

The initial attempt for creating point mutations in the *MIP1* locus took advantage of a previous study that showed the deletion of 205 C-terminal residues has virtually no effect on the functionality of the Mip1p protein (Young, 2006). Two DNA fragments were created via PCR (Figure 2.1). The first DNA fragment contained 40 bp of homology to the *MIP1* locus upstream of residue E1036, the point mutation E1036G, a stop codon following A1049, and sequence upstream of the *CaURA3* marker from plasmid pKT209. It was created by allowing primers EGMutFwd and EGMutRev to anneal at 50°C for 2 minutes followed by extension using Phusion DNA polymerase (New England Biolabs, Pickering, ON) in a 100 μ L reaction. The second DNA fragment was amplified from plasmid pKT209 and contained 40 bp of homology to the 3' end of the first DNA fragment, *CaURA3*, and 40 bp of homology downstream of the *MIP1* locus. This reaction was carried out using Phusion DNA polymerase according to manufacturer's recommendations in a separate 50 μ L reaction using primers EGMutUraFwd and CTEFcRev for the second DNA fragment. These two fragments were then combined in a 1:1 ratio and EtOH precipitated. The resulting DNA pellet was resuspended in 15 μ L sdH₂O and transformed into the S150 strain via electroporation. Selection after the transformation was done on Sc-URA plates at 30°C. Isolates harbouring the E1036G mutation and replacement of the 205 C-terminal residues with *CaURA3* were confirmed via PCR and sequencing.

2.3.4.2 Mip1pR1034G

This strategy for creating point mutations in the *MIP1* locus was adapted from the *delitto perfetto* method designed by Storici *et al.* (2006). It involves the insertion of a CORE (COunterselectable REporter) cassette into the desired genomic locus of the yeast strain through homologous recombination by cellular machinery (Figure 2.2). This cassette contains the gene for an I-*SceI* HO endonuclease under the control of a galactose promoter, an I-*SceI* target site, a *KIURA3* marker, and a *kanMX4* marker (Figure 2.2). The first step was the amplification of the CORE cassette using primers that contain ends homologous to the desired site in the genomic DNA. However, in the case of this study, it was necessary to first introduce a selectable marker immediately proximal to the *MIP1* gene. *SpHIS5* was amplified from pKT128 (Table 2.2) using primers Mip1SpHIS5Fwd and Mip1SpHIS5Rev (Table 2.3). This amplification was carried out using Phusion DNA polymerase in a 100 µL reaction. The *SpHIS5* PCR product was then gel extracted using the Qiaquick® gel extraction kit (Qiagen, Toronto, ON) and eluted in 30 µL of sdH₂O. Transformation of the *SpHIS5* marker in *Saccharomyces cerevisiae* S150 was adapted from the “High efficiency transformation” method outlined by Gietz *et al.* (2002) described above. Selection of transformants was done on Sc-HIS plates. Successful mutants were verified by the presence of a 2185 bp PCR fragment using primers Mip1SpHIS5VerFwd and Mip1SpHIS5VerRev (Table 2.3) on genomic DNA.

Amplification of the CORE cassette was performed using primers Mip1DSBFwd and Mip1DSBRev (Table 2.3). They contain homologous ends such that the CORE cassette replaced an area encoding residues N1033 to A1049 of the *MIP1* gene (Figure 2.1). This amplification, purification and transformation were carried out using

the Gietz method as above with a two notable exceptions. First, the CORE cassette was transformed into a yeast strain harbouring the *SpHIS5* marker described above and grown in Sc-HIS media prior to transformation. Second, the transformants were selected on Sc-URA plates followed by growth on YPD + G418 for selection of the *kanMX4* marker. Finally, PCR confirmation of the insertion yielded a 5.2 kb fragment.

DNA fragments with single point mutations were created using overlap extension polymerase chain reaction (OE-PCR) (Figure 2.2D). This mutagenesis utilizes a 2-step PCR protocol. In the first step, two mutant fragments were created using Phusion high-fidelity DNA polymerase in a 50 μ L reaction:

Fragment 1: DSBMutFwd + XXXXXGRM

Fragment 2: XXXXXGFM + DSBMutRev

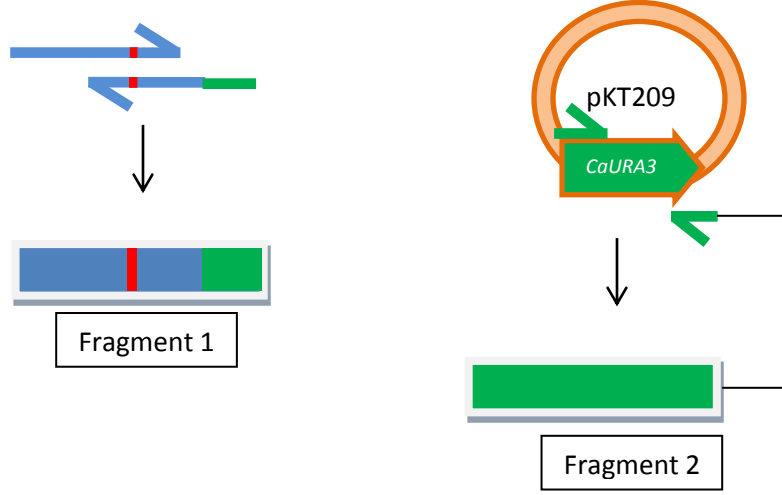
(replace XXXXX with the desired mutation, see Table 2.3)

Both the XXXXXGFM and XXXXXGRM primers contain the desired point mutation and 20 base pairs complementary to each other. The fragments generated from the reaction were then run on a 1.5% agarose gel for 30 minutes at 100V in 1xTris-Acetic Acid-EDTA buffer (1xTAE) and visualized by staining with ethidium bromide (EtBr). The desired bands were purified using the Qiaquick® Gel Extraction Kit (Qiagen). The second step of the protocol involves annealing the two fragments followed by extension and amplification with DSBMutFwd and DSBMutRev (Table 2.3) in a 100 μ L reaction using Vent® DNA polymerase (New England Biolabs, Pickering, ON) to generate a full-length mutant fragment 256-bp in size (Figure 2.2D). This PCR product was then ethanol precipitated and the DNA pellet was resuspended in 30 μ L sdH₂O.

Yeast cells harbouring the CORE cassette and the *SpHIS5* marker (RI003) to be transformed with a *MIP1* mutant DNA fragment were transformed following a procedure outlined by Storici (2003). RI004 cells were grown for 2 days in 10 mL YP10D broth at 30°C with shaking. The cells were subcultured to an OD_{600 nm} of 0.5 in 50 mL YP10D and grown further at 30°C to an OD_{600 nm} of 2.0. These cells were then centrifuged at 5,000 rpm for 5 minutes at room temperature and washed twice with sdH₂O. The cell pellet was resuspended in 50 mL of SC2Gal and incubated 4 hours at 30°C with shaking for the induction of the I-*SceI* HO endonuclease. Next, the cells were centrifuged at 5,000 rpm for 5 minutes at room temperature and washed with 50 mL of sdH₂O and washed again in 5 mL “solution 1” (0.1 M LiAc, 10 mM Tris-Cl, pH 7.5, 1 mM EDTA, Storici, 2003). The cell pellet was then resuspended in 250 µL of solution 1. 50 µL of this cell mixture was aliquoted to fresh microfuge tubes. To each aliquot 20 µL of purified full length mutant fragment and 300 µL of “solution 2” (0.1 M LiAc, 10 mM Tris-Cl, pH 7.5, 1 mM EDTA, in PEG 4000 50% w/v, Storici, 2003) were added and mixed. Transformation mixtures were incubated at 30°C for 30 minutes with gentle shaking and then heat shocked at 42°C for 15 minutes. Cells were pelleted by centrifugation at 5,000 rpm for 2 minutes and the supernatant was removed. The resulting cell pellet was resuspended in 100 µL of sdH₂O and plated in entirety onto a SC+FOA plate. Colonies were then picked onto a second SC+FOA plate and screened for sensitivity to G418. Mutant confirmation was done by PCR from isolated genomic DNA to verify the correct size using primers Mip1DSBVerFwd and Mip1DSBVerRev (Table 2.3) and sequencing.

Figure 2.1 Schematic of the one-step gene replacement cloning strategy employed to create *MIP1E1036G::CaURA3*. **A.** Fragment 1 mutant DNA fragments are created through primer extension of two 60 – 80 nt oligomers harbouring the mutation (in red) and homologous ends to the *MIP1* locus and *CaURA3*. Fragment 2 DNA was created through PCR amplification of the *CaURA3* gene located on pKT128. The 3'-end primer has homology to the area immediately following the *MIP1* locus. **B.** Fragments 1 and 2 were cotransformed by electroporation into S150 where they underwent homologous recombination with each other and with the *MIP1* locus. The result is a genomic replacement of the C-terminal 205 residues of *MIP1* with a *CaURA3* marker and a specific point mutation, E1036G.

A



B

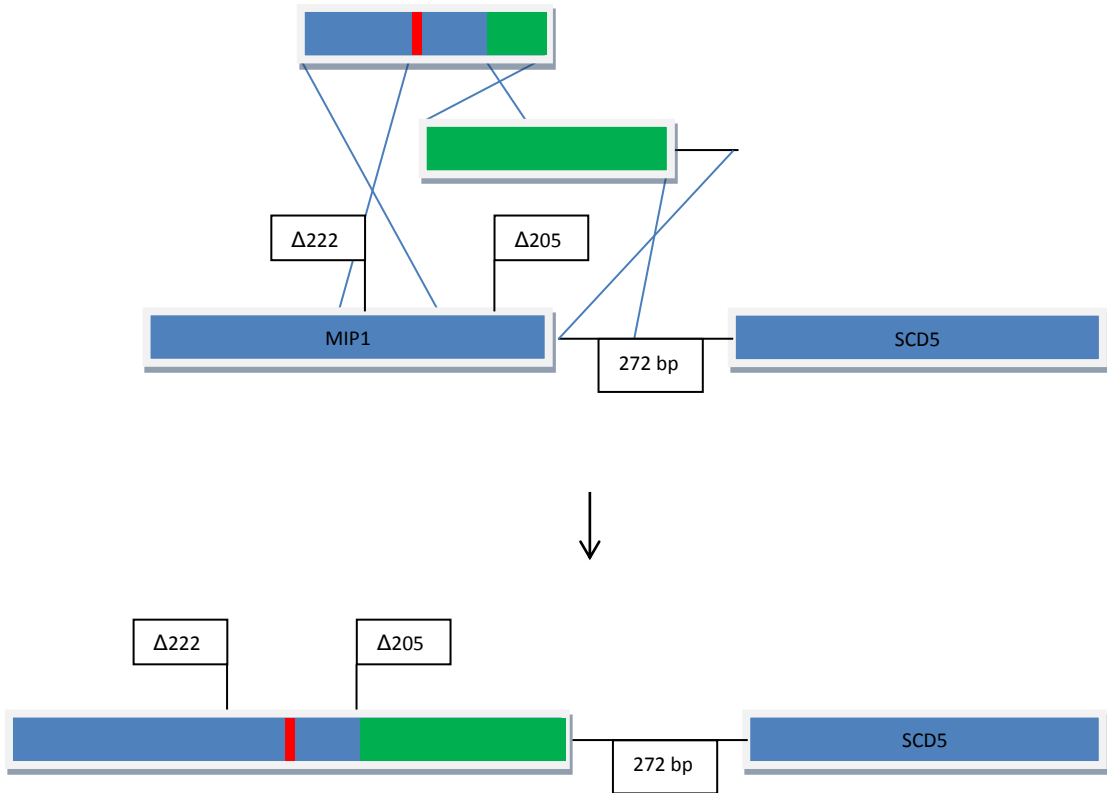
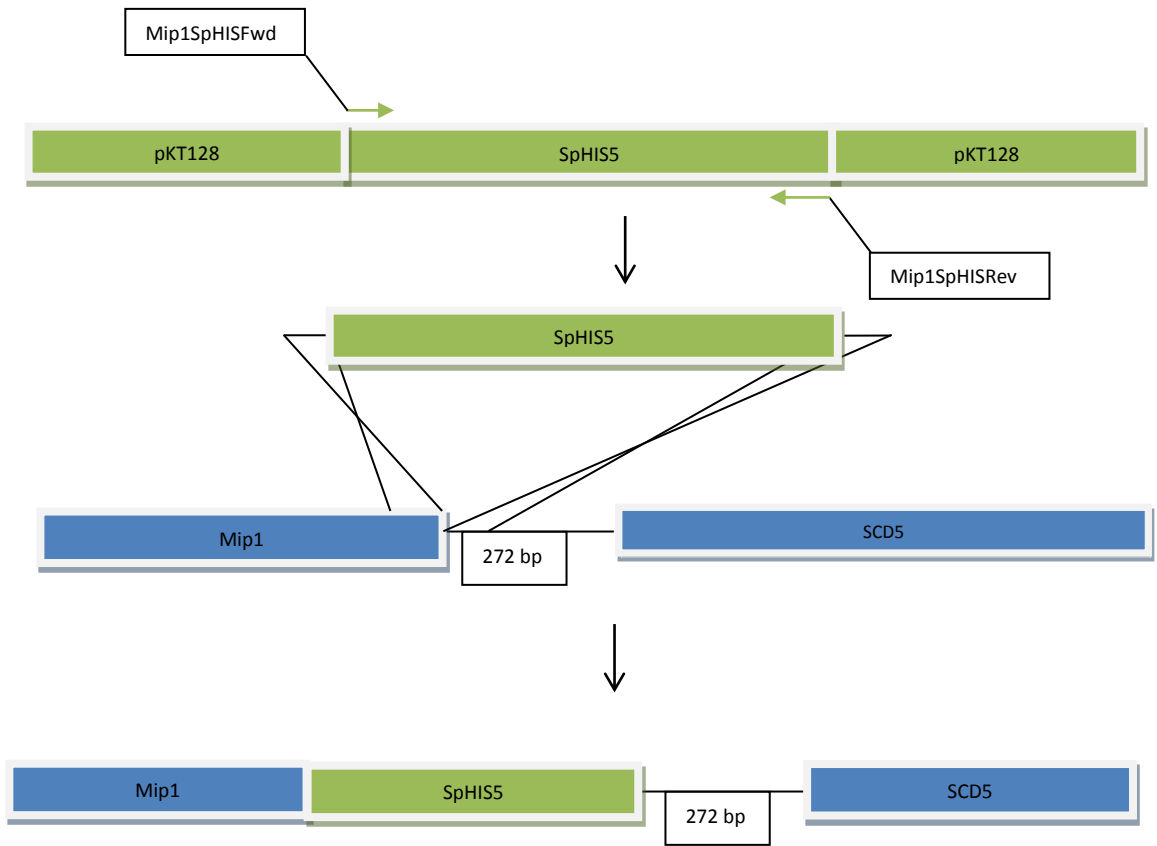


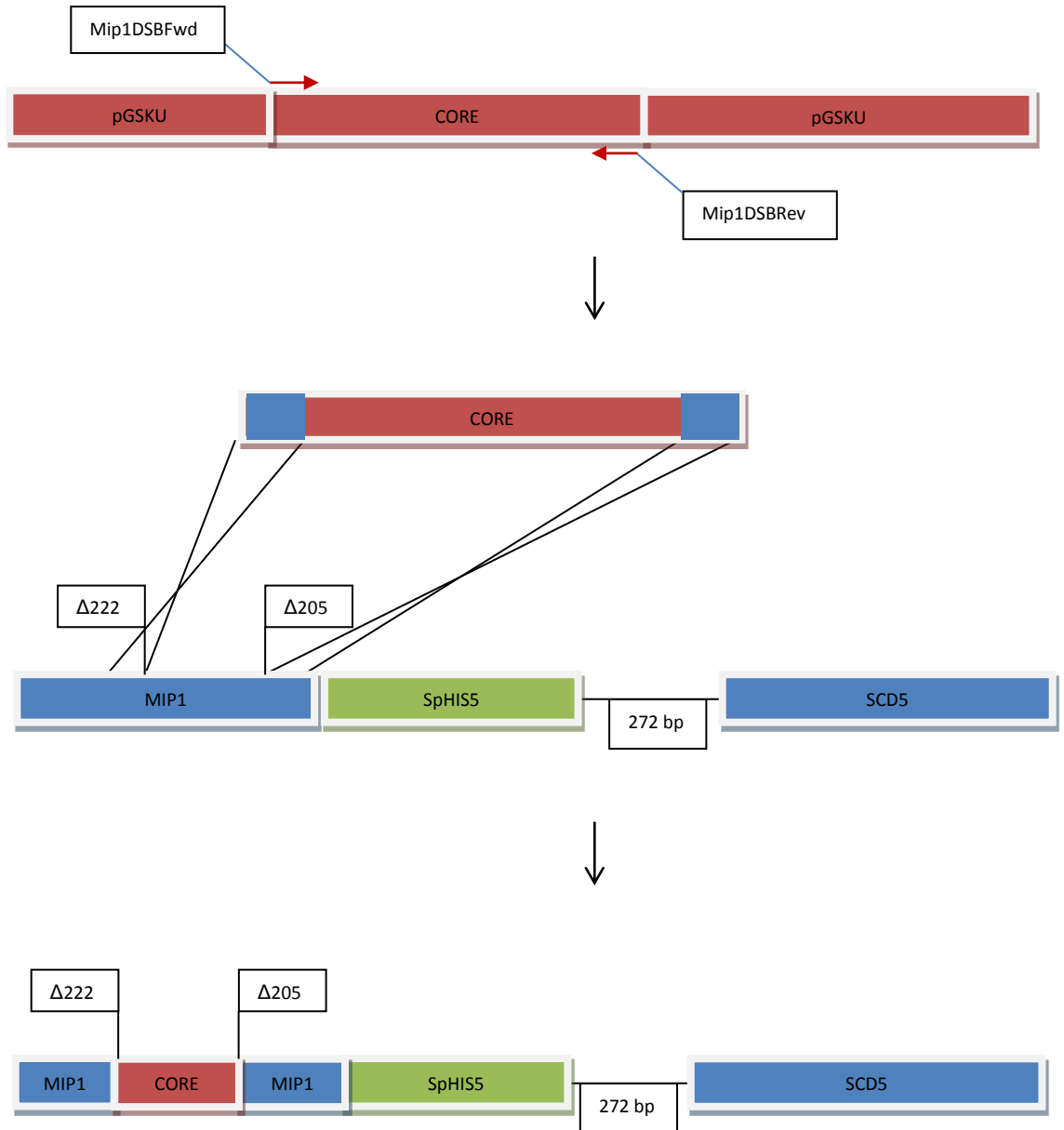
Figure 2.2 Adapted *delitto perfetto* cloning strategy for the creation of Mip1p genomic variants. A. *SpHIS5* auxotrophic marker was PCR amplified by primers Mip1SpHIS5Fwd and Mip1SpHIS5Rev. Mip1SpHIS5Fwd has homology to the C-terminus of the *MIP1* locus. Mip1SpHIS5Rev has homology to the locus immediately proximal to the *MIP1* locus. *SpHIS5* was transformed into S150 via the Gietz “High-efficiency method”. The result is the insertion of the *SpHIS5* auxotrophic marker immediately proximal to the C-terminus of the *MIP1* locus, which allows for the selection of downstream mutations introduced into the *MIP1* locus (RI002). B. Mip1DSBFwd and Mip1DSBRev have homology to the *MIP1* locus and are used to PCR amplify the CORE cassette from pGSKU and specifically target the cassette for replacement of Mip1p residues N1033 – A1049. The CORE cassette was transformed into RI002 using the Gietz “High-efficiency method”. The successful integration of the CORE cassette resulted in strain RI003. C. Full-length mutant DNA fragments were created by overlap extension PCR. First, primers 1 + 4, and primers 2 + 3 were used to PCR amplify the 5’ and 3’ fragments, respectively. The 5’ and 3’ fragments were then gel extracted (not shown) and both were added to a 100 µL reaction mixture containing primers 1 and 2. The result was a 256-bp fragment harbouring homologous to the *MIP1* locus except for a single point mutation. D. The CORE cassette in RI003 was induced by galactose for 4 hours to express the *I-SceI* endonuclease gene. The target sequence located within the CORE cassette is cut by the endonuclease resulting in a double-stranded break. Immediately after, the full-length mutant DNA fragments are transformed into the cell through a modified Gietz “High-efficiency” method. Endogenous cell DNA repair mechanisms are activated by the

double-stranded break and homologously recombine the full-length mutant DNA fragments with high specificity and efficiency.

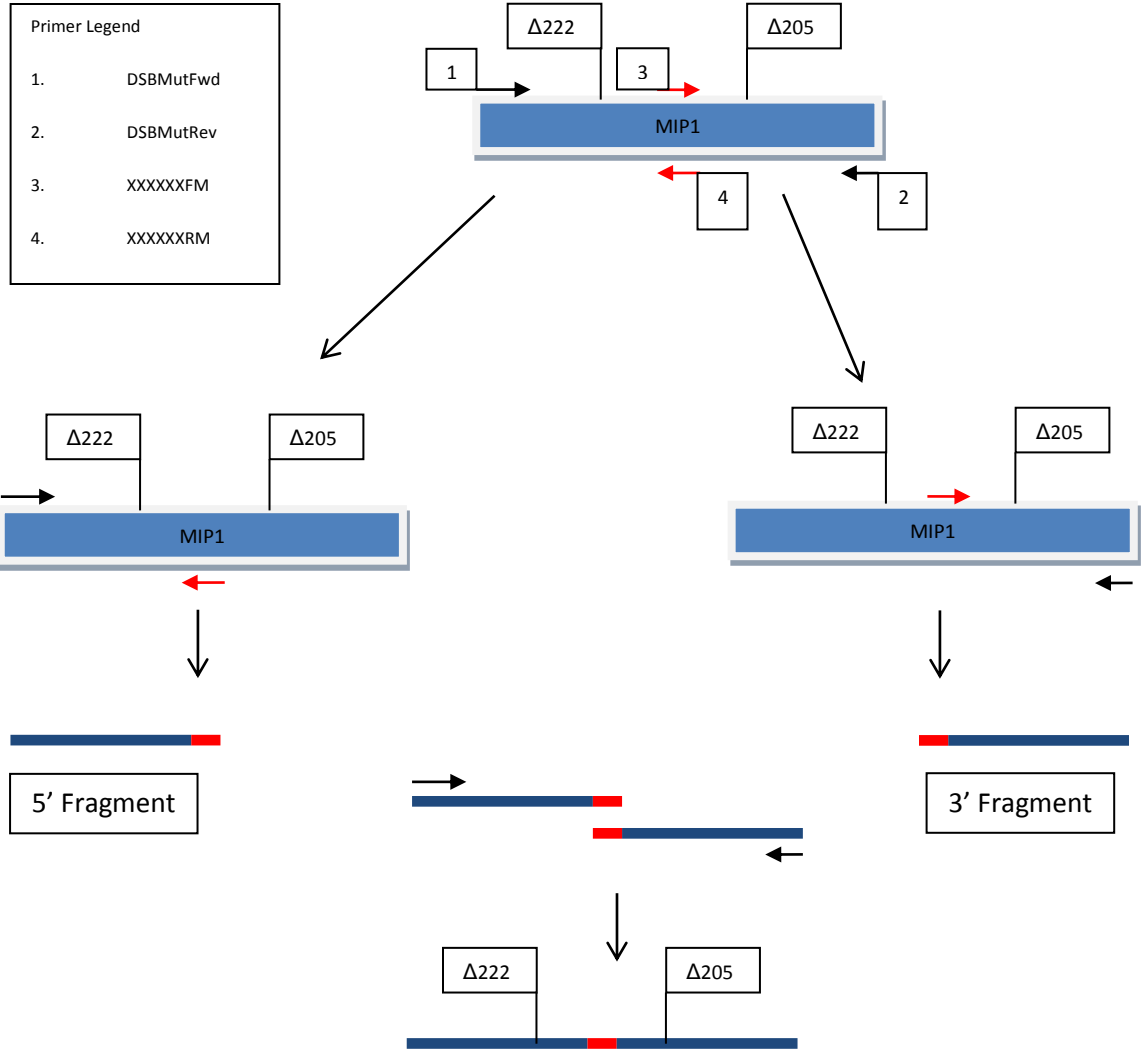
A



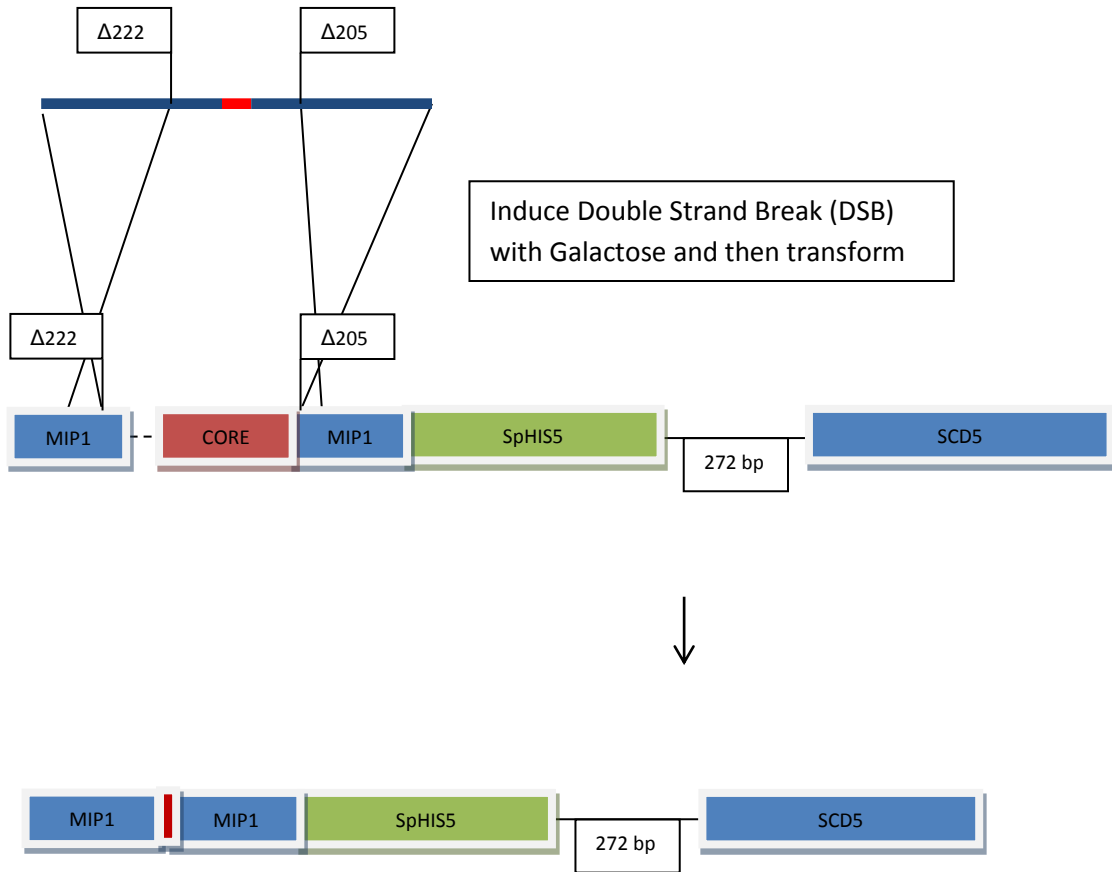
B



C



D



2.3.5 Replenishment of mitochondrial DNA

The insertion of the CORE cassette into the *MIP1* locus results in the loss of respiratory competence of the cell and depletion of mitochondrial DNA (mtDNA). To replenish mtDNA in the yeast cell following the replacement of the CORE cassette with a DNA fragment carrying a single point mutation, the strain was mated with another strain that is isogenic except for the absence of the point mutation and the presence of an auxotrophic marker. In this study, RI001 ([S150] *URA*⁺ *leu*⁻, *trp*⁻, *his*⁻, ρ ⁺) was used to mate with the mutant strain ([S150] *ura*⁻, *leu*⁻, *trp*⁻, *HIS*⁺, ρ ^o). Both strains were *MATa* and therefore had to undergo natural mating-type switching. RI001 and the mutant strain were grown separately overnight, each in 5 mL of YPD at 30°C with shaking. 1 mL of each culture was centrifuged at 5,000 rpm for 2 min and the supernatant was discarded. The cell pellets were resuspended in 1 mL of YPD and an OD_{600 nm} reading was taken. 1 mL of the mutant yeast strain was combined with RI001 such that the amount of RI001 cells in the mixture equalled 1/100th that of the mutant strain. This mixture was then topped up to 10 mL with YPD and grown for 2 days at 30°C with shaking to allow for mating-type switching and mating between the strains. A sample of the mating mixture was spotted onto a glass slide and viewed under oil-immersion microscopy for the presence of “shmooing” which is indicative of yeast sexual mating. 1 mL of the mating mixture was then centrifuged at 5,000 rpm for 2 minutes at room temperature. The supernatant was discarded and the cells were washed twice with sdH₂O, followed by resuspension in 200 μ L of sdH₂O and plating onto Sc-HIS-URA plates. After approximately 3 days of growth on Sc-HIS-URA, cells were scraped from plates and washed with sdH₂O into a microfuge tube and centrifuged at 5,000 rpm for 2 minutes at

room temperature. The cell pellets were then resuspended again in 200 μ L sdH₂O, plated onto sporulation media and grown at 30°C. Samples were taken from the plate over the course of 1 week and viewed under a microscope for the presence of asci. Plates with spore bearing asci were scraped and washed with 1 – 2 mL sdH₂O into a microfuge tube. These tubes were then centrifuged at 5,000 rpm for 2 minutes. The asci pellet was resuspended in 1 mL asci lysis buffer (0.1 M phosphate buffer, pH 7.5, 0.036 M β -mercaptoethanol, 400 μ g/mL lyticase). This suspension was incubated at 30°C for 2 hours and then centrifuged at 13,000 rpm for 2 minutes at 4°C. The lysed asci pellet was then washed twice with ice-cold sdH₂O, resuspended in 200 μ L of ice-cold sdH₂O and plated onto Sc-HIS media. These plates were incubated at 30°C for 3 days or until the appearance of His⁺ colonies. To determine whether or not the cells were respiratory competent, they were picked immediately following the appearance of on Sc-HIS onto YPG media.

2.3.6 Respiratory competence

Respiratory competence was measured according to a method first described by Ogur *et al.* (1957) and adapted by Young *et al.* (2006). Yeast cells were grown in YPG broth for 48 hours to ensure 100% respiratory competence prior to the experiment. On day 0, these cells were diluted down to an OD_{600 nm} of 0.01 in 15 mL YP10D broth for studies conducted at 30°C and an OD_{600 nm} of 0.16 in 15 mL YP10D broth for studies conducted at 37°C. Also, ~100 cells were plated onto YPD plates and allowed to grow at 30°C for 3 days. Every 24 hours, broth cultures from 30°C and 37°C cultures were diluted down to an OD_{600 nm} of 0.01 and 0.16, respectively. After 24, 72, and 96 hours, ~100 cells were plated onto YPD plates in duplicate and allowed to grow for 3 days at 30°C. Next,

each plate was overlaid with 2,3,5-triphenyl tetrazolium chloride (TTC, Sigma-Aldrich, St. Louis, MO) top agar (1% Bacto-agar, 0.067 M phosphate buffer, pH 7.0, 0.1% TTC) and allowed to sit in the dark at room temperature for at least one hour. Plates were then scored with red colonies representing respiratory competent cells and white colonies representing respiratory incompetent cells (Ogur, 1957).

2.3.7 Erythromycin resistance

The erythromycin resistance assay was conducted according to the protocol outlined by Young *et al.* (2006). Yeast cells were grown on YPG media and then inoculated in 30 mL of a 1:1 mixture of YPG:YPD overnight. 1×10^9 cells were plated onto YG-Er media in duplicate and a set of dilutions were also plated onto YPG media to determine the actual number of respiratory competent cells plated on YG-Er media.

2.3.8 Construction of mutant vectors for overexpression

To construct *MIP1* variant vectors for over-expression and *in vitro* analysis, plasmids were assembled in a $\Delta MIP1$ mutant (RI005). Full length mutant DNA fragments (described above, see Figure 2.2D) were transformed along with linearized and dephosphorylated pMIP Σ via electroporation (described above, see section 2.3.2). Prior to transformation, pMIP Σ was linearized with *PstI* (New England Biolabs, Pickering, ON) and dephosphorylated with Antarctic Phosphatase (New England Biolabs, Pickering, ON) according to manufacturer's specifications. Using cellular machinery, the linearized and desphosphorylated pMIP Σ vector undergoes homologous recombination with the full-length mutant DNA fragment to produce a circular plasmid with the desired mutation. Selection for cells containing these plasmids was done on Sc-TRP-LEU.

Isolation of potential mutant plasmids was performed using the “smash and grab” method (Hoffman and Winston, 1987) followed by transformation of the resulting DNA via electroporation into *Escherichia coli* DH5 α (described above). The cells growing on Sc-TRP-LEU plates following the transformation of RI005 with linearized and dephosphorylated pMIP Σ and full length mutant DNA fragments were scraped into a microfuge tube and centrifuged at 5,000 rpm for 2 minutes. The supernatant was aspirated off and the remaining pellet was resuspended in 200 μ L smash and grab lysis buffer (2% TritonX-100, 1% SDS, 100 mM NaCl, 10 mM Tris-Cl, 1 mM EDTA). 200 μ L of phenol:chloroform and 0.3 grams of 0.45 mm glass beads were added to the cells. The tube was sealed with parafilm and vortexed vigorously for 2 minutes. The tubes were then centrifuged at 13,000 rpm for 10 minutes. The aqueous layer was transferred to a fresh microfuge tube. To this tube, 95% EtOH was added at 3x the volume of the aqueous layer and 3 M sodium acetate, pH 5.2 was added at 1/10th the volume of the aqueous layer. This mixture was vortexed and incubated at -20°C overnight. The following day, the extracted DNA from the smash and grab was centrifuged 13,000 rpm for 15 minutes and washed with ice-cold 70% EtOH. The DNA pellet was air dried and resuspended in 30 μ L TE + RNaseA. 3 μ L of this DNA was then used to transform *E. coli* DH5 α by electroporation and plated onto LB+AMP. Plasmids were purified from potential *E. coli* isolates using the Qiagen Plasmid Mini Kit (Qiagen, Toronto, ON)

2.3.9 Induction

Induction of Mip1p variants was carried out following transformation of the overexpression vector into RI001 via electroporation described above (see section 2.3.2). RI001 cells harbouring the overexpression vector were selected on Sc-LEU plates. After

3 days growth at 30°C, these cells were scraped into a microfuge tube and centrifuged at 5,000 rpm for 2 minutes and resuspended in Sc-LEU media to a total volume of ~750 µL. 200 µL of sterile glycerol was added to the tube and vortexed. Next, 200 µL were aliquoted into fresh microfuge tubes and stored at -60°C. One aliquot was thawed at room temperature and used to inoculate 50 mL of Sc-LEU media. This culture was grown overnight at 30°C with shaking. The next morning, the starter culture was centrifuged at 5,000 rpm for 5 minutes at room temperature and resuspended in 50 mL of SRaff-LEU and grown for 9 hours at 30°C with shaking. This culture was subcultured into 500 mL of SRaff-LEU to an OD_{600 nm} of 0.1 and grown for 9 hours or to an OD_{600 nm} between 1 and 2 at 30°C with shaking. 250 mL of 3xYPGal were added to the culture and it was allowed to continue incubating at 30°C with shaking for another 5 hours. Induced cells were centrifuged at 6,000 rpm for 10 minutes at 4°C. The cell pellets were resuspended in 2 mL TG media (50 mM Tris-Cl, pH 8.0, 30% glycerol) and aliquoted into microfuge tubes. The wet weight of each aliquot was determined and the tubes were stored at -60°C.

2.3.10 Isolation of mitochondrial membrane fractions

Between 1 to 2 g of wet weight induced yeast cells were thawed on ice and centrifuged at 5,000 rpm for 2 minutes. The supernatant was aspirated off and the cell pellets were resuspend in an equivalent volume of yeast breaking buffer (YBB, 0.65 M sorbitol, 0.1 M Tris-Cl, pH 8.0, 5 mM EDTA, 0.2% Bovine Serum Albumin, (BSA), 1 mM Phenylmethanesulfonylfluoride, (PMSF)) to cell wet weight (i.e. 1.5 g of cells were resuspended in 1.5 mL of YBB). This mixture was transferred into a 15 mL Falcon tube and the microfuge tubes were rinsed with 2 volumes of YBB and transferred to the Falcon tube. 3 volumes of 0.45 mm glass beads were added to the YBB/cell mixture and

the tube was vortexed for 1 minute followed by cooling on ice for an additional minute. This process was repeated 5 more times to ensure lysis of the yeast cells. The tube was then centrifuged at 3,000 rpm for 5 minutes at 4°C, the supernatant was transferred to fresh microfuge tubes and referred to as “supernatant 1”. 2.2 volumes of YBB were added to the cell/glass bead pellet and the vortex-ice procedure was repeated 3 more times. The tube was centrifuged again at 3,000 rpm for 6 minutes at 4°C. This supernatant was transferred to fresh microfuge tubes and referred to as “supernatant 2”. Supernatant 1 was centrifuged at 12,000 rpm for 8 minutes at 4°C and the supernatant obtained from this step was transferred to new microfuge tubes and referred to as “supernatant 3”. Supernatant 2 and supernatant 3 were centrifuged at 12,000 rpm for 8 minutes at 4°C and their supernatants were discarded. The pellets from supernatants 1, 2 and 3 were washed with 500 µL SEM buffer (250 mM sucrose, 1 mM EDTA, 10 mM MOPS, pH 7.5). Following the wash, these tubes were resuspended in 500 µL SEM and centrifuged at 3,500 rpm for 4 minutes at 4°C. The resulting supernatants were combined and centrifuged at 12,000 rpm for 8 minutes at 4°C. The supernatants were discarded. For every 1.2 grams wet weight of cells, 0.6 mL of hypotonic lysis buffer (20 mM MOPS, pH 8.5, 3 mM β-mercaptoethanol, 1 mM PMSF, 1 µg/mL leupeptine) was used to resuspend the pellets into a single microfuge tube. The total volume of the suspension was estimated with a p1000 Pipetman™ (Gilson). Next, the suspension was subjected to homogenization by passage through a 27 ½ gauge needle 11 times followed by 6 cycles of vortexing for 1 minute followed by icing for 1 minute. This homogenization protocol was repeated one more time and hypotonic lysis buffer with 4 M NaCl at 1/10th of the volume previously measured was added. The suspension was subjected to the

homogenization protocol 2 more times and the slurry was loaded onto a sucrose gradient (250 μ L 60% sucrose w/v, 250 μ L 55% sucrose w/v, 2.25 mL 18% sucrose w/v in 20 mM Tris-Cl, pH 7.4, 0.5 mM EDTA, 5 mM β -mercaptoethanol). The gradient was centrifuged at 60,000 rpm for 1 hour at 4°C in a Beckman TLA 100.3 rotor. Fractions at the 60% - 55% interface were taken in 75 μ L aliquots. 3 μ L of each fraction was transferred to a fresh microfuge tube for Bradford analysis (Sigma-Aldrich, St. Louis, MO) and 12 μ L of each fraction was combined with 12 μ L of 2x SDS PAGE sample buffer (Sambrook *et al.* 2001) for Western Blot analysis (see below). The remaining ~60 μ L of fraction was combined with 50 μ L of sterile glycerol and mixed vigorously. 11 μ L aliquots were made and stored at -60°C.

2.3.11 Western blotting

12% SDS-PAGE gels were made according to Sambrook *et al.* (2001). Samples containing undiluted fractions combined with an equal volume of 2x SDS-PAGE loading buffer were loaded into the well of the SDS-PAGE gel and run for 1 hour and 54 minutes at 100 V.

Proteins separated in the SDS-PAGE gel were transferred overnight at 10 V in 4°C onto nitrocellulose membrane as described in the protocol outlined in Sambrook *et al.* (2001). Membranes were Ponceau S stained to confirm the transfer of proteins and then washed with 1x Tris-Buffered Saline (1x TBS, 50 mM Tris-Cl, pH 7.4, 150 mM NaCl). The ladder positions on the membrane were marked with a pencil and the blot was cut along the 37-kDa molecular weight band. Both pieces were blocked in 1x TBS/6.5% skim milk for 1 hour. The top piece of the membrane was then incubated with a 1:1000

dilution of Anti-HA Tag mouse monoclonal antibody (Applied Biological Material Inc., Richmond, BC) in 1x TBS/6.5% skim milk/0.2% Tween-20 for 1 hour. The bottom piece was incubated in a 1:1000 dilution of Anti-Tim17p rabbit polyclonal antibody (a gift from K. Hell, Universität Munchen) in 1x TBS/6.5% skim milk/0.2% Tween-20 for 1 hour. Next, both pieces were washed twice with 1x TBS/0.3% TritonX-100 followed by washing twice with 1x TBS. The secondary antibody used for the top part of the blot was a 1:3000 dilution of Anti-mouse IgG –Alkaline phosphatase polyclonal antibody (Sigma-Aldrich) in 1x TBS/6.5% skim milk. The secondary antibody used for the bottom part of the blot was a 1:6000 dilution of Anti-rabbit IgG – Alkaline phosphatase polyclonal antibody (Sigma-Aldrich) in 1x TBS/6.5% skim milk. Wash steps were repeated and the membranes were soaked in 10 mL of 1x CDP star assay buffer (New England Biolabs, Pickering, ON) and rinsed several times with 1 mL of a 1:100 dilution of CDP star substrate in 1x CDP star assay buffer. Western Blot signals were detected and relatively quantified using Fluorchem 8900 and AlphaEaseFC software (Alpha Innotech Corporation).

2.3.12 Non-radioactive *in vitro* DNA polymerase assay

10 μ L *in vitro* polymerase reactions consisted of digoxigenin-11-dUTP (DIG-11-dUTP, Roche Diagnostics, Mannheim, Germany), hexanucleotides (Roche), deoxynucleotides, REact 3 buffer (Invitrogen, Burlington, ON), *Eco*R1-linearized pMIP1F3 plasmid, aphidicholin (Sigma-Aldrich, St. Louis, MO) and isolated mitochondrial membrane fractions containing over-expressed Mip1p variants (described previously). A 10x deoxynucleotide mix was created from the following: 0.0875 mM DIG-11-dUTP, 0.9125 mM dTTP, and 1 mM each of dATP, dGTP and dCTP in 10 mM

Tris-Cl, pH 7.5. A working stock of aphidicolin was made by diluting a 10 mg/mL in DMSO stock solution to 1 mg/mL in sdH₂O. Mip1p variant containing fractions were diluted to a concentration of 2 mg/mL with a sucrose/glycerol/ β -mercaptoethanol mix (100 μ L 55% sucrose, 100 μ L glycerol, 0.34 μ L β -mercaptoethanol). Linearized pMIP1F3 plasmid was boiled for 10 minutes and cooled on ice prior to the start of the reaction. 1 μ L of 1x REact 3 buffer was combined with 0.5 μ L of 1 mg/mL aphidicolin, 1 μ L of 10x hexanucleotide mix, 1 μ L of 10x deoxynucleotide mix, 2 μ L of 2 mg/mL Mip1p variant containing fraction and 1 μ L and pre-incubated at either 30°C or 37°C for 15 minutes to allow the variants to acclimate to the temperature. To start the reaction, 675 ng of linearized and boiled pMIP1F3 DNA was added to the mixture. Over the course of the reaction incubated at 30°C or 37°C, 2 μ L samples were taken at 2.5, 5, 10, and 15 minutes and combined with 6 μ L stop solution (24.25 mM EDTA in 10 mM Tris-Cl, pH 8.5). 1 μ L from each time point was then spotted in triplicate onto Hybond-N membrane (GE Healthcare Life Sciences, Baie d'Urfe, QC). The membrane was UV-crosslinked for 3 minutes and submerged in maleic Acid Buffer (0.1 M maleic acid, 0.15 M NaCl, pH 7.5) for 2 minutes. The membrane was then blocked for 30 minutes with 1x blocking buffer (Roche). Next, the blot was incubated with a 1:10,000 dilution of Anti-Digoxigenin-AP conjugated antibody (Roche) in 1x blocking buffer for 1 hour. The blot was rinsed 3 times with sdH₂O and washed twice with wash buffer (maleic acid buffer with 0.3% Tween-20 and 0.015% SDS). Following the washes, the blot was submerged in 10 mL of 1x CDP star assay buffer and rinsed with a 1:100 dilution of CDP star substrate (New England Biolabs, Pickering, ON) in 1x CDP star assay buffer. Signal data was detected and quantified as described above for Western Blots.

2.3.13 Data analysis

Western blots and DNA dot blots, spot density was analysed using FluorChem 8900 and AlphaEaseFC software (Alpha Innotech Corporation). For western blots, background signal empty lanes were subtracted from band signals. Band signals for Mip1p (~140 kDa) and Tim17p (~16 kDa) were divided to give a ratio of Mip1p:Tim17p in a given fraction. These ratios were determined for each fraction of each Mip1p variant.

Dot blots were analysed similarly to Western blots. Hybond-N signal background was subtracted from DNA dot signals. The triplicates of each time point were averaged. The signal from untransformed S150 background activity was subtracted from each Mip1p variant at each point. The highest total amount of signal detected for Mip1p[Σ] was consistently detected at 15 minutes regardless of temperature. Activity from Mip1p variants were compared to Mip1p[Σ] at 15 minutes for each respective temperature and are quantified as Relative Light Units (RLU, Mip1p variant signal / Mip1p[Σ] at 15 minutes).

CHAPTER THREE: RESULTS

3.1 Computational results

Previously, efforts were made to analyze the CTE sequence *in silico* (Young *et al.* 2006). From this analysis, truncations were created and a region spanning 6 amino acids (N1033 – E1038) was identified to be essential for a functional, albeit “sloppy” polymerase. Therefore, this study was intended to build upon those results. PRALINE (<http://www.ibi.vu.nl/programs/pralinewww/>, Young, 2008) was used to align CTEs of *Saccharomycetales*. This alignment revealed conservation scores of 5, 4, 7, 9, 5, and 6 for residues N1033, R1034, L1035, E1036, D1037, and E1038, respectively, based on a 10-point scale. Secondary structure prediction software suggests that these residues compose the N-terminal portion of a putative 15-residue helix (Young *et al.*, 2006). This prediction is supported using NetSurfP ver 1.1 (Petersen *et al.* 2009, Figure 3.1).

NetSurfP also analyzes sequences and determines the probability of surface accessibility of each residue. Of the six Mip1p essential CTE residues, N1033, R1034, D1037, and E1038 are considered to be exposed (Table 3.1). Interestingly, L1035 and E1036, the two most conserved residues, are highly likely to be buried.

3.2 Creation of Mip1p mutants for *in vivo* studies

Several attempts were made using different cloning strategies to create the desired point mutations in the *MIP1* locus. First, it was previously shown that deletion of the 205 residues (Mip1p Δ 205) on the distal end of the 1254 residue protein had little or no effect on the functionality of the enzyme *in vivo* as seen in respiratory competence and erythromycin

Figure 3.1 NetSurfP alpha helix prediction plot of the Mip1p residues Q1026 – R1075 located in the CTE. Data points along the curve represent the percent probability each residue is part of a alpha-helical structure. Each letter in the second to bottom row of characters represents a residue. The bottom row of characters (B/E) indicates whether the residue is “buried” (B) or “exposed” (E).

Table 3.1 NetSurfP numerical analysis of the predicted 15-residue helix in the Mip1p CTE

	Amino Acid	Mip1p Residue	Relative Surface Accessibility (RSA) ^a	Absolute Surface Accessibility ^b	Z-Fit Score for RSA Prediction ^c	Probability for Alpha-Helix	Probability for Beta-Strand	Probability for Coil	Class Assignment ^d
Required for Function	N	1033	0.473	69.233	0.320	0.858	0.002	0.139	E
	R	1034	0.519	118.851	1.668	0.923	0.002	0.076	E
	L	1035	0.070	12.799	0.122	0.923	0.002	0.076	B
	E	1036	0.182	31.795	0.272	0.970	0.001	0.030	B
	D	1037	0.616	88.823	0.950	0.970	0.001	0.030	E
	E	1038	0.428	74.684	0.610	0.970	0.001	0.030	E
Required for Fidelity	Y	1039	0.097	20.793	0.793	0.970	0.001	0.030	B
	L	1040	0.180	33.013	0.069	0.970	0.001	0.030	B
	R	1041	0.418	95.768	0.692	0.923	0.002	0.076	E
	E	1042	0.412	72.046	0.198	0.923	0.002	0.076	E
	C	1043	0.133	18.645	0.613	0.858	0.002	0.139	B
	T	1044	0.285	39.543	-0.334	0.782	0.003	0.216	B
	S	1045	0.407	47.747	-0.626	0.802	0.014	0.185	E
	K	1046	0.409	84.131	0.309	0.802	0.014	0.185	E
	E	1047	0.393	68.675	-0.415	0.717	0.014	0.269	E
	Y	1048	0.184	39.257	-0.147	0.717	0.014	0.269	B
	A	1049	0.353	38.901	-0.631	0.522	0.016	0.462	E

^a Relative Surface Accessibility is the numeral prediction of whether the residue is “buried” or “exposed” based on NetSurfP algorithms. ^b Absolute Surface Accessibility is based on experimentally solved related structures ^c Z-Fit score represents how well the ASA fits the RSA ^d Residues are assigned either a B for “buried” or E for “exposed”

resistance analysis (Young *et al.* 2006). However, it should be noted that *in vitro* analysis of this mutation revealed a decrease in polymerase activity over 15 minutes at 30°C as compared to wild-type activity (Young, 2008). To this end, preliminary efforts to create mutations in the *MIP1* locus were conducted by transformation of linear DNA fragments that would recombine with the *MIP1* gene and replace the distal 205 residues with a stop codon followed by *CaURA3* (*URA3* gene from *Candida albicans*) to select for the mutant. This strategy was only successful in producing Mip1p(E1036G) Δ 205 for *in vivo* studies (Figure 3.1).

To increase efficiency and specificity, the *delitto perfetto* method introduced by Storici *et al.* (2003) was adapted for this study. This strategy involves the insertion of a CORE (COunterselectable REsistance) cassette into the desired locus; in this case, at the *MIP1* locus between residues N1033 and A1049. The CORE cassette contains an I-*SceI* (intron-encoded endonuclease in *Saccharomyces cerevisiae*) endonuclease under the control of a galactose inducible promoter, a target sequence for the I-*SceI* endonuclease, *KIURA3* counterselectable marker, and *kanMX4* resistance gene. The double-stranded break created by the I-*SceI* endonuclease after being induced causes the cell to initiate endogenous DNA repair mechanisms. This, subsequently, was reported to increase the efficiency and specificity of engineered DNA fragments being homologously recombined at or near the double-stranded break. The presence of the *KIURA3* gene allows for the selection of a yeast strain harbouring the CORE cassette within the *MIP1* locus and counterselection for the replacement of the CORE cassette with the mutant DNA fragment. *kanMX4* imparts resistance to G418, otherwise known as Geneticin™

(Invitrogen) and allows for further selection of the CORE cassette, which minimizes the occurrence of false positives.

While the insertion of the CORE cassette into the *MIP1* locus offers the benefits of efficiency and specificity, its presence creates a non-functional Mip1p enzyme. This leads to depletion of mitochondrial DNA (mtDNA, ρ^0). Therefore, measures were taken to be able to mate the mutant strain with a respiratory competent isogenic strain (ρ^+) and subsequently sporulate the resulting diploid to select for a potentially respiratory competent, ρ^+ , mutant strain. Prior to the cloning of the CORE cassette into the *MIP1* locus, the *SpHIS5* auxotrophic marker was successfully inserted in the intergenic region immediately downstream of the *MIP1* gene (strain RI002) (Figure 3.2a).

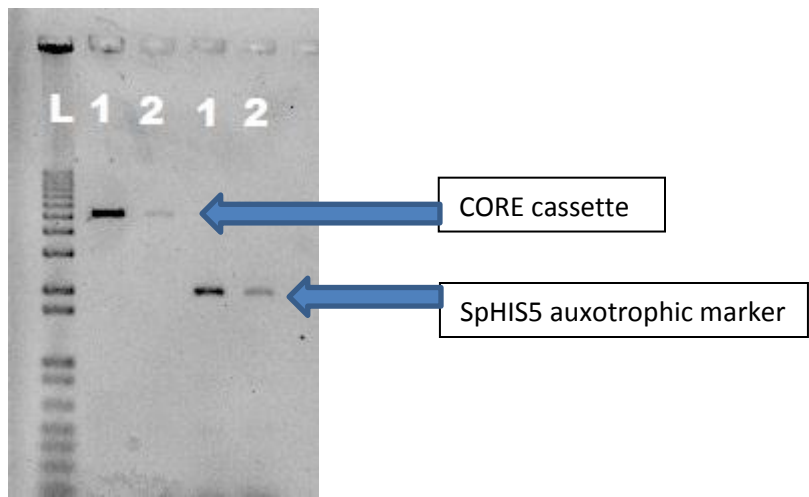
Insertion of the CORE cassette into the *MIP1* locus of RI001 was successful (Figure 3.2b). As expected, the resulting strain (RI003) was respiratory deficient and failed to grow on YPG media containing a non-fermentable carbon source. It also exhibited a substantially decreased growth rate, doubling once every 8 hours in YPD, likely attributed to the loss of the ability to respire.

Attempts were made to transform concentrated full-length mutant DNA created using overlap extension PCR fragments (see Figure 2.2D) into RI003 following induction of the *I-SceI* endonuclease. One mutant was obtained for *in vivo* studies. *mip1R1034G* (RI004) was sequenced and verified (Figure 3.2c).

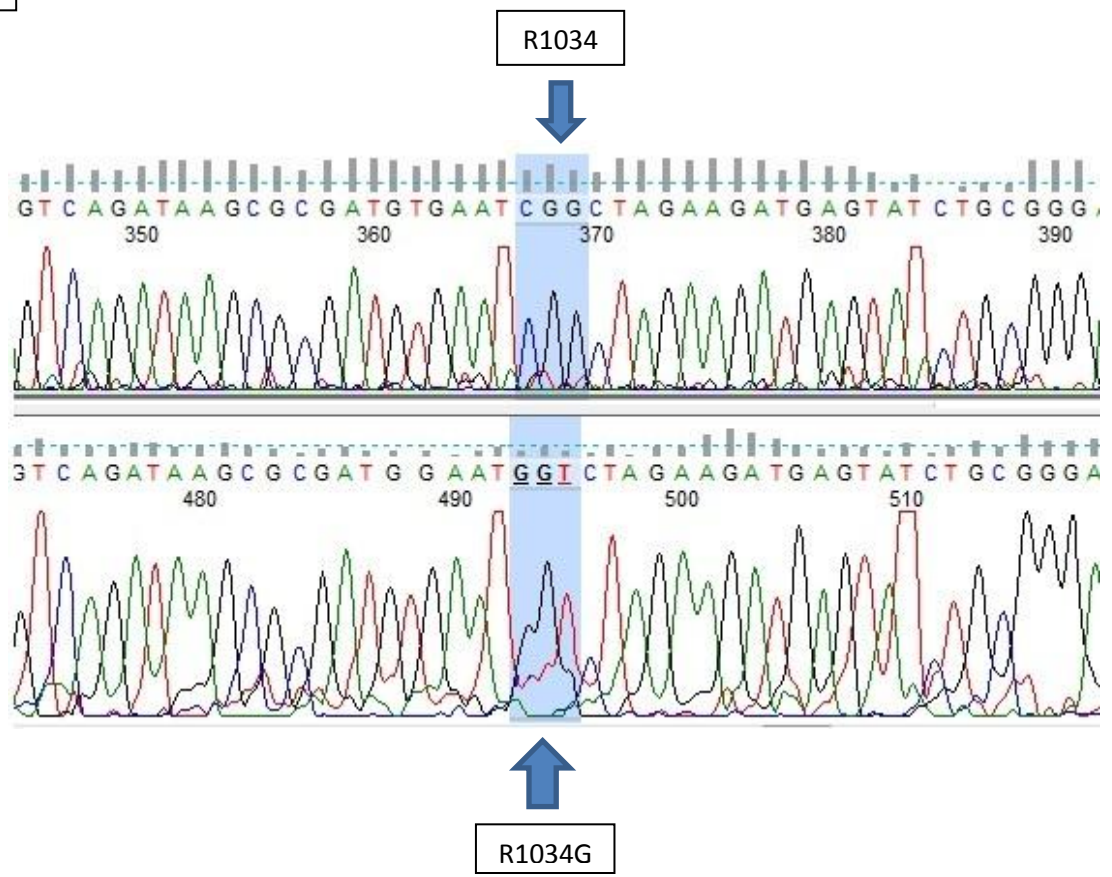
To replenish mtDNA in RI004 (*MATa*), the strain was mated with RI001 (*MATa*). The observance of “shmooing” indicated that the cells in the mixture underwent natural mating-type switching and were undergoing sexual mating. This mixture was plated onto

Figure 3.2 Verification of *delitto perfetto* cloning strategy in creating *mip1R1034G*. A. PCR verification of the CORE cassette inserted into the *MIP1* locus using primers Mip1DSBVerFwd and Mip1DSBVerRev to produce a 5.4 kb fragment. PCR verification of *SpHIS5* insertion in RI002 using primers Mip1SpHIS5VerFwd and Mip1SpHIS5VerRev produces a 2.1 kb fragment. L represents 1 kb-plus ladder (Invitrogen). Two potential isolates are shown and denoted as 1 and 2. C. Sequencing of strain RI004 shows the R1034G mutation.

A



B



sporulation media to induce the formation of spores. Over the course of 1 to 2 weeks of incubation at 30°C, samples were picked from the sporulation plates and examined under a microscope for the formation of spore-bearing asci. Asci were then lysed as described in section 2.3.5 and plated onto Sc-HIS selection media. RI004 isolates on this media were then plated on to a second Sc-HIS plate and a YPG plate to determine respiratory competency. RI004 was able to grow well on YPG indicating that mtDNA had been replenished in these cells.

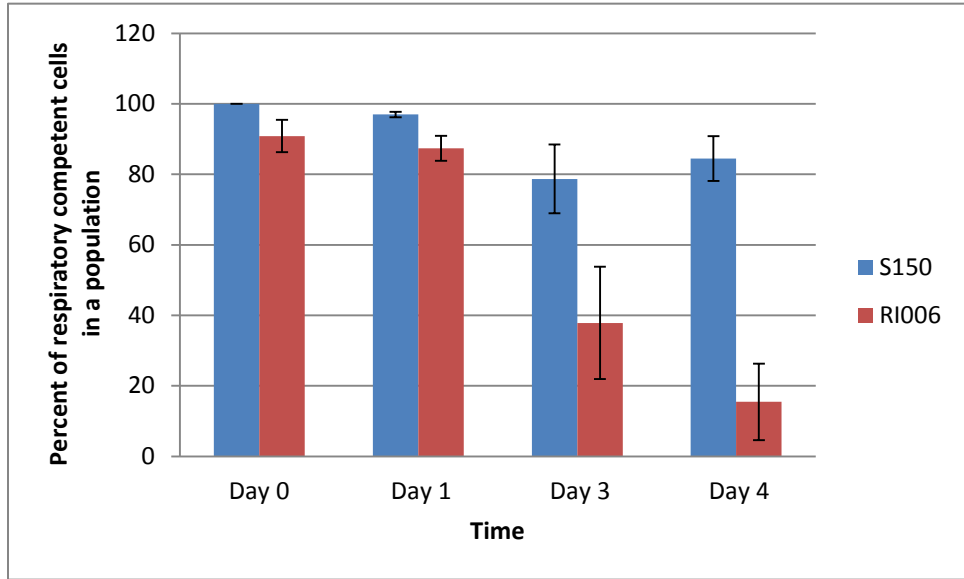
3.3 *In vivo* analysis

RI006 (*mip1E1036G::CaURA3*) was the only mutant created using the strategy in which the distal 205 residues of the wild-type protein were replaced with a *CaURA3* marker. It was possible to use this cloning strategy for *in vivo* studies because it was previously shown that Mip1p Δ 205 (removal of the distal 205 residues) had the same activity as Mip1p wild-type *in vivo* (Young, 2008). Over the period of 4 days at 30°C, *mip1 Δ 205* and S150 retained the ability to respire on a fermentable carbon source (95.9% of cells and 99% of cells, respectively, Young, 2008). RI006, however, had only 15% of cells still respiratory competent after 4 days growth at 30°C (Figure 3.3a). The enzyme was also found to be increasingly “sloppy” as demonstrated by increasing erythromycin resistance (Figure 3.4a). RI006 had a 2.5-fold increase in erythromycin resistant cells over S150.

The ρ^+ RI004 strain ([S150] *mip1R1034G*) was subjected to respiratory competence and erythromycin resistance testing (Figure 3.5). The results are similar to S150 and show an insignificant difference in respiratory competence. After 4 days

Figure 3.3 Respiratory competence of S150 and R1006 at 30°C. A. Chart representing the respiratory competence of a population of cells from strains S150 and R1006 grown for 4 days at 30°C on a fermentable carbon source. Respiratory competence on Days 1, 3 and 4 were determined by TTC agar-overlay (see section 2.3.6). B. YPD plate with TTC agar overlay depicting a respiratory competent cell (red arrow) and a non-respiring cell (white arrow).

A



B

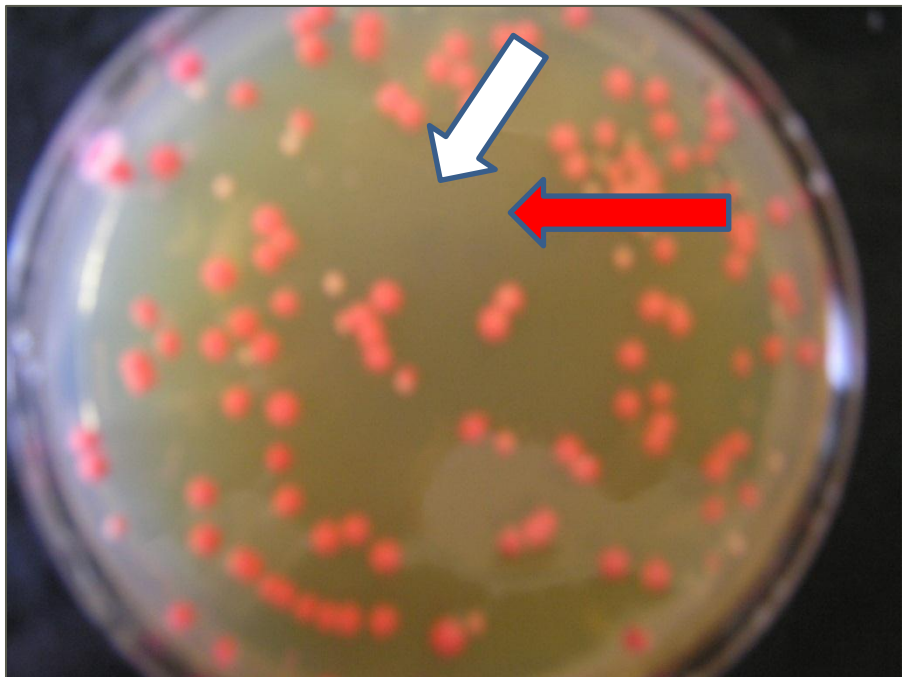
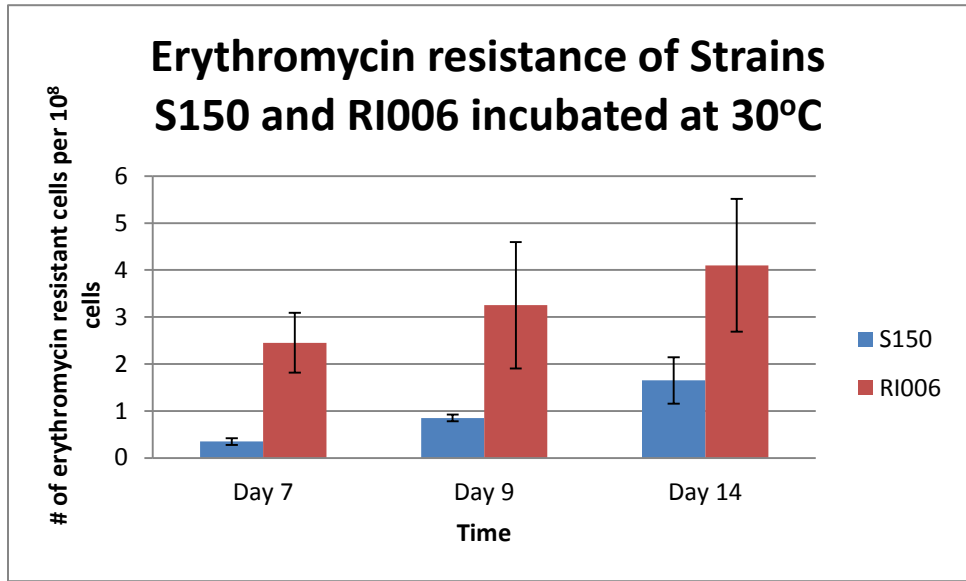


Figure 3.4 Erythromycin resistance of S150 and RI006 over the course of 2 weeks growth on a fermentable carbon source at 30°C. A. Chart representation of the number of erythromycin resistance cells of strains S150 and RI006 per population of 10^8 cells from averaged from 3 separate trials. B. Plates showing the erythromycin resistance after 14 days. Plates 1 and 2 represent growth of S150 and RI006 on YPG after 14 days, respectively. Plates 3 and 4 represent growth of S150 and RI006 on YG-Er after 14 days, respectively.

A



B

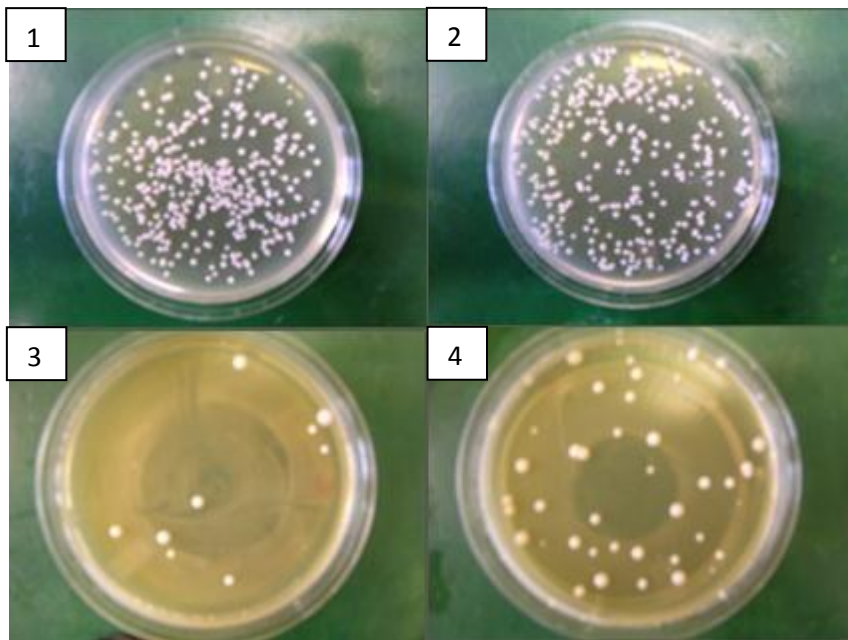
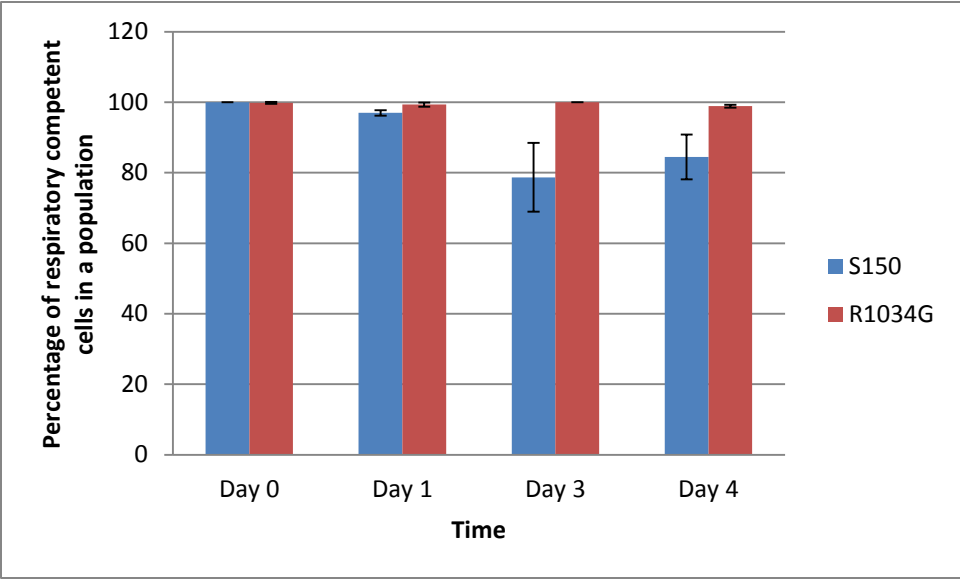


Figure 3.5 Respiratory competence of S150 and R1004 at 30°C. Strains were grown for 4 days at 30°C in media containing a non-fermentable carbon source and then transferred to glucose containing media. Respiratory competence on Days 1, 3 and 4 were determined by TTC agar-overlay (see section 2.3.6).



growth, at 30°C, on a fermentable carbon source, 97% of the cells remained respiratory competence. This non-mutagenic phenotype made it possible to forgo erythromycin testing. These results indicate that the mutation has virtually no detectable effect on the functionality of Mip1p *in vivo*.

3.4 Creation of plasmids for overexpression of *mip1* variants

To further investigate these mutations *in vitro*, plasmids were constructed for overexpressing Mip1p variants. *Pst*I-linearized pMIP Σ (Table 2.2) and full-length mutant DNA fragments were cotransformed into a *mip1* Δ mutant (RI001) where they underwent homologous recombination. pMIP Σ encodes wild-type Mip1p[Σ] under the control of a galactose-inducible promoter and C-terminally tagged with 6xHIS and HA epitope tags. Circularized plasmids were crudely isolated using the “smash and grab” DNA extraction method and transformed into *E. coli* DH5 α . Plasmids isolated from individual *E. coli* colonies were then purified and screened by sequencing (Figure 3.6).

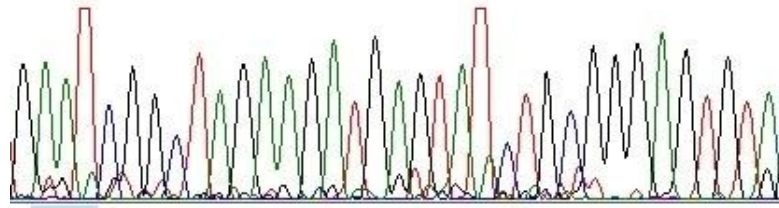
3.5 Overexpression and isolation of Mip1p variants

Verified overexpression Mip1p variant plasmids were transformed into wild-type *Saccharomyces cerevisiae* S150 for overexpression. Transformed cells were selected on Sc-LEU media, followed by culturing in SRaff-LEU to obtain a sufficient amount of cells in a glucose free environment. Induction was carried out by adding galactose to the culture and incubating at 30°C for 5 hours.

Mip1p was found to be associated with the inner mitochondrial membrane (Young, 2008).

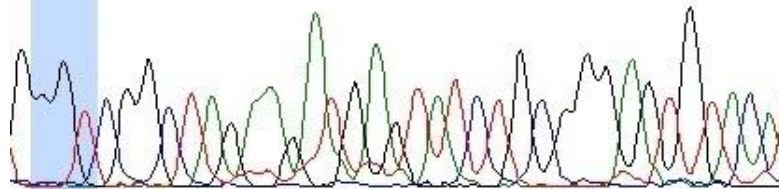
Figure 3.6 Sequencing chromatogram of *mip1* variant plasmids. Respective mutations are highlighted in blue.

GAATCGGC TAGAAGATGAGTATCTGCGGGAGTGTAT



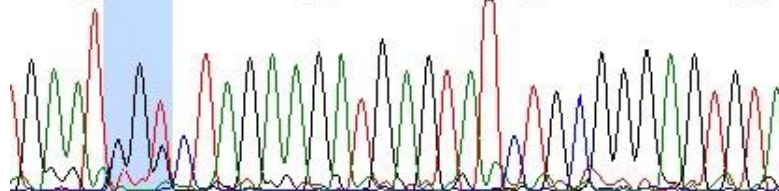
MIP1[Σ]

GGGTCGGCTAGAAGATGAGTATCTGCGGGAGTGTACA



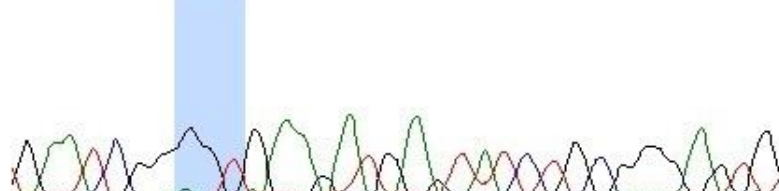
mip1N1033G

GAATGGTCTAGAAGATGAGTATCTGCGGGAGTGTAT
460 470 480 490



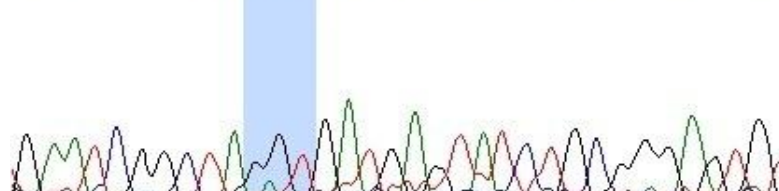
mip1R1034G

GAATCGGGGTGAAGATGAGTATCTGCGGGAGTG



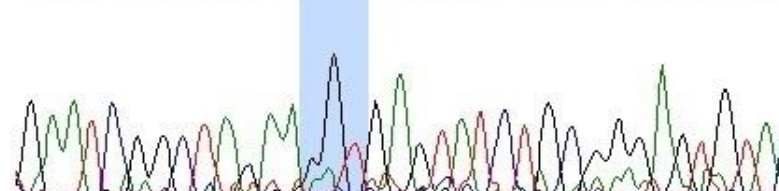
mip1L1035G

GAATCGGC TAGG TGAGTATCTGCGGGAGTGT



mip1E1036G

GAATCGGC TAGAAGGTGAGTATCTGCGGGAGTGTAC



mip1D1037G

Therefore, to obtain Mip1p variants for *in vitro* studies, mitochondrial membrane fractions were collected and assessed by Western blot.

3.6 Western blot

The presence of C-terminal-HA-tagged Mip1p variants was confirmed and relative levels were quantified. The ratio of chemiluminescent signal from HA-tagged variants to that of Tim17p was assessed (Figure 3.7)

3.7 Non-radioactive *in vitro* DNA polymerase assay

A non-radioactive *in vitro* DNA polymerase assay (Young, 2008) was optimized during the course of this study. Mip1p variants were incubated at pre-incubated for 15 minutes at 30°C or 37°C in a mixture containing hexanucleotides for random priming, nucleotides for polymerization, DIG-11-dUTP for DNA labelling, and aphidicolin to prevent activity of contaminating nuclear DNA polymerases to allow the variants to acclimate to each respective temperature prior to the start of the reaction. Boiled template DNA (linearized pMIP1F3, Table 2.2) was added to each reaction tube to initiate the reaction. Samples were taken at 2.5, 5, 10 and 15 minutes, stopped with EDTA and spotted in triplicate onto Hybond-N membrane (GE Healthcare Life Sciences, Baie d'Urfe, QC). Initial synthesis at 30°C or 37°C over the first 2.5 minutes was comparable for all variants except for Mip1pE1036G.

At 30°C, wild-type, Mip1p[Σ], showed steady synthesis over the 15 minute time period (Figure 3.8) with no significant increase in polymerization rate. This general trend was also observed for Mip1pN1033G, Mip1pR1034G and Mip1pL1035G. Although the rate of incorporation of DIG-11-dUTP was steady, the total amount of DNA synthesized

Figure 3.7 Western blot of a *mip1* variant. C-terminally HA-tagged Mip1p is indicated by Box A. Tim17p is indicated with Box B. Membrane background is indicated by Boxes C and D. Ratios of Mip1p:Tim17p were obtained by first subtracting the signal of Box C and D from both Box A and Box B respectively. The adjusted signal of Mip1p and Tim17p (- background) were divided to give a ratio of Mip1p:Tim17p. This calculation was carried out with each Mip1p variant. Mip1p_{variant}:Tim17p ratios were then compared to Mip1p[Σ] to give Mip1p_{variant}:Mip1p[Σ] ratios. The Mip1p_{variant}:Mip1p[Σ] ratios are used to adjust *in vitro* DNA polymerase data.

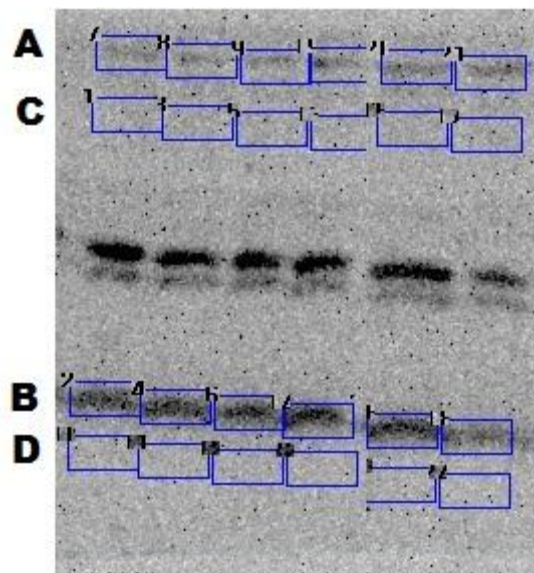


Figure 3.8 – 3.13 *In vitro* relative activity of Mip1p variants at 30°C and 37°C over 15 minutes. Panels 3.8A and 3.8B represent all of the *mip1* variants compared at 30°C and 37°C, respectively. Item A of Figures 3.9 – 3.13 shows the relative activities of Mip1p variants compared to Mip1p[Σ] at 30°C. Item B of Figures 3.9 – 3.13 shows the relative activities of Mip1p variants compared to Mip1p[Σ] at 37°C. Item C of Figures 3.9 – 3.13 shows the comparison of the activity of each Mip1p variant at 30°C and 37°C (Mip1pN1033G, Mip1pR034G, Mip1pL1035G, Mip1pE1036G and Mip1pD1037G, respectively).

Figure 3.8

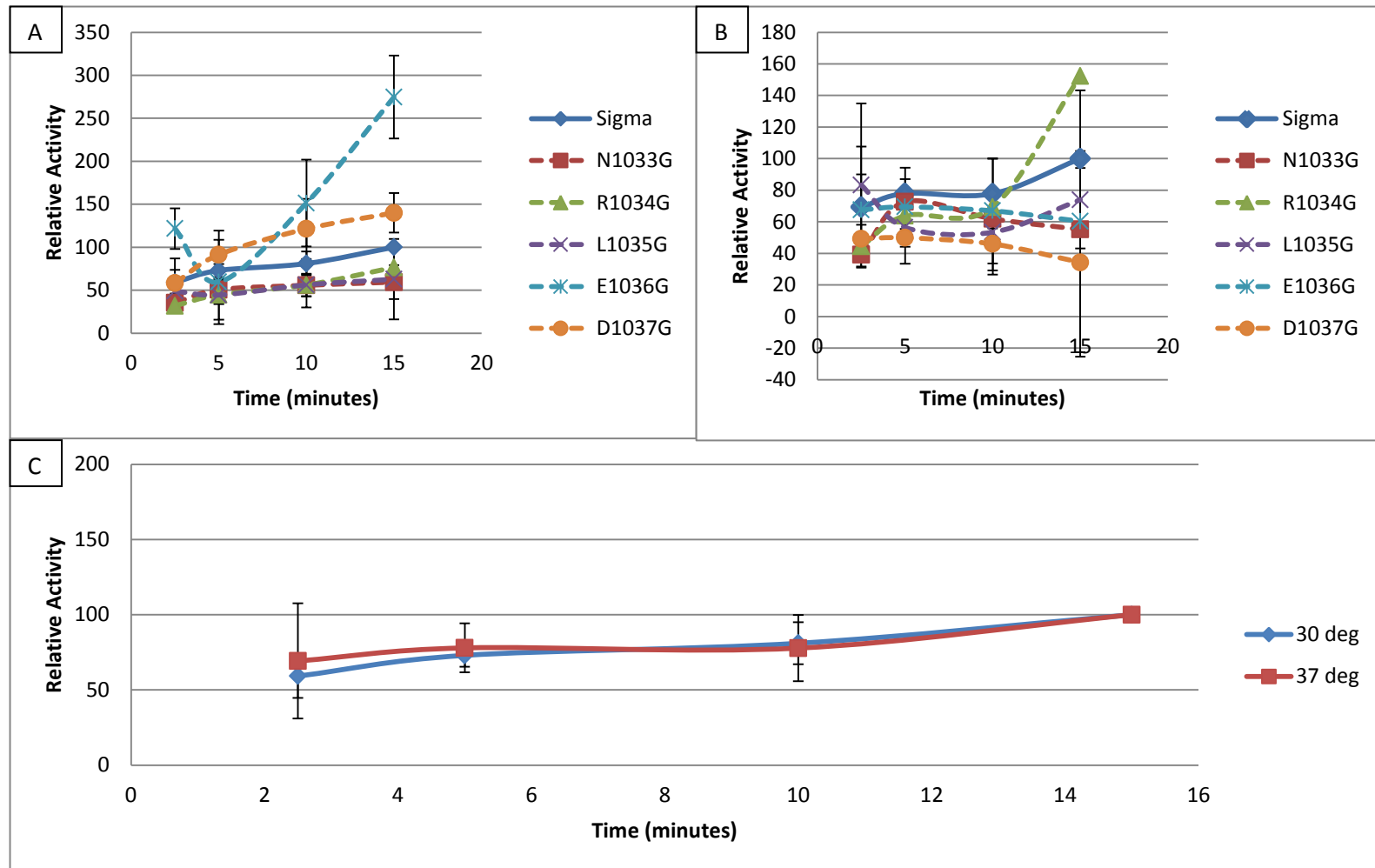


Figure 3.9

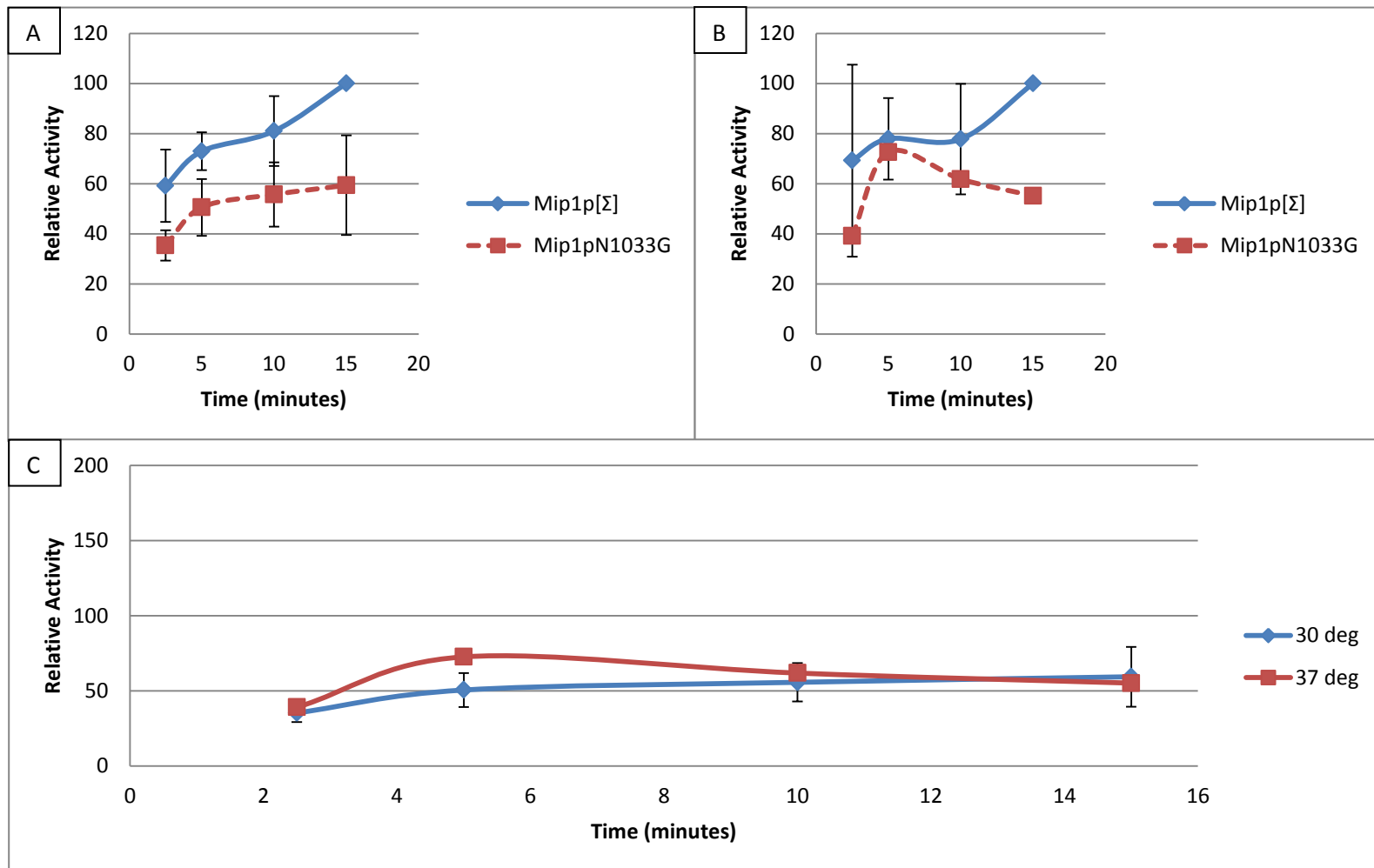


Figure 3.10

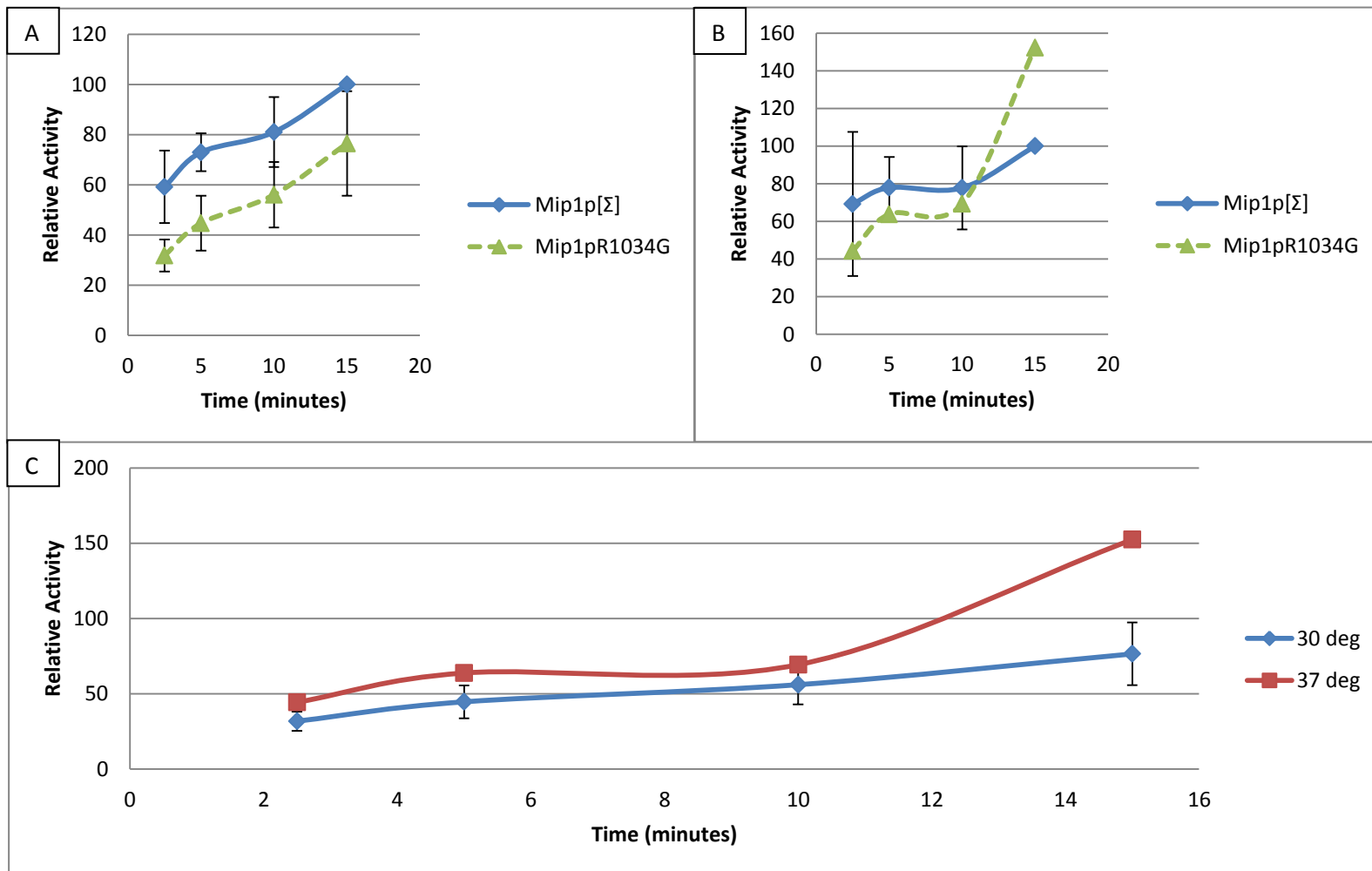


Figure 3.11

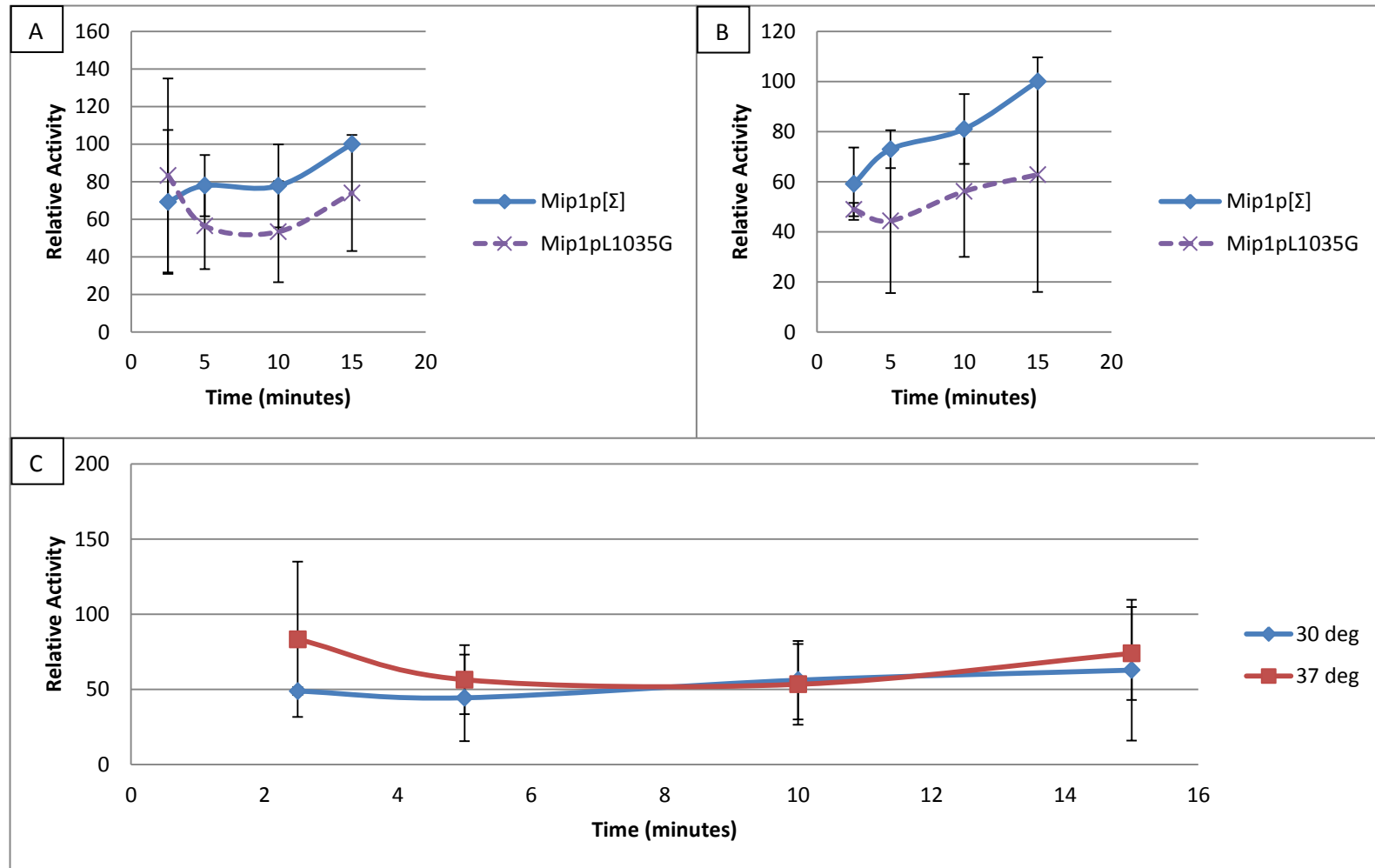


Figure 3.12

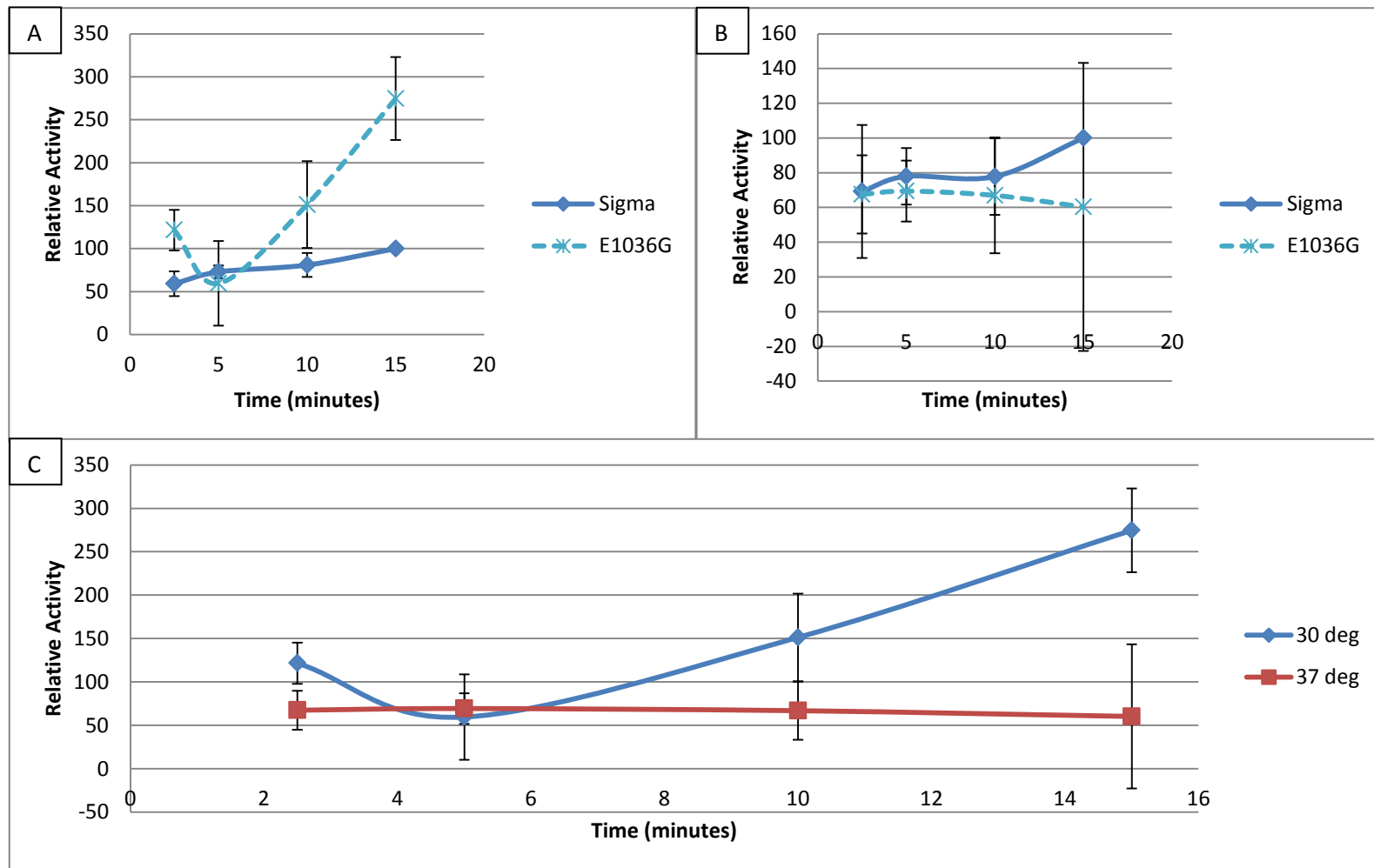
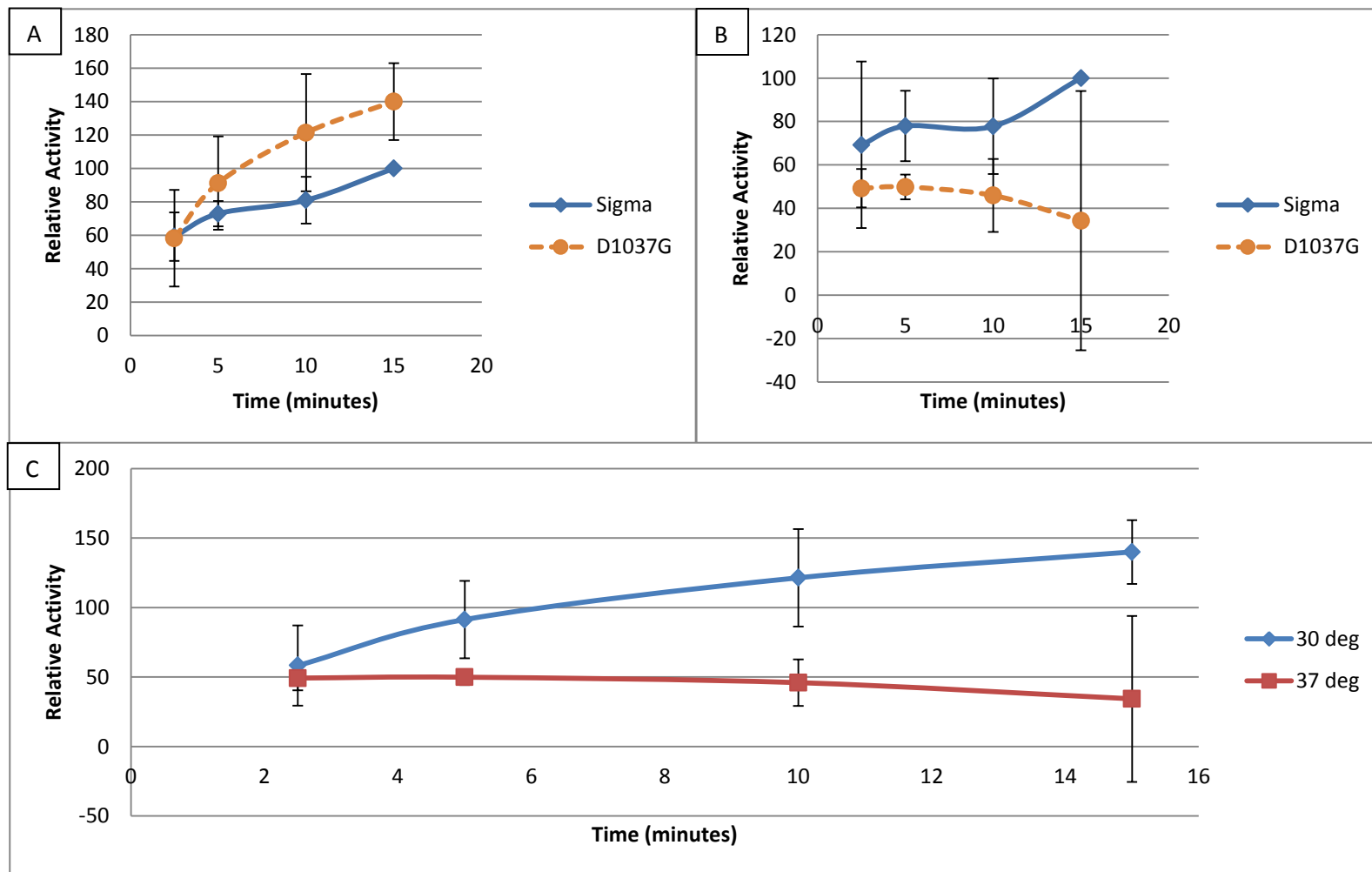


Figure 3.13



was less than wild-type (Figures 3.9, 3.10 and 3.11, respectively). Mip1pD1037G, however, was able to synthesize more DNA overall than wild-type over the 15 minute period and had a slightly higher polymerization rate over the first 5 minutes (Figure 3.13).

Interestingly, between 2.5 and 5 minutes, both, Mip1pL1035G and Mip1pE1036G (Figure 3.11 and Figure 3.12) had a decrease in signal in 2 of the 3 trials (Table 3.2). While the decrease for Mip1pL1035G was not as pronounced, Mip1pE1036G gave over a 3-fold drop in signal (Table 3.2). This drop was not mirrored in any of the Mip1p[Σ] trials carried out at the same time, indicating a variant-specific effect.

Furthermore, at 30°C, prior to the drastic decrease in signal, Mip1pE1036G initially synthesized more DNA in 2.5 minutes than Mip1p[Σ] did in 15 minutes (Figure 3.12). Following the drop in signal, Mip1pE1036G had a drastic increase in polymerization activity over the next 10 minutes. The incorporation of DIG-11-dUTP was almost 10 times greater than Mip1p[Σ] (Table 3.4).

Mip1p[Σ] activity at 37°C was fairly consistent with the results at 30°C (Figure 3.8c). These results agree with those published by others, using a radioactive assay (Baruffini *et al.* 2007). Mip1p[Σ] did not seem to be affected by the increase in temperature. Similar results were seen with Mip1pN1033G and Mip1pL1035G enzymes (Figures 3.9c and 3.11c, respectively). The amount of incorporated DIG-11-dUTP at 37°C in the Mip1pN1033G mutant was not significantly different from the amount incorporated at 30°C over the 15 minute trial. However, at 30°C, synthesis by Mip1pN1033G was gradual over that period, while, at 37°C, Mip1pN1033G initially had

a higher polymerization activity, followed by a gradual decrease in signal. The amount of incorporated DIG-11-dUTP by Mip1pL1035G at 30°C was not significantly different from that at 37°C. Much like Mip1pN1033G, Mip1pL1035G had a sharp increase in polymerase activity at 37°C, initially. This high rate of synthesis was followed by a sudden drop in signal. However, unlike Mip1pN1033G, Mip1pL1035G seemed to recover after the 10 minute mark and returned to synthesizing DNA during the last 5 minutes at 37°C.

Mip1pR1034G, Mip1pE1036G and Mip1pD1037G all show altered activity at 37°C. Mip1pR1034G might be the most interesting at this temperature. All of the variants show some degree of signal loss over the course of the experiment at 37°C, with the exception of Mip1pR1034G (Figure 3.10). Mip1pR1034G shows gradual synthesis of DNA over the first 10 minutes followed by a drastic increase in synthesis (Table 3.3). Not only was the rate of DIG-11-dUTP incorporation accelerated, but, the total amount of DIG-labelled DNA synthesized is 1.5-fold more than Mip1p[Σ] synthesized over 15 minutes at 30°C. It should be noted, however, that the results of Mip1pR1034G at 37°C currently stem from a single trial.

With the exception of 1 trial, Mip1pE1036G and Mip1pD1037G and showed a marked decrease in signal over the last 5 minutes of the experiment (Table 3.4). Mip1pE1036G and Mip1pD1037G had an approximately 5-fold drop in signal those trials. This is in stark contrast to their activities at 30°C in which both were able to synthesize more DNA than Mip1p[Σ].

Table 3.2 Activity of Mip1p variants at 30°C

Variant	Time (minutes)	Trial 1 (RLU)	Trial 2 (RLU)	Trial 3 (RLU)	Trial 4 (RLU)	Trial 5 (RLU)	Average (RLU)	Standard Deviation						
Mip1p[Σ]	2.5	60.17	49.24	83.43	47.50	55.65	59.20	14.47						
	5	64.02	67.10	83.01	74.26	76.39	72.96	7.56						
	10	104.45	77.03	81.96	69.60	71.98	81.00	13.95						
	15	100.00	100.00	100.00	100.00	100.00	100.00	0.00						
Mip1pN1033G	2.5				31.11	39.67	35.39	6.05						
	5				42.59	58.59	50.59	11.31						
	10				46.66	64.75	55.71	12.79						
	15				45.37	73.44	59.41	19.85						
Mip1pR1034G	2.5							27.35	36.36	31.86	6.37			
	5							36.95	52.42	44.68	10.94			
	10							46.83	65.29	56.06	13.05			
	15							61.77	91.23	76.50	20.83			
Mip1pL1035G	2.5							49.34	46.05	51.29			48.89	2.65
	5							77.49	31.04	24.74			44.42	28.81
	10							86.28	39.95	42.17			56.13	26.13
	15							116.83	35.18	36.42			62.81	46.79
Mip1pE1036G	2.5	113.66	148.27	103.09						121.68			23.63	
	5	114.04	46.30	18.53						59.62			49.13	
	10	207.83	135.36	110.78						151.32			50.46	
	15	304.49	300.59	218.95						274.68			48.30	
Mip1pD1037G	2.5	26.82	83.48	64.49			58.26			28.84				
	5	60.14	113.99	99.75			91.29			27.91				
	10	82.62	150.72	130.81			121.38			35.01				
	15	113.50	153.77	152.67			139.98			22.94				

Table 3.3 Activity of Mip1p variants at 37°C

Variant	Time (minutes)	Trial 1 (RLU)	Trial 2 (RLU)	Trial 3 (RLU)	Trial 4 (RLU)	Average (RLU)	Standard Deviation			
Mip1p[Σ]	2.5	39.17	123.92	67.16	46.70	69.24	38.33			
	5	63.46	79.43	68.65	100.18	77.93	16.26			
	10	70.66	74.40	57.21	108.92	77.80	22.03			
	15	100.00	100.00	100.00	100.00	100.00	0.00			
Mip1pN1033G	2.5				39.13	39.13				
	5				72.63	72.63				
	10				61.87	61.87				
	15				55.18	55.18				
Mip1pR1034G	2.5							44.40	44.40	
	5							63.83	63.83	
	10							69.35	69.35	
	15							152.36	152.36	
Mip1pL1035G	2.5	57.63	142.70	49.62					83.32	51.58
	5	63.46	75.14	30.77					56.46	23.00
	10	83.71	43.82	32.60					53.38	26.86
	15	106.99	68.88	45.90					73.92	30.86
Mip1pE1036G	2.5	92.64	60.62	49.25		67.50	22.50			
	5	88.60	65.48	54.19		69.43	17.54			
	10	105.03	42.74	53.03		66.94	33.39			
	15	156.01	8.26	16.65		60.31	82.98			
Mip1pD1037G	2.5	58.52	48.28	40.92			49.24	8.84		
	5	54.35	43.49	51.77			49.87	5.67		
	10	65.17	34.16	38.55			45.96	16.78		
	15	102.78	-6.76	6.91			34.31	59.69		

Table 3.4 Relative activity rates of Mip1p variants at 30°C and 37°C between sampled time points

Mip1p Variant		2.5 – 5 minutes		5 – 10 minutes		10 – 15 minutes	
	Temperature	Average (RLU/min)	Std Dev	Average (RLU/min)	Std Dev	Average (RLU/min)	Std Dev
Mip1p[Σ]	30°C	5.50	4.62	1.61	3.81	3.80	2.79
	37°C	3.48	16.54	-0.03	1.95	4.44	4.41
Mip1pN1033G	30°C	6.0	2.10	1.02	0.30	0.74	1.41
	37°C	13.40	-	-2.15	-	-1.34	-
Mip1pR1034G	30°C	5.13	1.83	2.28	0.42	4.09	1.56
	37°C	7.77	-	1.10	-	16.60	-
Mip1pL1035G	30°C	-1.79	11.53	2.34	0.99	1.34	4.14
	37°C	-10.70	14.93	-0.62	5.22	4.11	1.27
Mip1pE1036G	30°C	-24.82	21.90	18.34	0.48	24.67	7.34
	37°C	0.77	2.07	-0.50	3.92	-1.33	9.98
Mip1pD1037G	30°C	13.21	0.95	6.02	1.43	3.72	2.84
	37°C	0.25	3.54	-0.78	2.58	-2.33	8.58

Positive values indicate polymerase activity. Negative values (green) indicate loss of signal, presumably due to exonuclease activity

CHAPTER FOUR: DISCUSSION AND FUTURE STUDIES

4.1 Discussion

Saccharomyces cerevisiae has long been considered a very good model for investigating eukaryotic processes. Researchers have exploited this tool by introducing equivalent mutations of human disease in these cells and studying their effects. More specifically, diseases such as Alpers' syndrome, progressive external ophthalmoplegia, Parkinson's disease, cancer as well as ageing are caused by mitochondrial DNA mutations caused by a dysfunctional mitochondrial DNA polymerase. Variants of POLG, the human mitochondrial DNA polymerase, found in patients diagnosed with these disorders have been sequenced and equivalent mutations have been introduced into Mip1p, the yeast mitochondrial DNA polymerase for study.

Despite differences in mitochondrial nucleoid interactions, mitochondrial DNA topology and mitochondrial polymerase structure, researchers still use Mip1p to model POLG. Furthermore, the exact DNA replication mechanism in both yeast and human has yet to be completely elucidated. The purpose of this study is to examine one of the more salient features of Mip1p, the Carboxy-terminal extension (CTE) in the hopes of determining its function.

Previous studies have shown that only 74 residues proximal to the polymerase domain of the 279 residue CTE are required for wild-type function (Young *et al.*, 2006). Within this area are two predicted helices. The first helix is 11 residues in length and has moderate to high conservation among *Saccharomycetales*. The second helix is 15 residues in length and has low to moderate conservation. Disruption of the second helix

through removal of 9 residues on the C-terminal portion of the helix, leaving behind the N-terminal 6 residues decreases the fidelity of the enzyme (Young *et al.*, 2006). Removal of all of the residues to the C-terminal side of, and including the entire 15 residue helix abolishes enzyme function. From these results, this study took a closer look at the region critical for Mip1p function, Mip1p residues N1033 – E1038.

Each amino acid in the critical region of the CTE was systematically replaced with a glycine residue to examine the significance, if any, they play in Mip1p function. *In vitro* analysis suggests that N1033, R1034 and L1035 do not play a significant role in the activity of Mip1p. Substitution of these residues with glycine did not significantly disrupt *in vitro* synthesis. With the exception of Mip1pR1034G activity at 37°C, DNA was synthesized at a rate comparable to wild-type (Table 3.3). It should be noted that the data from Mip1pR1034G at 37°C was gathered from a single trial. More trials are necessary to determine its effect at this temperature. Similar to Mip1p Δ 205, the total amount of DNA synthesized by these variants was reduced but they had comparable DNA synthesis rates to Mip1p[Σ]. Therefore, the capacity of variants to stably maintain mtDNA copies is not affected. When studied *in vivo*, cells harbouring Mip1p Δ 205 displayed no mutagenic growth phenotypes associated with mitochondrial DNA polymerase dysfunction (Young, 2008). Likewise, Mip1pR1034G cells showed no significant increase in *petite* frequency over the period of 4 days growth on a fermentable carbon source at 30°C. *In vivo* study of Mip1p(E1036G) Δ 205, however, revealed a drastic increase in *petite* frequency under those conditions. After 4 days growth, only 15% of the population of Mip1p(E1036G) Δ 205 cells remained respiratory competent on average over 2 trials (Figure 3.3). Furthermore, there was a 2.5-fold increase in erythromycin resistance on

average over 2 trials after 14 days growth on YG-Er (Figure 3.4). E1036 is the most conserved CTE residue among *Saccharomycetales* with a conservation score of 9 on a 10-point scale (Young *et al.*, 2006). *In silico* analysis using NetSurfP gives the residue a low relative surface accessibility score and has suggested that this residue is “buried” rather than exposed for interactions with other factors (Table 3.1). *In vitro* study of Mip1pE1036G also suggests that this residue plays a critical role in the function of Mip1p (Figure 3.12). Replacement of this glutamate residue with glycine affected the rates of polymerase and exonuclease activity (Table 3.3). The incorporation rate was not steady throughout the 15 minute time period as was seen with Mip1p[Σ]. Instead, at 30°C, Mip1pE1036G had a maximal synthetic rate of 24.6 RLU/min between 10 and 15 minute time points (Figure 3.12). Furthermore, it had a degradative rate of 24.8 RLU/min between 2.5 and 5 minutes (Figure 3.12). Neither of these phenomena were observed in the background strain and thus is assumed to be caused only by the *mip1E1036G* mutation. Interestingly, no significant difference between Mip1p[Σ] and Mip1pE1036G was observed at 37°C; although, activity of Mip1pE1036G was harder to determine considering the large standard deviations of the data at this temperature (Figure 3.12). In two out of the three trials the signal intensity dropped approximately 6-fold and had an average degradative rate 12.4 RLU/min over the final 5 minutes, while the third trial exhibited no loss in signal. Altogether, the *in vitro* and *in vivo* data gathered from E1036G suggests that this residue functions in the exonuclease-polymerase coupling mechanism of the enzyme. For long stretches, as seen in the *in vitro* data, the enzyme stays in either proofreading or polymerase mode with minimal switching, resulting in

increased rates of synthesis or degradation. Prolonged proofreading activity could result in the depletion of mtDNA and the ρ^0 phenotype.

The Mip1pE1036G *in vitro* results were also seen in Mip1pD1037G. D1037 is moderately conserved in the CTEs of *Saccharomycetales* with a conservation score of 5 (Young, 2008). *In silico* analysis predicts this residue as be “exposed” (Table 3.1). As for Mip1pE1036G, the experiments using Mip1pD1037G had highly variable results at 37°C, particularly at the 15 minute time point. Two trials exhibited a drastic drop in signal with an average degradative rate of 11.3 RLU/min over the final 5 minutes. The third trial exhibited no exonuclease activity. At 30°C, Mip1pD1037G had markedly different activity; it had a faster initial synthesis rate (Figure 3.13). In the first 5 minutes, it synthesized approximately the same amount of DNA that Mip1p[Σ] did after 15 minutes and had synthesized 40% more DNA than Mip1p[Σ].

In summary, this study has developed a cloning strategy that successfully created a point mutation in *MIP1* and replenished mitochondrial DNA in this cell line for *in vivo* analysis. Furthermore, through *in vivo* and *in vitro* analysis, this study has identified 2 residues essential for a proper functioning Mip1p, E1036 and D1037. Their roles have yet to be determined. However, data from this study suggests that they may be involved in exonuclease-polymerase coupling. N1033, R1034 and L1035, conversely, do not appear to have a significant function in Mip1p activity.

4.2 Future studies

The results of this study have identified 2 CTE residues essential to Mip1p function. Unfortunately, *in vivo* analysis of all the variants in this study was not

completed, due to problems in mutant generation. It is very likely that the lack of transformation efficiency in the modified *delitto perfetto* method is due to the induction step. Cells at this step exhibit a growth defect due to the insertion of the CORE cassette in the *MIP1* locus. Induction of the I-SceI endonuclease increases the transformation efficiency by creating a double-stranded break at a desired locus, thus, invoking endogenous DNA repair mechanisms. These DNA repair mechanisms increase the efficiency of homologous recombination by *mip1* mutant DNA fragments. This induction step, according to the protocol outlined by Storici *et al.* (2003), involved incubation of the culture at 30°C for 4 hours in galactose. For future studies, mutations using this strategy should employ incubation times of 8 and 12 hours given that the doubling time of ρ^0 cells is increased approximately 2-fold (data not shown).

The increased rates of polymerase and exonuclease activity in Mip1pE1036G and Mip1pD1037G suggest that these residues may participate in switching between these functions and cause the enzyme to remain in either mode for longer periods of time. Xie *et al.*, (2007) proposed a model for exonuclease-polymerase coupling of “right hand” DNA polymerases based on affinities of the enzyme domains and the free energy state of DNA. This model uses three assumptions: (1) the “fingers” subdomain has affinity for 5'-3' ssDNA (template strand), (2) the exonuclease domain has 3'-5' ssDNA affinity (primer strand) and (3) the “thumb” and “palm” subdomains have dsDNA affinity (see Figure 1.3). Implicit in their model is that the preferred conformational state is that of polymerization. Polymerization proceeds as follows: the enzyme is in an “open” state, where the fingers are outstretched and the polymerase active site is sampling dNTPs. Association of a dNTP to the polymerase active site causes a conformational change in

the protein and results in the fingers rotating 40° inward to the “closed” state (Xie *et al.*, 2007). The polymerase transitions from the “open” to “closed” state, to allow the incoming dNTP to attach to the phosphate backbone of the primer strand and allow base pairing with the template strand. The fingers subdomain then moves the DNA molecule down by distance, l , in order to bind to the next unpaired base on the template strand due to its 5'-3' ssDNA binding affinity. Upon binding to the unpaired base, the DNA molecule is moved down further by distance, p , the distance between two successive bases. The release of pyrophosphate after attached the nucleotide to the phosphate backbone causes the polymerase to transition back to the “open” state. This transition drives the DNA molecule back up by a distance, l . Therefore, the net movement of DNA upon successful insertion of a matched nucleotide is distance, p . During polymerization, these steps are repeated. When a mismatched nucleotide is integrated into the phosphate backbone, the enzyme transitions into from the “open” to “closed” states, moving the DNA molecule down by distance, l . The fingers domain continues to have affinity for its current position on the template strand and thus there is no movement of the DNA molecule by distance, p . Therefore, upon transition back to the “open” state, there is no net movement by the DNA molecule.

Attempts to integrate a new dNTP in the polymerase active site cause the polymerase to stall due to steric hindrance with the mismatched base on the primer strand. The fingers domain continues to have affinity for its current position on the template strand and thus there is no movement of the DNA molecule by distance, p . Therefore, upon transition back to the “open” state, there is no net movement by the DNA molecule and this stall allows the polymerase to switch to exonuclease activity.

The authors note that the switch to exonuclease activity does not only occur in the event of polymerase stalling and the mechanism of the switch is dependent upon the ssDNA binding affinities of the exonuclease active site (E_x), fingers domain (E_p) as well as free energy of the DNA molecule (E_{bp} – energy required to unwind DNA, E_{DNA} – energy required to deform dsDNA). The mechanism of the switch can occur in two ways:

$$(1) (E_{bp} + E_x < E_p + E_{DNA})$$

$$(2) (E_{bp} + E_x > E_p + E_{DNA}),$$

In case (1), the energy required to unwind the DNA molecule such that the primer strand can associated with the exonuclease active and the 3'-5' ssDNA binding affinity of the exonuclease site, together, is less energetically costly than moving the entire molecule to the exonuclease site (overcome binding affinity of the fingers domain and deform dsDNA either by bending dsDNA or overcoming dsDNA binding affinity of thumb and palm domains) then only the primer strand will translocate to the exonuclease active site. Conversely, in case (2), the energy from the ssDNA binding affinity of the exonuclease active site and the energy required to unwind dsDNA, together, are greater than the binding affinity of the fingers domain and energy required to deform dsDNA, then, both strands will translocate to the exonuclease active site.

Using this model for Mip1p, it is possible that the CTE could alter the energy requirements for translocation between the active sites. If the CTE were to decrease the energy required to shuttle the primer DNA strand between the active sites, then any impairment of CTE function would make translocation energetically expensive. Thus,

switching between active sites would be less common, leading to enzymes with relatively higher rates of either polymerization or exonucleolytic activity.

Recently, Viikov *et al.* (2010) have been able to express a recombinant form of Mip1p in *E. coli* and characterize it *in vitro*. Their findings suggest that Mip1p acts as an extremely processive monomer in replicating DNA. Comparatively, the POLG catalytic subunit, POLGA, has been found to be moderately processive in the absence of its accessory subunit due to a mammalian-conserved *IP* (Intrinsic Processivity) subdomain in the linker region of the protein (Lee *et al.* 2009; Figure 4.1). Processivity is the extent of polymerization following a single binding event (Foury, 1992). The *IP* subdomain and accessory subunit are absent in Mip1p and *S. cerevisiae* (Figure 4.1, Lee *et al.* 2009, Lucas *et al.* 2004). It is tempting to suggest that the 74 proximal residues of the CTE may be involved in the processivity of Mip1p. Processivity is achieved through different mechanisms. For example, thioredoxin enhances T7 DNA polymerase processivity by prolonging the time of each binding event (Huber *et al.*, 1987) and POLGB enhances POLG processivity by accelerating the polymerization (Johnson *et al.*, 2000). The CTE could conceivably enhance Mip1p processivity by accelerating the polymerization rate through maintenance of a favourable polymerase:exonuclease activity ratio. Processivity assays should be carried out to test this hypothesis.

Respiratory competence of cells harbouring Mip1(E1036G) Δ 205 drastically decreased over 4 days at 30°C yet erythromycin resistance only had a modest increase over wild-type cells. Thus, mitochondrial DNA dysfunction is likely due to complete loss, deletions or rearrangements of mitochondrial DNA and could be caused by a DNA

Figure 4.1 Amino acid alignment of representative mitochondrial DNA polymerases from *Homo sapiens* (HS), *Xenopus laevis* (XI) mouse (mm), *Drosophila melanogaster* (Dm), *Saccharomyces cerevisiae* (Sc) and *Schizosaccharomyces pombe* (Sp). Boxed in red are the *Intrinsic Processivity* (IP) and *Accessory Interacting Domains* (AID) which are highly conserved among higher metazoans. Only the exonuclease, linker and portion of the polymerase domains are shown. The fungal CTE is not shown polymerase domains are shown. The fungal CTE is not shown. (This figure was adapted with permission from Lee *et al.* 2009).

polymerase stuck in exonuclease mode. To confirm the loss of mtDNA *in vivo*, DAPI staining could be performed on these respiratory deficient cells.

The CTE may still have other functions. Viikov *et al.* (2010) noted that Mip1p can undergo DNA strand-displacement synthesis. This ability is intrinsic as the experiment was carried out with a purified enzyme expressed in *E. coli*. POLG is unable to do this alone and requires single-stranded binding proteins and DNA helicase, TWINKLE. Furthermore, a recent study by Cheng *et al.* (2010) found that Mip1p was likely involved in a protein-protein interaction with another protein in the nucleoid and was not interacting exclusively with mitochondrial DNA. Following centrifugation of fractions containing percoll-gradient purified mitochondria treated with DNA restriction endonuclease *EcoRV*, Mip1p was almost exclusively located in the pellet along with the inner mitochondrial membrane. DNA binding protein, Abf2p, however, was released into the supernatant with digested mitochondrial DNA.

This study developed a strategy for creating point mutations in the critical region of the CTE for *in vivo* studies as well as optimized a non-radioactive *in vitro* DNA polymerase developed previously. Through these methods, 2 residues were found to be important for Mip1p function, E1036 and D1037. Their exact function is unknown, but, data from this study implicates them in polymerase-exonuclease coupling. It is with great hope that these findings contribute to the overall knowledge of the enigmatic mechanism of mitochondrial DNA replication and lead to discoveries that could contribute to solving issues related to human mitochondrial disease.

REFERENCES

Barrientos, A., (2003) Yeast Models of Human Mitochondrial Diseases. *IUBMB* **55**: 83-95.

Baruffini, E., Lodi, T., Dallabona, C., Puglisi, A., Zeviani M. and Ferrero, I., (2006) Genetic and chemical rescue of the *Saccharomyces cerevisiae* phenotype induced by mitochondrial DNA polymerase mutations associated with progressive external ophthalmoplegia in humans. *Hum Mol Genet* **15**: 2846-55.

Baruffini, E. and Lodi, T., (2010) Construction and validation of a yeast model system for studying *in vivo* the susceptibility to nucleotide analogues of DNA polymerase gamma allelic variants. *Mitochondrion* **10**: 183-187.

Bateman, J., Perlman, P. and Butow, R., (2002) Mutational bisection of the mitochondrial DNA stability and amino acid biosynthetic functions of Ilv5p of budding yeast. *Genetics* **161**: 1043-52.

Baudin, A., Ozier-Kalogeropoulos, O., Denouel, A., Lacroute, F. and Cullin, C., (1993) A simple and efficient method for direct gene deletion in *Saccharomyces cerevisiae*. *Nucleic Acids Res* **21**: 3329-30.

Beese, L., Derbyshire V. and Steitz, T., (1993) Structure of DNA polymerase I Klenow fragment bound to duplex DNA. *Science* **260**: 352-5.

Berger, K. and Yaffe, M., (2000) Mitochondrial DNA inheritance in *Saccharomyces cerevisiae*. *Trends Microbiol* **8**: 508-13.

Blank, H., Li, C., Mueller, J., Bogomolnaya, L., Bryk, M. and Polymenis, M., (2008) An increase in mitochondrial DNA promotes nuclear DNA replication in yeast. *PLoS Genet* **4**: e1000047.

Boldogh, I., Nowakowski, D., Yang, H., Chung, H., Karmon, S., Royes, P. and Pon L., (2003) A protein complex containing Mdm10p, Mdm12p and Mmm1p links mitochondrial membranes and DNA to the cytoskeleton-based segregation machinery. *Mol Biol Cell* **14**: 4618-27.

Brachmann, C., Davies, A., Cost, G. J., Caputo, E., Li, J., Hieter, P. and Boeke, J. D., (1998) Designer deletion strains derived from *Saccharomyces cerevisiae* S288c: a useful

set of strains and plasmids for PCR-mediated gene disruptions and other applications. *Yeast* **14**: 115-32.

Brown, M. A., (1997) Tumor suppressor genes and human cancer. *Adv Genet* **36**: 45-135.

Carrodegua, J. A., Kobayashi, R., Lim, S. E., Copeland, W. C., Bogenhagen, D. F., (1999) The accessory subunit of *Xenopus laevis* mitochondrial DNA polymerase gamma increases processivity of the catalytic subunit of human DNA polymerase gamma and is related to class II aminoacyl-tRNA synthetases. *Mol Cell Biol* **19**: 4039-46.

Carrodegua, J. A. and Bogenhagen, D. F., (2000) Protein sequences conserved in prokaryotic aminoacyl-tRNA synthetases are important for the activity of the processivity factor of human mitochondrial DNA polymerase. *Nucleic Acids Res* **28**: 1237-44.

Chang, D. D. and Clayton, D. A., (1985) Priming of human mitochondrial DNA replication occurs at the light-strand promoter. *Proc Natl Acad Sci U S A* **82**: 321-5.

Cheng, X. and Ivessa, A. S., (2010) Association of the yeast DNA helicase Pif1p with mitochondrial membranes and mitochondrial DNA. *Eur J Cell Biol* **89**: 742-7.

Chiappini, F., Teicher, E., Saffory, R., Debuire, B., Vittecog, D. and Lemoine A., (2009) Relationship between polymerase gamma (POLG) polymorphisms and antiretroviral therapy-induced lipodystrophy in HIV-1 infected patients: a case-control study. *Curr HIV Res* **7**: 244-53.

Cohen, B. H. and Naviaux, R. K., (2010) The clinical diagnosis of POLG disease and other mitochondrial DNA depletion disorders. *Methods* **51**: 364-73.

Chomyn, A., Martinuzzi, A., Yoneda, M., Daga, A., Hurko, O., Johns, D., Lai, S. T., Nonaki, I., Angelini, C. and Attardi, G., (1992) MELAS mutations in mtDNA binding site for transcription termination factor causes defects in protein synthesis and in respiration but no changes in levels of upstream and downstream mature transcripts. *Proc Natl Acad Sci U S A* **89**: 4221-5.

Davidzon, G., Greene, P., Mansuco, M., Klos, K. J., Ahlskog, J. E., Hirano, M. and DiMauro S., (2006) Early-onset familial parkinsonism due to POLG mutations. *Ann Neurol* **59**: 859-62.

Desler, C., Marcker, M. L., Singh, K. K. and Rasmussen, L. J., (2011) The importance of mitochondrial DNA in aging and cancer. *J Aging Res* **2011**: 407536.

Di Fonzo, A., Bordoni, A., Crimi, M., Sara, G., Del Bro, R., Bresolin N. and Comi, G. P., (2003) POLG mutations in sporadic mitochondrial disorders with multiple mtDNA deletions. *Hum Mutat* **22**: 498-9.

Diffley, J. F. and Stillman, B., (1991) A close relative of the nuclear, chromosomal high-mobility group protein HMG1 in yeast mitochondria. *Proc Natl Acad Sci U S A* **88**: 7864-8.

Diffley, J. F. and Stillman, B., (1992) DNA binding properties of an HMG1-related protein from yeast mitochondria. *J Biol Chem* **267**: 3368-74.

Dimmer, K. S., Jakobs, S., Vogel, F., Altmann, K. and Westermann B., (2005) Mdm31 and Mdm32 are inner membrane proteins required for maintenance of mitochondrial shape and stability of mitochondrial DNA nucleoids in yeast. *J Cell Biol* **168**: 103-15.

Doubl  , S., Tabor, S., Long, A. M., Richardson, C. C. and Ellenberg, T., (1998) Crystal structure of a bacteriophage T7 DNA replication complex at 2.2   resolution. *Nature* **391**: 251-8.

Dujon, B., (1981) Mitochondrial genetics and functions.

Elledge, S. J. and Davis, R. W., (1987) Identification and isolation of the gene encoding the small subunit of ribonucleotide reductase from *Saccharomyces cerevisiae*: DNA damage-inducible gene required for mitotic viability. *Mol Cell Biol* **7**: 2783-93.

Eom, S. H., Wang, J. and Steitz T. A., (1996) Structure of Taq polymerase with DNA at the polymerase active site. *Nature* **382**: 278-81.

Ephrussi, B., Jakob, H. and Grandchamp, S., (1966) Etudes Sur La Supressivite Des Mutants a Deficiencie Respiratoire De La Levure, II Etapes De La Mutatoin Grande En Petite Provoquee Par Le Facteur Suppressif. *Genetics* **54**: 1-29.

Fan, L., Sanschagr  n, P. C., Farr, C. L., Schaefer, K. T., Randolph, K. M, Tainer, J. A. and Kaguni, L. S., (1999) The accessory subunit of mtDNA polymerase shares structural homology with aminoacyl-tRNA synthetases: implications for a dual role as a primer recognition factor and processivity clamp. *Proc Natl Acad Sci U S A* **96**: 9527-32.

Fan, L., Kim, S., Farr, C. L., Schaefer, K. T., Randolph, K. M., Tainer, J. A. and Kaguni, L. S., (2006) A Novel Processive Mechanism for DNA Synthesis Revealed by Structure, Modelling and Mutagenesis of the Accessory Subunit of Human Mitochondrial DNA Polymerase. *J Mol Biol* **358**: 1229-1243.

Fangman, W. L., Henly, J. W. and Brewer, B. J., (1990) RPO41-independent maintenance of [rho-] mitochondrial DNA in *Saccharomyces cerevisiae*. *Mol Cell Biol* **10**: 10-5.

Filee, J., Forterre, P., Sen-Lin, T. and Laurent, J., (2002) Evolution of DNA polymerase families: evidence for multiple gene exchange between cellular and viral proteins. *J Mol Evol* **54**: 763-73.

Foury, F., (1989) Cloning and sequencing of the nuclear gene MIP1 encoding the catalytic subunit of the yeast mitochondrial DNA polymerase. *J Biol Chem* **264**: 20552-60.

Foury, F. and Vanderstraeten, S., (1992) Yeast mitochondrial DNA mutators with deficient proofreading exonucleolytic activity. *Embo J* **11**: 2717-26.

Fridde, R. W., Klare, J. E., Martin, S. S., Corzett, M, Balhorn, R., Baldwin E. P., Baskin, R.J. and Noy, A., (2004) Mechanism of DNA compaction by yeast mitochondrial protein Abf2p. *Biophys J* **86**: 1632-9.

Gilkerson, R. W., Schon, E. A., Hernandez, E and Davidson, M. M., (2008) Mitochondrial nucleoids maintain genetic autonomy but allow for functional complementation. *J Cell Biol* **181**: 1117-28.

Graziewicz, M. A., Longley, M. J. and Copeland, W. C., (2006) DNA polymerase gamma in mitochondrial DNA replication and repair. *Chem Rev* **106**: 383-405.

Hanahan, D., (1985) Techniques for transformation of *E. coli*. *DNA Cloning: A practical approach* In: Glover, D. M., editor. Vol. 1 Washington, DC: IRL Press. 109-135.

Hobbs, A. E., Srinivasam M., McCaffery, J. M. and Jensen, R. E., (2001) Mmm1p a mitochondrial outer membrane protein, is connected to mitochondrial DNA (mtDNA) nucleoids and required for mtDNA stability. *J Cell Biol* **152**: 401-10.

Holt, I. J., He, J., Mao, C.C., Boyd-Kirkup, J. D., Martinsson, P., Sembongi, H., Reyes A. and Spelbrink, J. N., (2007) Mammalian mitochondrial nucleoids: organizing an independently minded genome. *Mitochondrion* **7**: 311-21.

Holt, I. J., (2009) Mitochondrial DNA replication and repair: all a flap. *Trends Biochem Sci* **34**: 358-65.

Horvath, R., Hudson, G., Ferrari, G., Futterer, N., Ahola, S., Lamantea, E., Prokisch, H., Lochmuller, H., McFarland, R., Ramesh, V., *et al.*, (2006) Phenotypic spectrum associated with mutations of mitochondrial polymerase gamma gene. *Brain* **129**: 1674-84.

Hu, J. P., Vanerstraeten, S. and Foury, F., (1995) Isolation and characterization of ten mutator alleles of the mitochondrial DNA polymerase-encoding *MIP1* gene from *Saccharomyces cerevisiae*. *Gene* **160**: 105-10.

Hudson, G, Schaefer, A. M., Taylor, R. W., Tiangyou, W., Gibson, A., Venables, G., Griffiths, P., Burn, D. J., Turnbull, D. M., Chinnery, P. F., (2007) Mutation of the linker region of polymerase gamma-1 (POLG-1) gene associated with progressive external ophthalmoplegia and Parkinsonism. *Arch Neurol* **64**: 553-7.

Hughes, J. A., Sweeney, M. G., Cooper, J. M., Hammans, S. R., Brockington, M., Schapira, A. H.V., Harding, A. E. and Clark, J. B., (1995) Mitochondrial DNA (mtDNA) diseases: correlation of genotype to phenotype. *Biochim Biophys Acta* **1271**: 135-40.

Ishikawa, K. and Hayashi, J., (2010) A novel function of mtDNA: its involvement in metastasis. *Ann N Y Acad Sci* **1201**: 40-3.

Ito, J. and Braithwaite, D. K., (1990) Yeast mitochondrial DNA polymerase is related to the family A DNA polymerases. *Nucleic Acids Res* **18**: 6716.

Iyengar, B., Luo, N., Farr, C. L., Kaguni, L. S. and Campos, A. R., (2002) The accessory subunit of DNA polymerase gamma is essential for mitochondrial DNA maintenance and development in *Drosophila melanogaster*. *Proc Natl Acad Sci U S A* **99**: 4483-8.

Jacobs, H. T., Lehtinen, S. K. and Spelbrink, J. N., (2000) No sex please, we're mitochondria: a hypothesis on the somatic inheritance of mammalian mtDNA. *Bioessays* **22**: 564-72.

Johnson, A. A., Tsai, Y., Graves, S. W. and Johnson, K. A., (2000) Human mitochondrial DNA polymerase holoenzyme: reconstitution and characterization. *Biochemistry* **39**: 1702-8.

Joyce, C. M. and Steitz, T. A., (1995) Polymerase structures and function: variations on a theme? *J Bacteriol* **177**: 6321-9.

Kaguni, L. S., (2004) DNA polymerase gamma, the mitochondrial replicase. *Annu Rev Biochem* **73**: 293-320.

Kaufman, B. A., Newman, S. M., Hallberg, R. L., Slaughter, C. A., Perlman, P. S. and Butow, R. A., (2000) In organelle formaldehyde crosslinking of proteins to mtDNA: identification of bifunctional proteins. *Proc Natl Acad Sci U S A* **97**: 7772-7.

Kaufman, B. A., Kolesar, J. E., Perlman, P. S. and Butow, R. A., (2003) A function for the mitochondrial chaperonin Hsp60 in the structure and transmission of mitochondrial DNA nucleoids in *Saccharomyces cerevisiae*. *J Cell Biol* **163**: 457-61.

Kohlhaw, G. B., (2003) Leucine biosynthesis in fungi: entering metabolism through the back door. *Microbiol Mol Biol Rev.* **67**: 1-15.

Kornman, B. and Walter, P., (2010) ERMES-mediated ER-mitochondria contacts: molecular hubs for the regulation of mitochondrial biology. *J Cell Sci* **123**: 1389-93.

Kucej, M. and Butow, R. A., (2007) Evolutionary tinkering with mitochondrial nucleoids. *Trends Cell Biol* **17**: 586-92.

Kucej, M., Kucejova, B., Subramanian, R., Chen, X. J. and Butow, R. A. (2008) Mitochondrial nucleoids undergo remodelling in response to metabolic cues. *J Cell Sci* **121**: 1861-8.

Kunkel, T. A., Patel, S. S. and Johnson, K. A., (1994) Error-prone replication of repeated DNA sequences by T7 DNA polymerase in the absence of its processivity subunit. *Proc Natl Acad Sci U S A* **91**: 6830-4.

Lecrenier, N., Van Der Bruggen, P. and Foury F., (1997) Mitochondrial DNA polymerases from yeast to man: a new family of polymerases. *Gene* **185**: 147-52.

Lecrenier, N. and Foury, F., (2000) New features of mitochondrial DNA replication system in yeast and man. *Gene* **246**: 37-48.

Lee, Y. S., Kennedy, W. D. and Yin, Y. W., (2009) Structural Insight into Processive Human Mitochondrial DNA Synthesis and Disease-Related Polymerase Mutations. *Cell* **139**: 312-24.

Ling, F. and Shibata, T., (2002) Recombination-dependent mtDNA partitioning: *in vivo* role of Mhr1p to promote pairing of homologous DNA. *EMBO J* **21**: 4730-40.

Ling, F. and Shibata, T., (2004) Mhr1p-dependent concatameric mitochondrial DNA formation for generating yeast mitochondrial homoplasmic cells. *Mol Biol Cell* **15**: 310-22.

Lipinski, K. A., Kaniak-Golik, A. and Golik, P., (2010) Maintenance and expression of the *S. cerevisiae* mitochondrial genome—from genetics to evolution and systems biology. *Biochim Biophys Acta* **1797**: 1086-98.

Lohr, D., Kovacic, R. T. and Van Hold, K. E., (1977) Quantitative analysis of the digestion of yeast chromatin by staphylococcal nuclease. *Biochemistry* **8**: 463-71.

Lorenz, M. C., Muir, R. S., Lim, E., McElver, J., Weber, S. C. and Heitman J. (1995) Gene disruption with PCR products in *Saccharomyces cerevisiae*. *Gene* **158**: 113-7.

Lorimer, H. E., Brewer, B. J. and Fangman, W. L., (1995) A test of the transcription model for biased inheritance of yeast mitochondrial DNA. *Mol Cell Biol* **15**: 4803-9.

Lucas, P., Lasserre, J. P., Plissonneau, J. and Costeviejo, M., (2004) Absence of accessory subunit in the DNA polymerase gamma purified from yeast mitochondria. *Mitochondrion* **4**: 13-20.

Luoma, P. T., Eerola, J., Ahola, S., Hakonen, A. H., Hellstrom, O., Kivisto, K. T., Tienari, P. J. and Suomalainen, A., (2007) Mitochondrial DNA polymerase gamma variants in idiopathic sporadic Parkinson disease. *Neurology* **69**: 1152-9.

Macierzanka, M., Plotka, M., Pryputniewicz-Drobinska, D., Lewandowska, A., Lightowers, R. and Marszalek, J., (2008) Maintenance and stabilization of mtDNA can be facilitated by the DNA-binding activity of Ilv5p. *Biochim Biophys Acta* **1783**: 107-17.

Maleszka, R., Skelly, P. J. and Clark-Walker, G. D., (1991) Rolling circle replication of DNA in yeast mitochondria. *EMBO J* **10**: 3923-9.

McBride, H. M., Neuspiel, M. and Wasiak, S., (2006) Mitochondria: more than just a powerhouse. *Curr Biol* **16**: 551-60.

Meeusen, S., Tieu, Q., Wong, E., Weiss, E., Schieltz, D., Yates, J. R. and Nunnari J., (1999) Mgm101p is a novel component of the mitochondrial nucleoid that binds DNA and is required for the repair of oxidatively damaged mitochondrial DNA. *J Cell Biol* **145**: 291-304.

Meeusen, S. and Nunari, J., (2003) Evidence for a two membrane-spanning autonomous mitochondrial DNA replisome. *J Cell Biol* **163**: 503-10.

Midzak, A., Rone, M., Aghazadeh, Y., Culty, M. and Papadopoulos V., (2011) Mitochondrial protein import and the genesis of steroidogenic mitochondria. *Mol Cell Endocrinol* **336**: 70-9.

Miyakawa, I., Fujimura, R. and Kadowaki, Y., (2008) Use of the *nuc1* null mutant for analysis of yeast mitochondrial nucleoids. *J Gen Appl Microbiol* **54**: 317-25.

Netter, P., Petrochilo, E., Slonimski, P. P., Bolotin-Fukuhara, M., Coen, D., Deutsch, J. and Dujon B. (1974) Mitochondrial genetics VII Allelism and mapping studies of ribosomal mutants resistant to chloramphenicol, erythromycin and spiramycin in *S. cerevisiae*. *Genetics* **78**: 1063-100.

Ogur, M., St. John, R. and Nagai, S., (1957) Tetrazolium overlay technique for population studies of respiratory deficiency in yeast. *Science* **125**: 928-9.

Oliveira, M. T. and Kaguni, L. S., (2009) Comparative purification strategies for *Drosophila* and human mitochondrial DNA replication proteins: DNA polymerase gamma and mitochondrial single-stranded binding protein. *Methods Mol Biol* **554**: 37-58.

Phadnis, N., Mehta, R., Meednu, N. and Sia, E.A., (2006) Ntg1p, the base excision repair protein generates mutagenic intermediates in yeast mitochondrial DNA. *DNA Repair (Amst)* **5**: 829-39.

Polesky, A. H., Steitz, T. A., Grindley, N. D. and Joyce, C. M., (1990) Identification of residues critical for the polymerase activity of the Klenow fragment of DNA polymerase I from *Escherichia coli*. *J Biol Chem* **265**: 14579-91.

Rinaldi, T., Dallabona, C., Ferrero, I., Frontali, L. and Bolotin-Fukuhara, M., (2010) Mitochondrial diseases and the role of the yeast models. *FEMS Yeast Res* **10**: 1006-22.

Sheff, M. A. and Thorn, K. S., (2004) Optimized cassettes for fluorescent protein tagging in *Saccharomyces cerevisiae*. *Yeast* **21**: 661-70.

Sia, R. A., Carrol, S., Kalifa, L., Hochmuth, C. and Sia E. A., (2009) Loss of the mitochondrial nucleoid protein, Abf2p, destabilizes repetitive DNA in the yeast mitochondrial genome. *Genetics* **181**: 331-4.

Solieri, L., (2010) Mitochondrial inheritance in budding yeasts: towards an integrated understanding. *Trends Microbiol* **18**: 521-30.

Sor, F. and Fukuhara, H., (1982) Identification of two erythromycin resistant mutations in the mitochondrial gene coding for the large ribosomal RNA in yeast. *Nucleic Acids Res* **10**: 6571-7.

Spelbrink, J. N., (2010) Functional organization of mammalian mitochondrial DNA in nucleoids: history, recent developments and future challenges. *IUBMB Life* **62**: 19-32.

Steger, H. F., Sollner, T., Kiebler, M., Dietmeier, K. A., Pfaller, R., Trulzsch, K. S., Tropschug, M., Neupert, W. and Pfanner, N., (1990) Import of ADP/ATP carrier into mitochondria: two receptors act in parallel. *J Cell Biol* **111**: 2353-63.

Stella, C., Burgos, I., Chapela, S. and Gamondi, O., (2011) Ischemia – reperfusion: A look from yeast mitochondria. *Curr Med Chem* (Epub ahead of print).

Stigter, D., (2004) Packaging of single DNA molecules by the yeast mitochondrial protein Abf2p: reinterpretation of recent single molecule experiments. *Biophys Chem* **110**: 171-8.

Storici, F., Durham, C. L., Gordenin, D. A. and Resnick, M. A., (2003) Chromosomal site-specific double-stranded breaks are efficiently targeted for repair by oligonucleotides by yeast. *Proc Natl Acad Sci U S A* **100**: 14994-9.

Stros, M., Launholt, D. and Grasser, K. D., (2007) The HMG-box: a versatile protein domain occurring in a wide variety of DNA-binding proteins. *Cell Mol Life Sci* **64**: 2590-606.

Stuart, G. R., Santos, J. H., Strand, M. K., Van Houten, B. and Copeland, W. C., (2006) Mitochondrial and nuclear DNA defects in *Saccharomyces cerevisiae* with mutations in DNA polymerase gamma associated with progressive external ophthalmoplegia. *Hum Mol Genet* **15**: 363-74.

Stumpf, P. L., (1969) Metabolism of fatty acids. *Annu Rev Biochem* **38**: 159-212.

Stumpf, J. D., Bailey, C. M., Spell, D., Stillwagon, M., Anderson, K. S. and Copeland, W. C., (2010) mip1 containing mutations associated with mitochondrial disease causes mutagenesis and depletion of mtDNA in *Saccharomyces cerevisiae*. *Hum Mol Genet* **19**: 2123-33.

Szczepanowska, K. and Foury, F., (2010) A cluster of pathogenic mutations in 3'-5' exonuclease domain of DNA polymerase gamma defines a novel module coupling DNA synthesis and degradation. *Human Mol Genet* **19**: 3516-29.

Tabor, S., Huber, H. E. and Richardson, C. C. (1987) *Escherichia coli* thioredoxin confers processivity on the DNA polymerase activity of the gene 5 protein of bacteriophage T7. *J Biol Chem* **262**: 16212-23.

Tiangyou, W., Hudson, G., Ghezzi, D., Ferrari, G., Zeviani, M., Burn, D. J. and Chinnery, P. F., (2006) POLG1 in idiopathic Parkinson disease. *Neurology* **67**: 1698-700.

Tiranti, V., Savoia, A., Forti, F., D'Apolito, M. F., Centra, M., Rocchi, M. and Zeviani, M., (1997) Identification of the gene encoding the human mitochondrial RNA polymerase (h-mtRPOL) by cyberscreening of the Expressed Sequence Tags database. *Human Mol Genet* **6**: 615-25.

Travers, A. A., (2003) Priming the nucleosome: a role for HMGB proteins?. *EMBO Rep* **4**: 131-6.

Tifunovic, A., Wredenberg, A., Falkenberg, M., Spelbrink, J., Rovio, A. T., Bruder, C. E., Bohlooly, M., Gidlof, S., Oldfors, Anders., Wibom, R., Tornell, J., Jacobs, H. T. and Larson, N., (2004) Premature ageing in mice expressing defective mitochondrial DNA polymerase. *Nature* **429**: 417-23.

Van Goethem, G., Dermaut, B., Lofgren, A., Martin, J. J. and Van Broeckhoven, C., (2001) Mutation of POLG is associated with progressive external ophthalmoplegia characterized by mtDNA deletions. *Nat Genet* **28**: 211-2.

Veatch, J. R., McMurray, M. A., Nelson, Z. W., Gottschling, D. E., (2009) Mitochondrial dysfunction leads to nuclear genome instability via an iron-sulfur cluster defect. *Cell* **137**: 1247-58.

Viikov, K., Valjamae, P. and Sedman, J., (2011) Yeast mitochondrial DNA polymerase is a highly processive single-subunit enzyme. *Mitochondrion* **11**: 119-26.

Williamson, D., (2002) The curious history of yeast mitochondrial DNA. *Nat Rev Genet* **3**: 475-81.

Yamanaka, H., Gatanaga, H., Kosalaraksa, P., Matsuoka-Aizawa S., Takahashi, T., Kimura, S. and Oka S. (2007) Novel mutation of human DNA polymerase gamma associated with mitochondrial toxicity induced by anti-HIV treatment. *J Infect Dis* **195**: 1419-25.

Ylikallio, E. and Suomalainen, A., (2011) Mechanisms of mitochondrial diseases. *Ann Med* [Epub ahead of print].

Young, M. J., Theriault, S. S. Li, M. and Court, D. A., (2006) The carboxyl-terminal extension on fungal mitochondrial DNA polymerases: identification of a critical region of the enzyme from *Saccharomyces cerevisiae*. *Yeast* **23**: 101-16.

Young, M. J., (2008) Analysis of *Saccharomyces cerevisiae* genetic background and mitochondrial DNA polymerase variants on maintenance of the mitochondrial genome. Ph.D. dissertation, University of Manitoba.

Youngman, M. J., Hobbs, A. E., Burgess, S. M. Srinivasan, M. and Jensen R. E., (2004) Mmm2p, a mitochondrial outer membrane protein require for yeast mitochondrial shape and maintenance of mDNA nucleoids. *J Cell Biol* **164**: 677-88.

Zeleneya-troitskaya, O ., Newman, S. M., Okamoto, K., Perlaman, P. S. and Butow, R. A., (1998) Functions of the high mobility group protein, Abf2p, in mitochondrial DNA segregation, recombination, and copy number in *Saccharomyces cerevisiae*. *Genetics* **148**: 1763-76.

Zhao, X., Muller, E. G. and Rothstein, R., (1998) A suppressor of two essential checkpoint genes identifies a novel protein that negatively affects dNTP pools. *Mol Cell* **2**: 329-40.